

**International
Progress Report**

IPR-02-67

Äspö Hard Rock Laboratory

**Geological study on block scale
water-conducting structures
representative in the tunnel**

Junichi Goto

JNC

July 2002

Svensk Kärnbränslehantering AB

Swedish Nuclear Fuel
and Waste Management Co
Box 5864
SE-102 40 Stockholm Sweden
Tel +46 8 459 84 00
Fax +46 8 661 57 19



**Äspö Hard Rock
Laboratory**

Report no.	No.
IPR-02-67	F13K
Author	Date
Goto	02-07-01
Checked by	Date
Leif Stenberg	03-02-05
Approved	Date
Christer Svemar	03-02-27

Äspö Hard Rock Laboratory

Geological study on block scale water-conducting structures representative in the tunnel

Junichi Goto

JNC

July 2002

Keywords: Geology, hydrology, Äspö HRL, tunnel mapping, fractures, radionuclide migration, fracture zones, microscopy, mineralogical investigations, XRD analysis

This report concerns a study which was conducted for SKB. The conclusions and viewpoints presented in the report are those of the author(s) and do not necessarily coincide with those of the client.

Abstract

A geological study on block scale (ca. 10-100 m) water-conducting structures were conducted at Äspö Hard Rock Laboratory (HRL). The main objective is to geologically characterise the "minor structure" and "connecting structure", and acquire information relevant to construct conceptual hydrogeological models. The "minor structure" is defined here as a relatively small and less transmissive water-conducting structure that can be a candidate for block scale tracer tests, and the "connecting structure" is as a geometrically and hydrogeologically moderate water-conducting structure that connect the minor structure and the large highly transmissive water-conducting structure. In the reconnaissance mapping in the tunnel to select targets for the study, a certain connecting structure was not identified. Six alternative structures that could potentially be considered as connecting structures, and minor structures crosscutting each other were then selected. Detailed mapping in the tunnel, microscopic and mineralogical study, and mapping of drill core were performed on these structures. It is concluded in terms of geology that most of the studied structures are faults that re-activated existing structure as faults, cataclasites and mylonites. The potential connecting structures have more activity events and larger aperture than the minor structures. In terms of hydrogeology, NW trending structures are more water-conductive, position and amount of discharge in a structure are very heterogeneous, and the effect of intersection of structure is not positively recognised. Information relevant to transport of solutes is that all the studied water-conducting structures have gouge materials that contain clay minerals up to 50% of weight.

Sammanfattning

En geologisk studie på vattenförande sprickor i blockskala (ca 10-100 m) har genomförts i Äspölaboratoriet. Det huvudsakliga syftet var att karakterisera s k ”mindre sprickor” och ”konnekterade sprickor”, samt att samla information som är betydelsefull för att bygga konseptuella, hydrogeologiska modeller. ”Mindre sprickor” definieras här som relativt små och obetydligt transmissiva, vattenförande sprickor, som kan vara kandidater till blockskaleförsök med spårämnen, och ”konnekterande sprickor” som måttligt vattenförande sprickor, vilka sammanbinder mindre sprickor med större, högre transmissiva, vattenförande sprickor. I rekognoseringskarteringen i tunneln, som gjordes för att välja föremål för studien, identifierades aldrig någon särskilt konnekterande spricka. Sex alternativa sprickor, som potentiellt kunde betraktas som konnekterande sprickor, och mindre sprickor som korsar varandra, valdes istället. Detaljerad kartering gjordes av dessa sprickor i tunneln och i borrhälar, och prover studerades med mikroskopi och mineralogiska undersökningar. Slutsatsen är att de flesta studerade sprickor är förkastningar som reaktiverar förekommande sprickor till förkastningar samt bildning av kataklasit-och mylonitfyllningar. De potentiellt sammanbundna sprickorna har utsatts för fler händelser och har större spricköppningar än de mindre sprickorna. NW-riktade sprickor är mer vattenförande. Plats för och mängd av vattenflöde i en spricka är mycket oregelbundna. Effekten av korsande sprickor har inte kunnat fastställas. Alla de studerade sprickorna har sprickmineral som innehåller upp till 50 vikts-% lermineral.

Contents

1 Introduction	9
1.1 Background	9
1.1.1 Investigations at Äspö	9
1.1.2 TRUE Block Scale Project	10
1.1.3 FCC project	12
1.1.4 Task 6	13
1.2 Objectives	15
1.3 Terminology and definitions	16
1.4. Outline of investigations	17
2 Target selection	19
2.1 Objectives	19
2.2 Area for the target selection	19
2.3 Methods	19
2.4 Results	21
3 Detailed tunnel mapping	27
3.1 Objectives	27
3.2 Methods	27
3.3 Results	28
3.3.1 Site 1	28
3.3.2 Site 2	32
3.3.3 Site 3	35
3.4 Summary of interpretations	38
3.4.1 Potential connecting structures and minor structures	38
3.4.2 Intersection of the minor structures	39
4 Microscopic and mineralogical investigations	51
4.1 Objectives	51
4.2 Methods	51
4.2.1 Sampling	51
4.2.2 Microscopy	52
4.2.3 XRD	52
4.3 Results	52
4.3.1 Microscopic observation	52
4.3.2 XRD analysis	55
4.4 Summary of interpretations	56
5 Core mapping	63
5.1 Objectives	63
5.2 Methods	63
5.3 Results	64
5.4 Summary of interpretations	68
6 Conclusions	69
Acknowledgements	71
References	73
Appendix 1: Table of description for the target selection	
Appendix 2: Maps of the detailed tunnel mapping	
Appendix 3: Tables of descriptions for the detailed mapping	
Appendix 4: Report of the XRD measurement	
Appendix 5: Maps of the core mapping	
Appendix 6: Tables of descriptions for the core mapping	

1 Introduction

1.1 Background

1.1.1 Investigations at Äspö

Extensive scientific investigations have been conducted at Äspö since 1986. Three experimental phases, the pre-investigation phase, construction phase and operation phase were set that correspond the intervals before, during and after construction of the laboratory. Location and layout of the Äspö Hard Rock Laboratory (HRL) are illustrated in Figure 1-1.

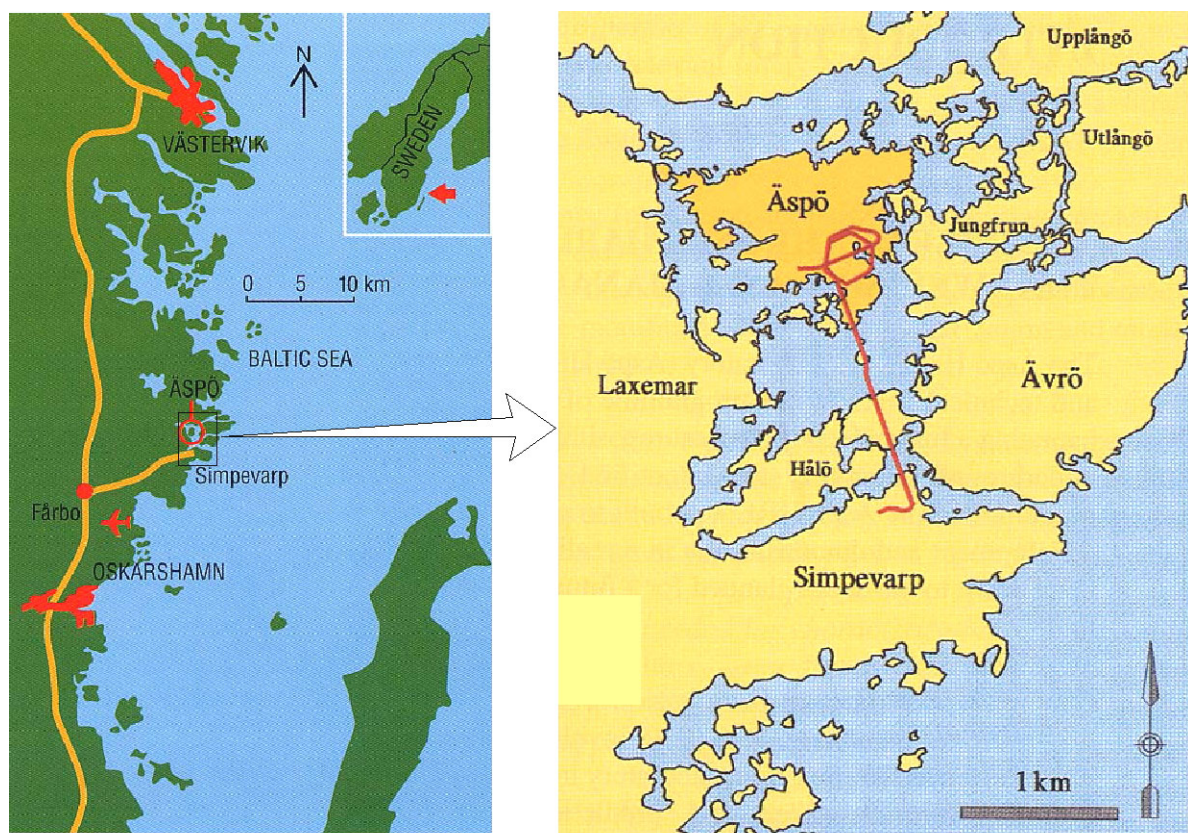


Figure 1-1: Locations of Äspö, ramp and spiral tunnel (Rhén, et al., 1997).

In terms of geology in the pre-investigation phase, lithology and structures were characterized from surface based investigations and the occurrences of structures in the underground predicted are shown in Figure 1-2, (left). In the construction phase, vast amount of data were taken and the predictions were verified (Figure 1-2, right). In the operation phase, various investigation programs for both natural and engineered barrier have been performed in the tunnel to date. The TRUE Block Scale and the Task 6 are one of the active projects relevant to both site characterisation and performance assessment for a deep repository of radioactive waste.

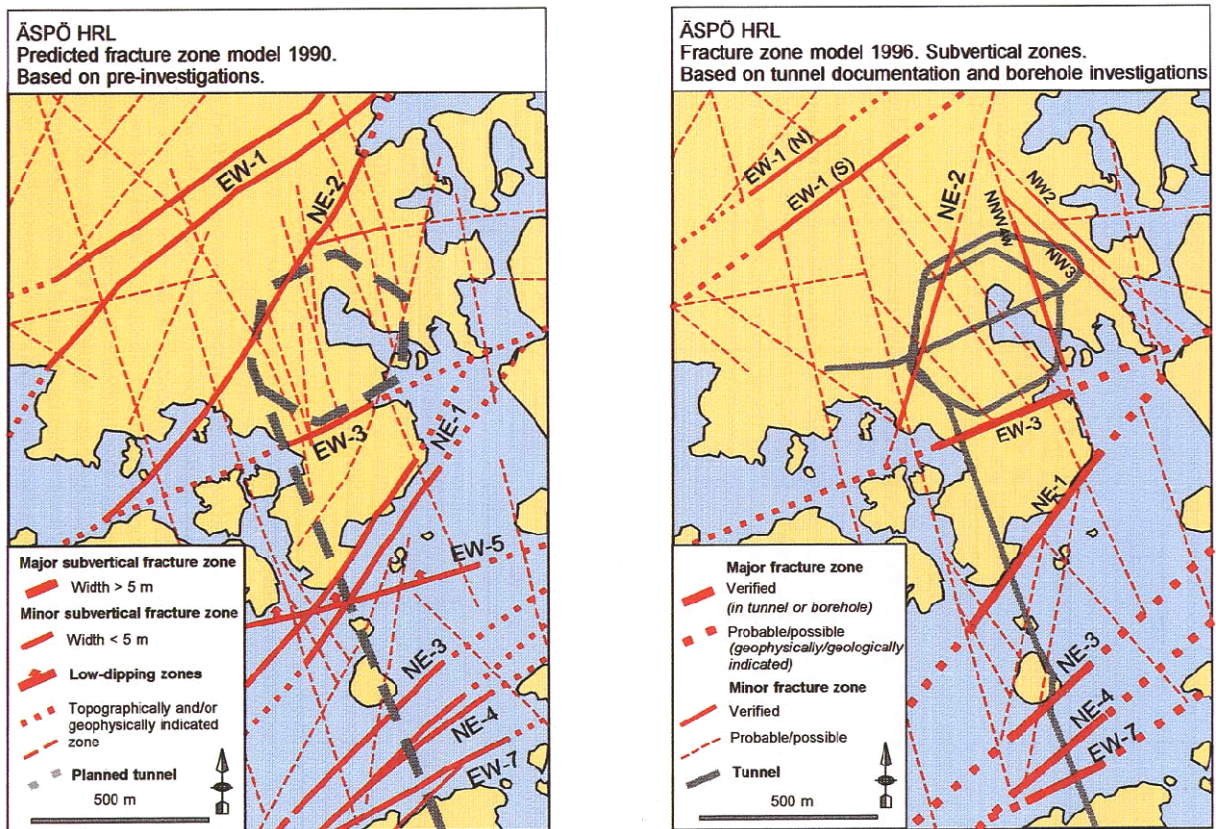


Figure 1-2: Structural models before (left) and after (right) construction of the HRL (after Rhén, et al., 1997).

1.1.2 TRUE Block Scale project

TRUE Block Scale is a part of the TRUE (Tracer Retention Understanding Experiment) project (Bäckblom and Olsson, 1994). Overall objectives of the TRUE project are,

- to develop the understanding of radionuclide migration and retention in fractured rock,
- to evaluate the realism in applied model concepts,
- to assess whether the necessary input data to the models can be collected from site characterisation,
- to evaluate usefulness and feasibility of different model approaches, and
- to provide in-situ data on radionuclide migration and retention,

in the detailed scale (1 – 10 m) and block scale (10 – 100 m). In each scale of experiments, geological characterisation of the test site, hydraulic and tracer tests, injection of epoxy resin and excavation of the tested volume, and finally analysis of flow paths and tracer concentration are planned. The TRUE First Stage (TRUE-1) for the detailed scale has been completed (Winberg, et al, 2000). The TRUE Block Scale for the block scale has the following objectives (Winberg, 1997):

- to increase understanding and ability to predict tracer transport in a fracture network,
- to assess the importance of tracer retention mechanisms (diffusion and sorption) in a fracture network, and
- to assess link between flow and transport data as means for predicting transport phenomena.

Tracer tests are close to complete and the results are going to be reported.

In the TRUE Block Scale project, a network of NW trending water-conducting structures for tracer tests has been identified (Figure 1-3). The network complies with a series of NW trending structures, the core structure #20 and associated structures #13, #21, #22 and #23 (Winberg, 2000; Hermanson and Doe, 2000). These are bounded by and some are in connection with the larger and more conductive NW trending structures #6 and #19 (Winberg, personal communication). These boundary structures may connect with the water-conducting major fracture zones outside the block.

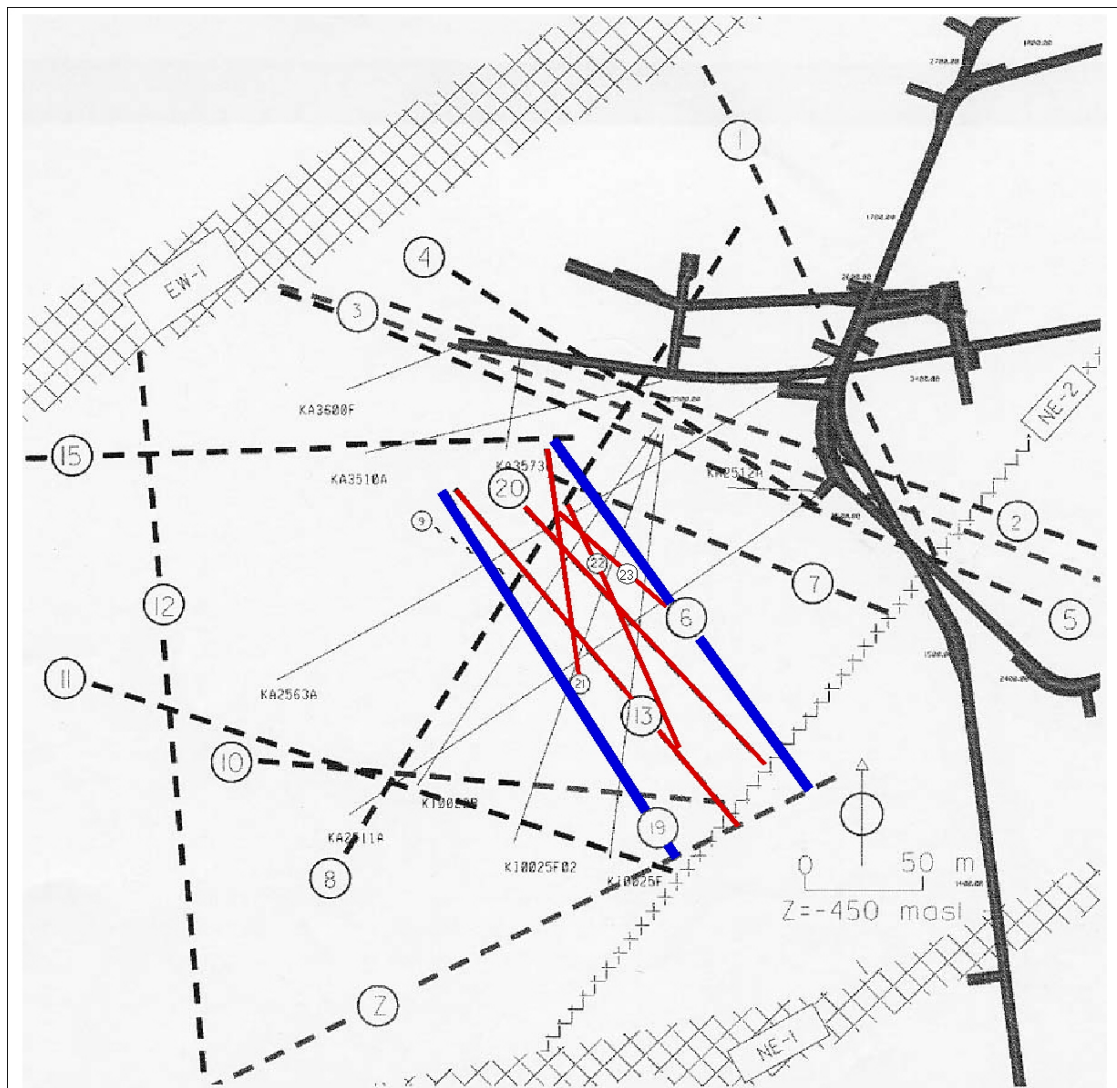


Figure 1-3: A fracture network in the TRUE Block Scale project (modified from Winberg, 2000). Structures #13, #20, #21, #22 and #23 (narrow red) for tracer tests, and boundary structures #6 and #19 (thick blue).

The geological characterisation for the conceptual structural model in this project has been limited on the drill core and boreholes. Existence of a fracture network similar to the TRUE Block Scale provides confidence of the model. Natures of intersection of minor structure and connecting structure, and the fracture intersection zone (FIZ) (Eiben, et al., 1999) have not been verified in the tunnel. Additionally, genesis and deformation mechanisms of the block scale water-conducting structure have not been fully explained. The construction of a micro scale conceptual model of the water-conducting structure has also been one of the issues in this project. Characterisation has been intensively done on the minor structures for tracer tests and less on the boundary structures. In the context of understanding of heterogeneity or consistency in water-conducting structures, to correlate block scale water-conducting structures between borehole and tunnel is important, but has not been studied in detail.

1.1.3 FCC project

Mazurek et al. (1996) conducted a comprehensive study on the outcrop scale water-conducting features in the phase II of FCC (Fracture Classification and Characterisation) project. Results are summarised as follows.

- All the water-conducting features consist of the master faults and splay cracks, which are steep and strike dominantly NW to NNW, often indicate strike-slip displacements.
- Water-conducting features are classified only by geometry into five types; 1) single fault, 2) swarm of single faults, 3) fault zone, 4) fault zone with rounded geometry and 5) fault zone with long splays (Figure 1-4). Those types blend each other in a water-conducting feature along strike.
- Repeated brittle reactivation of water-conducting features is indicated from fracture fillings formed in several events.
- Shear senses of faults may explain a conjugate system of NW dextral and NNW sinistral strike-slip movements.
- Small scale and micro scale pore volume of the studied water-conducting features are characterised and conceptualised.

The connecting structure and minor structure are not classified here, and their structural connectivity is not discussed in detail.

Bossart et al. (2001) in the phase III of FCC project characterized small-scale fracture network in the TRUE-1 site and discussed about fracture geometries in different scales. Structures on different scales are not self-similar with regard to fracture geometry and mechanistic principles. Structures are linear in regional to site scale while structure system consists of master faults and splays in block to outcrop scale, and only fracture cluster and random background fractures exist in small scale. These structures are interconnected hydrogeologically and hydrochemically. They proposed a conceptual model where the small-scale fracture networks are connected to the outcrop scale water-conducting faults, then to the smaller and larger HPF (High Permeability Features, Rhén and Forsmark (2000)) including deterministically known fault zones (Figure 1-5).

Both models in the TRUE Block Scale and the FCC III projects exhibit certain structures that connect between smaller and less conductive structures and much larger and highly conductive deterministic fault zones. These structures correspond to the boundary structure in the TRUE Block Scale and the smaller HPF in the FCC III project, and are termed as "connecting structure" in this study. The smaller and less conductive outcrop to block scale structures are termed as "minor structures". Details of these definitions are described later.

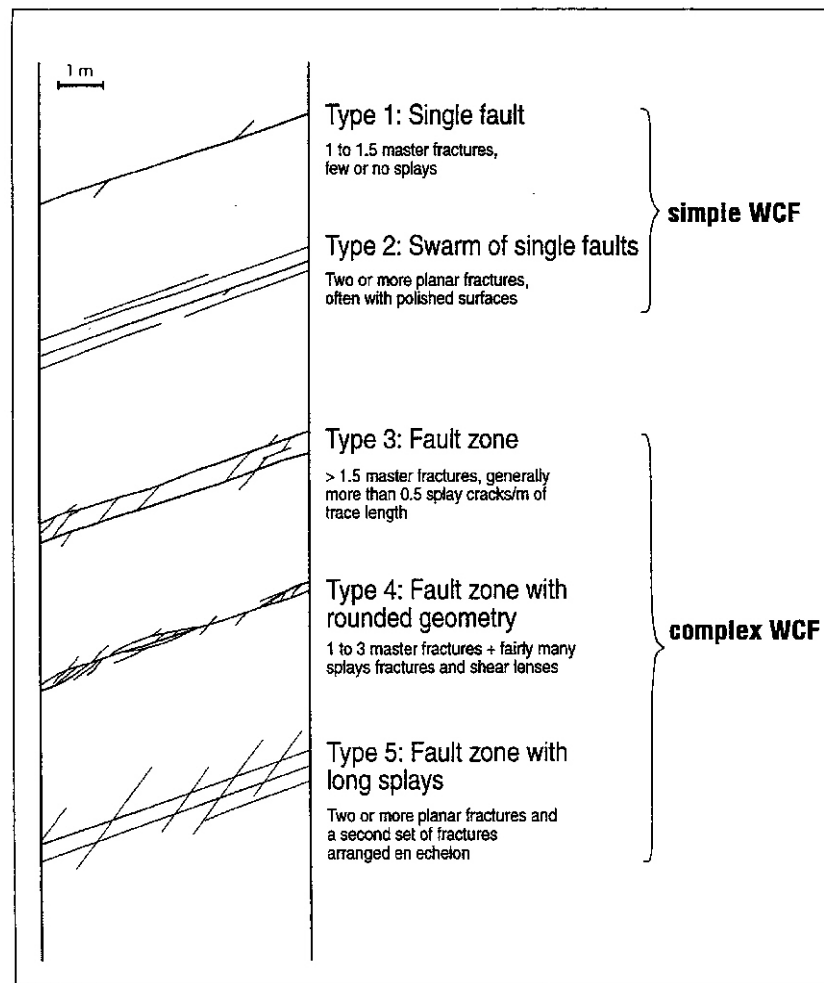


Figure 1-4: Classification of water-conducting features in the FCC-project (after Mazurek, et al., 1996).

1.1.4 Task 6

Task 6 is the sixth task of the Äspö Task Force on Modelling of Groundwater Flow and Transport of Solutes. The Task 6 seeks to provide a bridge between site characterisation and performance assessment. One of the specified tasks, the Task 6C aims at development of a 50 – 100 m synthetic structural model using data from the Prototype Repository, TRUE Block Scale, TRUE-1 and FCC projects (Morosini, 2001). Geological and structural information and concepts of block scale fracture network are required in this specific task. Therefore issues in the TRUE Block scale project are relevant for the Task 6C.

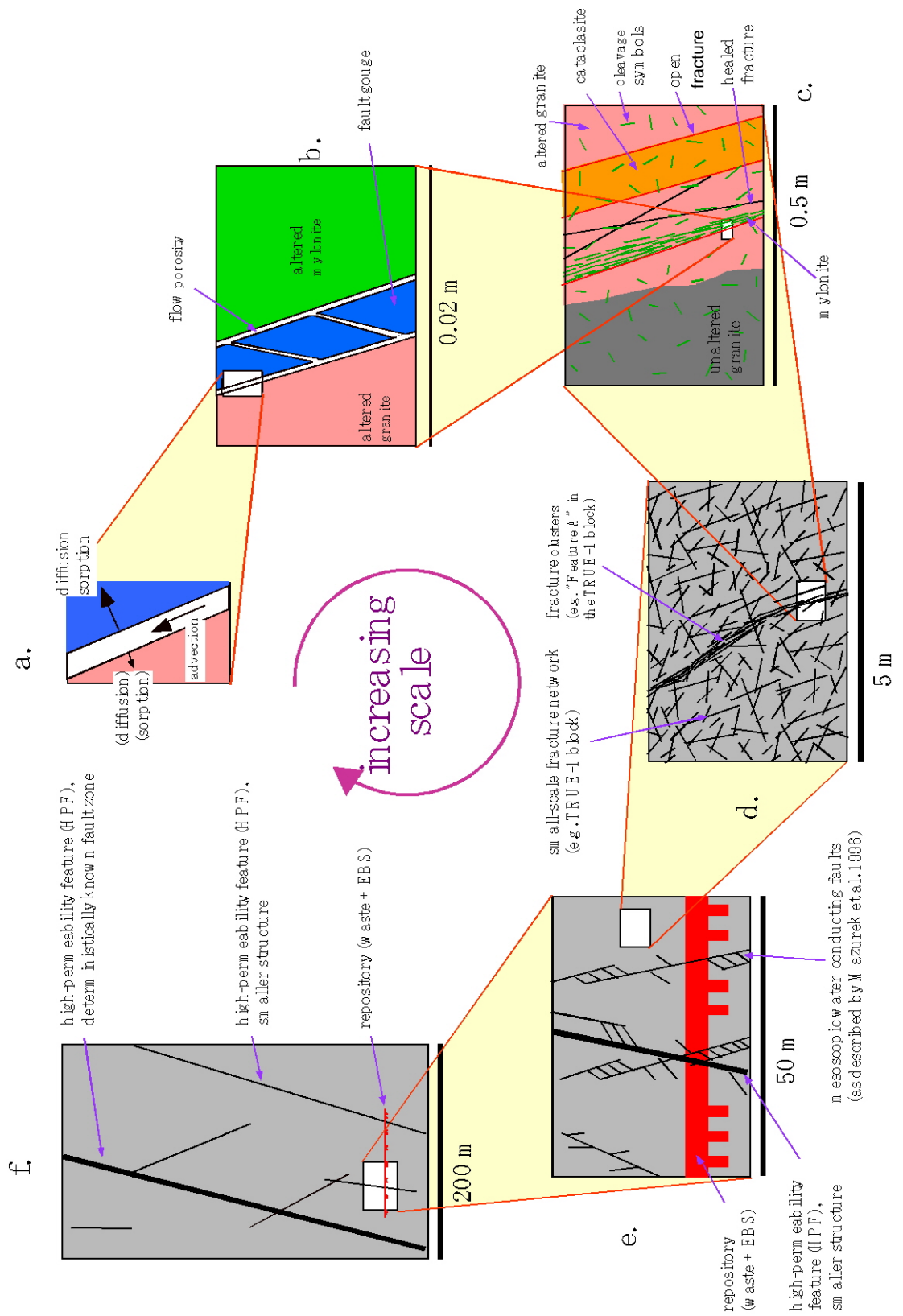


Figure 1-5: Conceptual models with increasing scales in the FCC-III project (after Bossart, et al., 2001).

1.2 Objectives

Based on the above background, the following objectives are established,

- to characterise the connecting and minor water-conducting structures in the tunnel in terms of geometry, deformation, mineralogy, heterogeneity, structural connectivity and fracture intersection,
- to increase understanding of micro scale structures relevant to flow/transport within water-conducting structures in block scale, and
- to correlate the mapped target structures in the tunnel with those on the drill core to assess consistency of characteristics.

The target structures for this study and their structural settings are schematically displayed on Figure 1-6. Results of the study are expected to provide basis for the understanding and conceptual modelling of a fracture network in block scale, particularly for the TRUE Block Scale and the Task 6C.

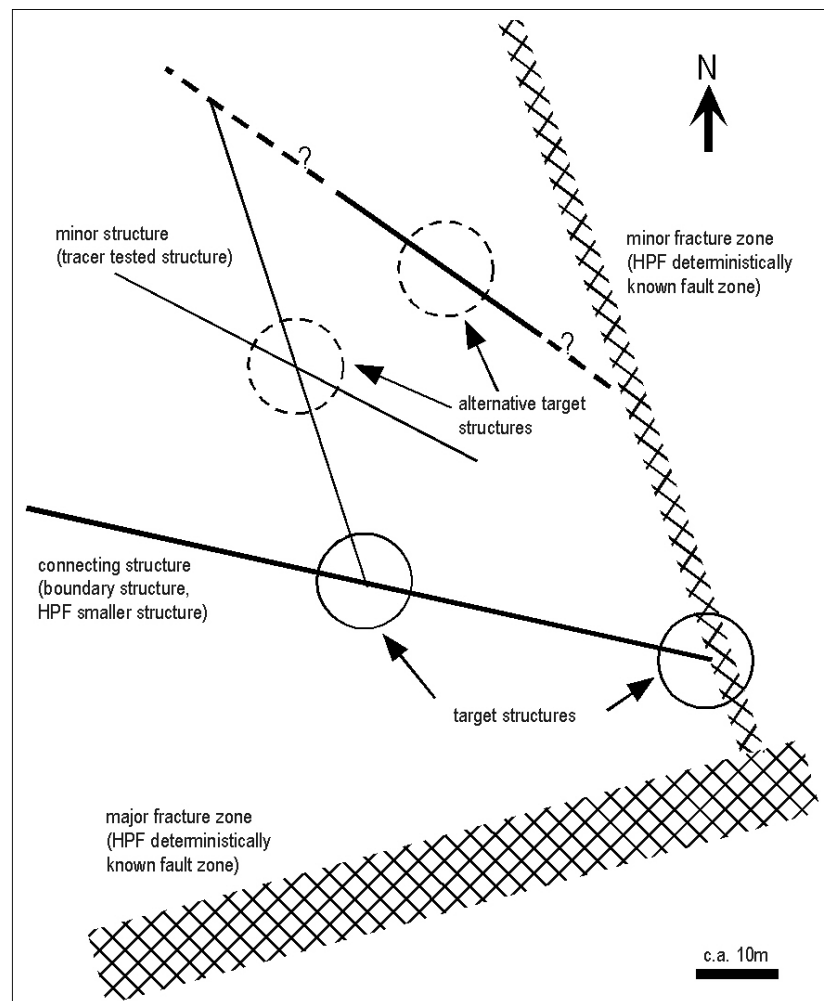


Figure 1-6: Schematic illustration of the target structures. Alternative target structures after the target selection are also presented (see the following chapter).

1. 3 Terminology and definitions

Scales used in this report are based on the following definitions.

- block scale: 10 to 100 m in definition by SKB (for example, Rhén, et al., 1997).
- outcrop scale: Metres to tens of metres in Mazurek, et al. (1996).
- small scale: 1 mm to 1 m in Mazurek, et al. (1996).
- micro scale: Less than 0.1 m in Mazurek, et al. (1996).

The following terms are based on the definitions by Munier (1995), Hermanson (1995) and Mazurek, et al. (1996).

- fracture:* *A general term for any discontinuity or break in rock irrespective of displacement. The term covers fault and joint.*
- fault: A fracture or zone of fractures where slip has displaced the walls along the discontinuity.
- joint: A fracture where no displacement has occurred between the opposing surfaces.

Hydrogeologically important structures are described below.

- water-conducting structure: Used in this report only for the relevance with the "structure" in the TRUE Block Scale. It is equivalent to the terms as water-conducting features, hydraulic conductors, water-bearing fractures, and so on, in the other reports.
- HPF: The High Permeability Features defined by Rhén and Forsmark (2000) for a feature where flow-rate ≥ 100 l/min or transmissivity $\geq 10^{-5}$ m²/s is recorded in the surface or tunnel boreholes.

Structures of interest in this study are defined in detail as below.

- connecting structure: In structural and hydraulic connection with smaller and less conductive structures, and much larger and highly conductive deterministic fault zones. Corresponding to the boundary structure in the TRUE Block Scale and to the smaller HPF. NW trending, in more detail WNW to NNW trending, striking ca. 280 to 350 degrees or 100 to 170 degrees, vertical to steeply-dipping as dominant water-conducting structures in Munier (1995), Hermanson (1995), Mazurek et.al. (1996), Rhén and Forsmark (2000), and Hermanson and Doe (2000). Trace length longer than 10 m as structures in the TRUE Block Scale, and width less than 5 m to exclude the major fracture zone in SKB definition. All types of geometry in Mazurek, et al. (1996) are considered. As a reference, transmissivity in the probe holes is in orders of 10^{-6} to 10^{-5} m²/s as in the TRUE Block Scale.
- minor structure: In structural and hydraulic connection with the connecting structure, corresponding to the tested structure in the TRUE Block Scale. The other aspects are same as the connecting structure except its smaller extent of trace length and width, and the lower transmissivity in orders of 10^{-8} to 10^{-7} m²/s.

1. 4 Outline of investigations

Outline of investigations in this study are described.

Target selection:

Target structures and study sites for this study are selected by surveying existing data and reconnaissance tunnel mapping.

Detailed tunnel mapping:

The selected target structures and study sites are characterized in detail by mapping and description.

Microscopic and mineralogical investigations:

Samples are taken from the studied structures and characterised in terms of micro scale structure and mineralogy.

Core mapping:

Extension of the studied water-conducting structure are identified on the drill core nearby the tunnel and characterised by mapping and description.

2 Target selection

2.1 Objectives

Objectives of the target selection are:

- to identify the structures that match with the overall objectives of this study, and set areas for the detailed mapping,
- to understand general characteristics of water-conducting structures in the tunnel for reasonable target selection.

2.2 Area for the target selection

Area for the target selection was set from 1500 m to 3600 m in the main tunnel, from the beginning of the spiral to the end of the tunnel. Additionally all the connected experimental drifts and niches were included by the following reasons:

- Many NW trending water-conducting structures have been mapped and reported.
- A water-conducting structure may crosscut the tunnel at plural points, and it makes easier to understand its spatial distribution.
- Experimental sites are concentrated and many boreholes have been drilled.

2.3 Methods

Existing data survey

Locations of water-conducting structures in Mazurek, et al. (1996), Hermansson (1995) and Rhèn and Forsmark (2000) were surveyed. Since there were not exact location maps for those structures, locations were correlated with the water-bearing structures on the comprehensive tunnel description map in Markström and Erlström (1996) (Figure 2-2 and 2-3 for example). Existence and available information of boreholes nearby the structures were also surveyed on the map of Hermansson (1995) and tables in Stanfors, et al. (1997).

Reconnaissance tunnel mapping

The above water-conducting structures as well as structures reported in the SELECT, ZEDEX and TRUE Block Scale projects were visited in the tunnel to check locations, conditions and characteristics, also to re-evaluate previous works. Checked and observed items are location, host rock, orientation of structure, lineation on fracture plane, structure type in Mazurek (1996), intensity of associated mylonite, kind of fault rock, fracture coating/filling minerals, wet % (percentage of wet area on the fracture trace in the tunnel), type and description of water discharge, existence of grout and shotcrete, outcrop condition and other remarks. Results of existing data survey and

reconnaissance mapping were stored in a table. If the target structures are identified in this stage, they are to be investigated in the detailed mapping. If not, alternative target structures are selected on the following procedure.

Alternative target selection

Structures in the table were evaluated in three steps, and target structures and study sites were selected.

1) 1st selection

The structures are evaluated in the following criteria:

- a: Any of occurrence is observed;
 - intersection of water-conducting structures,
 - possible connection with deterministic water-conducting fault zone,
 - considerable water discharge to observe its distribution,
 - grouted structures to see the flow path (transmissivity more than $1.0 \text{ E-}6 \text{ m}^2/\text{s}$ in probe holes)
- b: Any special disadvantage or advantage to be ranked in "a " or "c ".
- c: Any of occurrence is observed;
 - dominantly hosted in Fine-grained granite or green stone (not extensive in Äspö, distinct characteristics),
 - poor exposure condition,
 - not NW trending,
 - trace length less than 7 m,
 - no indication of water discharge.
- d: Any of occurrence is observed;
 - not exist or identified,
 - completely covered with shotcrete,
 - more than two items in "c" are observed.

2) 2nd selection

The structures ranked as "a" in the 1st selection were further ranked based on the numbers of prioritised criteria.

higher priority:

- intersection of water-conducting structure
- trace length more than 10 m

lower priority:

- cored borehole near by the tunnel
- representative water-conducting structures stated in the FCC study

A: two in the higher priority plus one or two in the lower priority are applied

B: three in both priorities are applied

C: one in the higher priority, or, one or two in the lower priority are applied

3) Final selection

The target structures were finally selected from the rank "A" structures mostly based on practicality and time constraints. Then certain ranges of intervals covering the selected structures were set as study sites.

2.4 Results

126 water-conducting structures were picked up from previous reports and maps.

In the reconnaissance mapping, existence of the connecting structure was not confirmed, i.e. no clear evidence of the connection to the minor structures or to the deterministic water-conducting fault zone was identified. Therefore, alternative target structures as intersecting minor structures and "potential" connecting structures (Figure 1-6) were selected according to the procedure. In total, 149 structures are listed in Appendix 1 for the alternative target selection including the newly found 23 structures.

In the 1st selection, 20 structures were ranked "a", 42 were "b", 55 were "c" and 32 were "d". In the 2nd selection, 6 structures were ranked "A", 8 were "B" and 6 were "C". In the final selection, 6 target structures in 3 sites are selected (Appendix 1).

Site 1: tunnel 1544 to 1576 m (Figure 2-1 and 2-2)

Structures: 1555 m, 1558 m, 1570 m (hereafter, structures are called by the location where the structure cross the centre line of the tunnel)

Structures 1555 m and 1558 m cross at the tunnel ceiling. Structure 1570 m may be terminated or cut by 1555 m at B¹ wall (right hand side toward tunnel depth direction). The most discharging structure, at 1558 m, has a transmissivity value of $1.8 \cdot 10^{-8} \text{ m}^2/\text{s}$. Therefore, all the structure in Site 1 are regarded as the minor structures. Unfortunately, no borehole exists near Site 1.

Site 2: tunnel 2150 to 2170 m and niche 2156B (Figure 2-1 and 2-3)

Structure: 2163 m (and 2154 m)

Structure 2163 m is a highly discharging structure extending to niche 2156B. Simple linear extension of this structure to the southeast intersects the water-conducting minor fracture zone NNW-4 about 10 m from the tunnel. Its transmissivity values range in the order of 10^{-7} to $10^{-5} \text{ m}^2/\text{s}$ in different probe-holes. Structure 2154 m was ranked as "B" because of its trace length in the tunnel is less than 10 m, but considered as a potential target because its vicinity with the NNW-4, high transmissivity possibility to be a grouted HPF, also "typical type 1, simple water-conducting feature"² in the FCC project together with the 2163 m. The extension of these structures is expected to intersect the borehole KA2048B running parallel to the tunnel.

Site 3: 2194 to 2202 m and niche 2198A (Figure 2-1 and 2-3)

Structure: 2198 m

This structure may be considered as the connecting structure. It is a grouted HPF with transmissivity $3.4 \cdot 10^{-5} \text{ m}^2/\text{s}$ in probe holes. It is possible to assume that this structure connects with the NNW-4 to the southeast. Extension at the niche 2198A is highly discharging while B wall of tunnel is only wet due to grouting. This structure is reported as "typical type 3, complex water-conducting feature" in the FCC project. The extension of this structure is also expected to intersect the borehole KA2048B.

¹ In the tunnel, the letter "A" accounts for the left hand side toward tunnel depth and the "B" does the opposite. It is put at the end of the name of boreholes and niches to indicate their relative positions.

² The types 1 and 3 occupy 77% of all the FCC features.

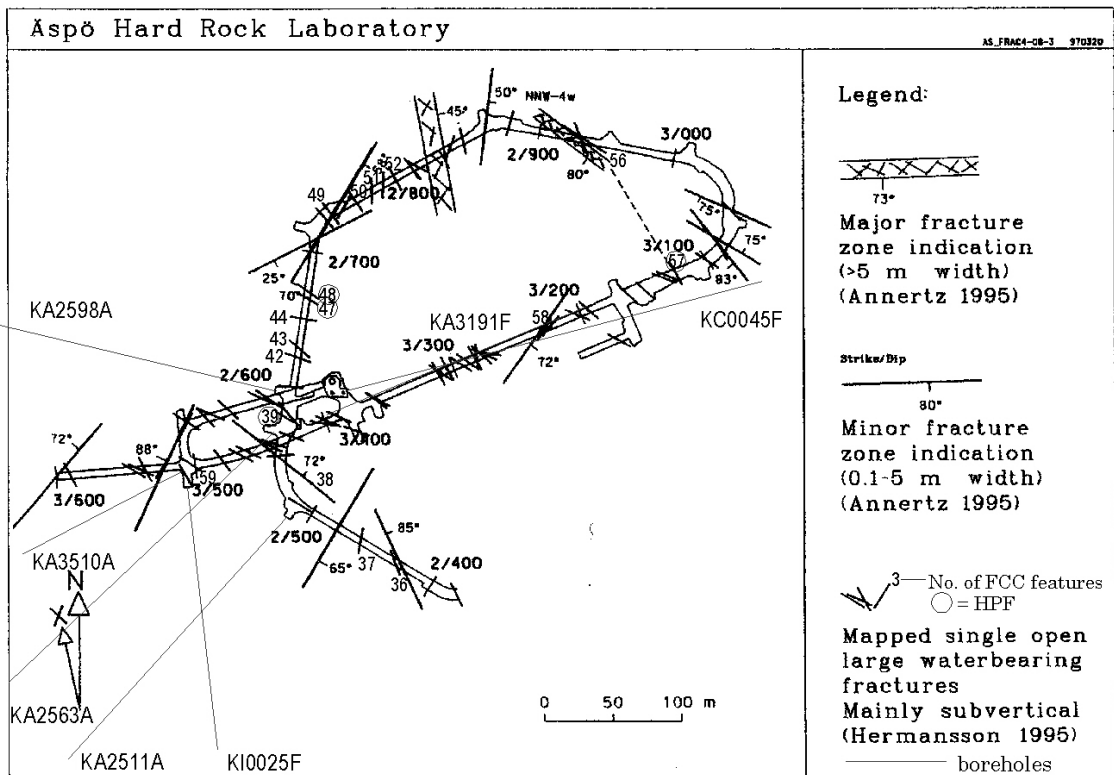
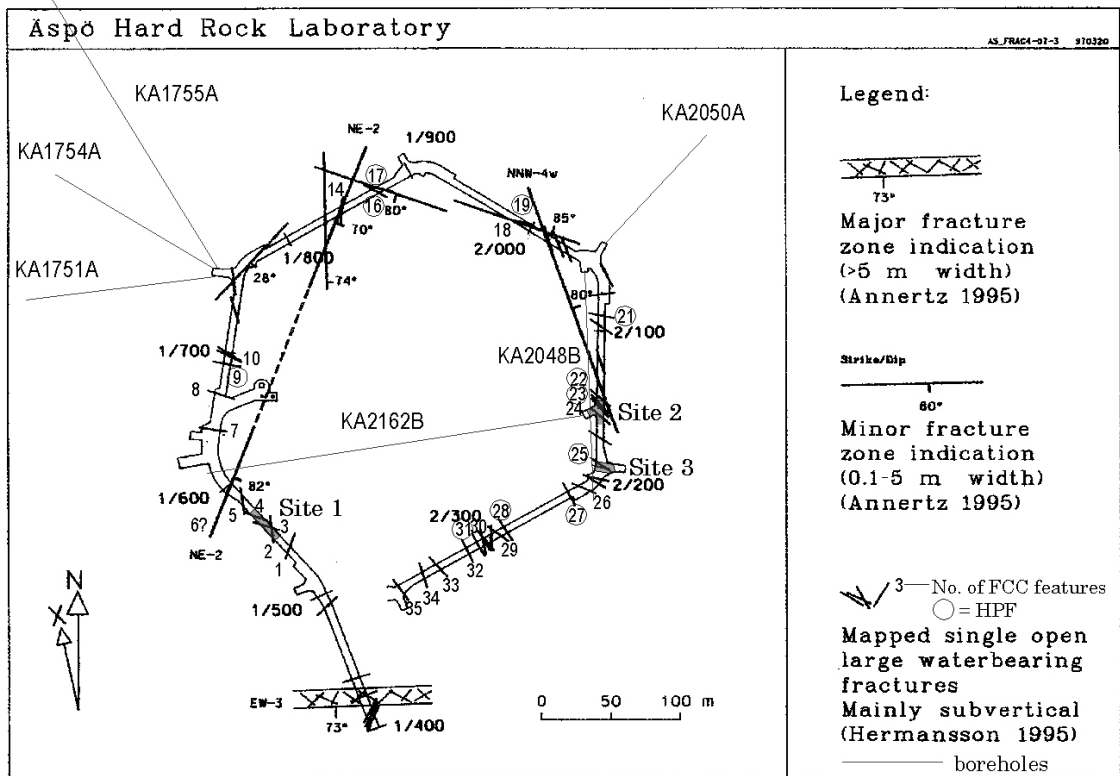


Figure 2-1: Locations of waterbearing fractures, FCC features, HPF, boreholes and the selected study sites (base map modified from Rhén, et al., 1997).

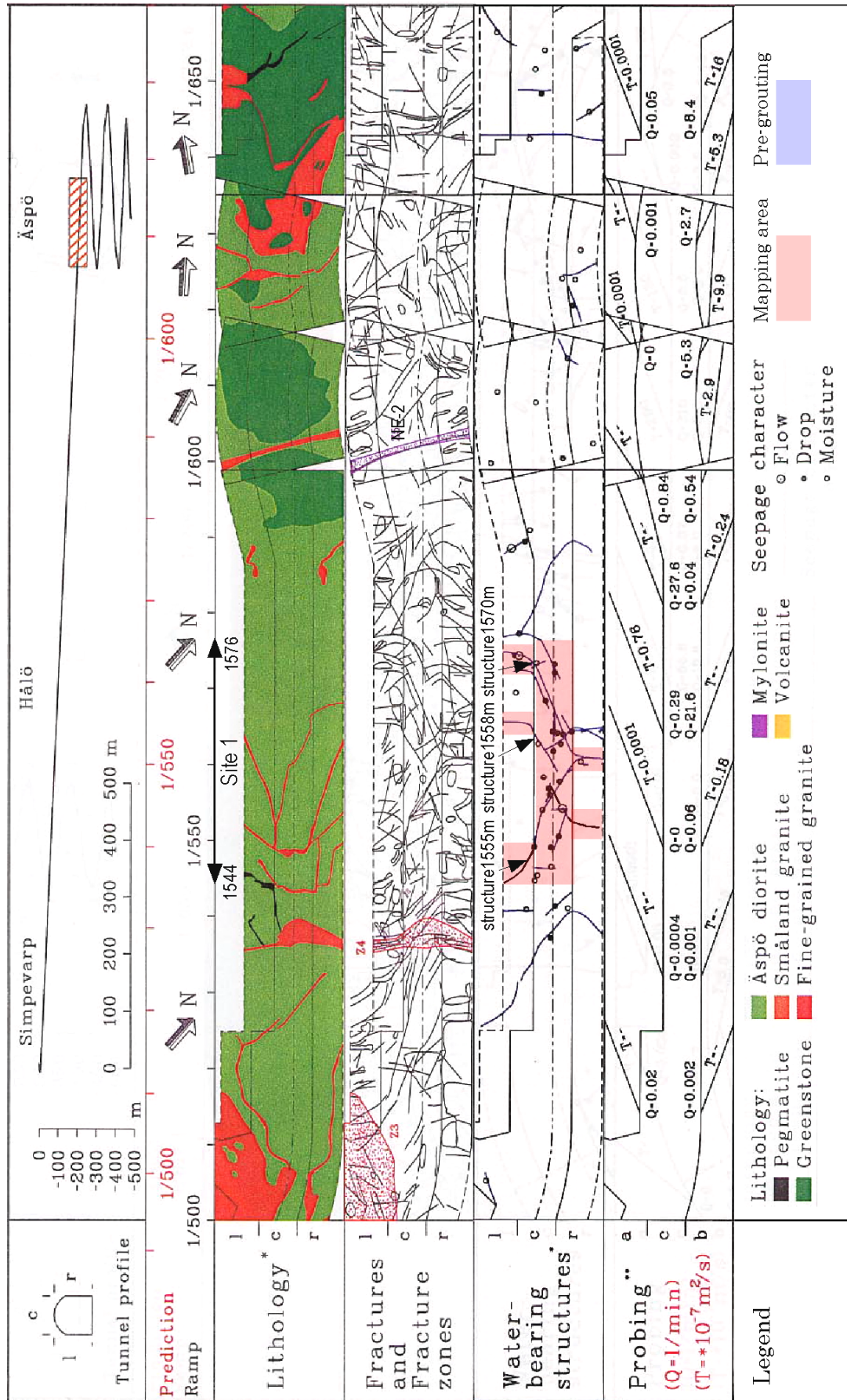


Figure 2-2: Location of Site 1 and target structures (modified from Markström and Erlström, 1996).

3 Detailed tunnel mapping

3.1 Objectives

Objectives of the detailed tunnel mapping apply to the first objective of this study:

- to characterise the connecting and minor water-conducting structures in the tunnel in terms of geometry, deformation, mineralogy, heterogeneity, structural connectivity and fracture intersection.

The specific objective for each site is, Site 1:

- to characterise the minor structures and their intersection zone,

Site 2:

- to characterise the minor or potential connecting structures, and typical simple structures,

Site 3:

- to characterise the potential connecting structure, and typical complex structure.

3.2 Methods

Preparation:

- Sidewalls of tunnel and niches were cleaned by a high pressure hot water sprayer. Tunnel ceiling was not cleaned because it looked less dirty before preparation.
- Two 1000 W halogen lamps with tripods were prepared to light up the site.
- 1 m grids were set on the floors and on sidewalls of tunnel and niches. Grids on the floors were set to make projection maps of the ceiling. Based on the centre line in the coordinate system of Äspö HRL, precise location of each grid point was surveyed by total station, and dotted by a spray marker. Grids on sidewalls were set perpendicular to the floors in the same manor. A wheel loader with a cage was employed for the work at higher positions.

Mapping:

Accurate maps are essential to understand geometry of structures. All maps were drawn in scale 1/50 on grid papers. Mapping for the tunnel ceiling was performed by projecting the features onto the floor. For sidewalls, if a target structure intersects in an oblique angle, the structure and a few metres to both sides was mapped toward the wall. In case of an acute angle, the structure and features in a few metres to both sides were projected onto an imaginary plane perpendicular to the structure. Error in location on the ceiling map and wall map in the oblique case is about 25 cm for both sides, and larger in the acute case.

The following features were mapped to characterise both the study sites and target structures:

lithology: lithological boundaries, altered zones, foliation,

structure: faults and other fractures with trace lengths more than 0.5 m, and the associated mylonite, cataclasite, fault breccia and crush.

hydrology: wet area, discrete points of flow, drop and moist on fracture trace.

reference number for the description.

Description:

Fractures with trace length more than 1 m were described on the format in Appendix 3. The following items were described (see legend of Appendix 3 for the definitions); host rock, relation to the host rock, intensity and width of mylonite, type and width of fault rocks (cataclasite, breccia, crush and gouge), strike and dip of fracture, trend and plunge of linear structure on surface, trace length in tunnel and niche, aperture (including coating/filling), roughness of surface, coating/filling material and thickness, percentage of coated/filled fracture area, type and width of alteration along fracture, wet % (percentage of wet area on the fracture trace in the tunnel), type and description of water discharge, and other remarks. If a structure on ceiling extends to sidewalls, the more accurate information from sidewalls is included in the description.

Photograph:

Important observations are photographed with aid of halogen lamps. It was impossible to photograph whole area of mapping due to lack of light.

3.3 Results

Maps and descriptions are presented in Appendix 2 (Maps 1 to 6) and Appendix 3. Description and interpretation for each site and structure are presented below.

3.3.1 Site 1

Site: tunnel 1544 to 1576 m

Structures: 1555 m, 1558m, 1570 m

Site and mapping area:

The tunnel orients 320 degrees and dips 8 degrees continuously. Three thick pipes run along B wall causing obstacles for observation. Mapping was performed for ceiling from 1544 to 1574 m. For sidewalls, only near the target structures were mapped because they intersect with the sidewalls in acute angles. No borehole except probe holes has been drilled near the site.

Characterisation of site:

Lithology

Äspö diorite occupies most area of the site. In this site, it is relatively rich in quartz and heterogeneous in place that it locally contains oriented lenses of mafic enclaves striking NE and dipping moderately to NW. No foliation or ductile deformation is observed. A few Fine-granite dikes in different generations crosscut the diorite. Some fractures follow margins of the dikes while some fractures are stepped, branched and dispersed when they cross the dikes. Rock types of the dikes vary from pegmatite to leuco-granite, and to aplite.

Structure

There are three dominant orientations in 79 structures on the ceiling, the two sub-vertical NW sets including target structures, and the steep NNE set (Figure 3-1). On sidewalls, the two NW sets are significant for faults, and the other fractures are rather scattered.

Average and mode trace length of all structures on the ceiling are 3.7 m and 2 m respectively (Figure 3-2).

Striations are observed in 8 fault planes on sidewalls, of which 6 are from target structures (Figure 3-3). All of them plunge subhorizontal suggesting strike slip displacement. Slip senses were estimated from steps on coatings as chlorite, epidote and asymmetric growth of calcite on 6 planes. Three NNW faults show sinistral sense and other three WNW faults do dextral, implying a conjugate arrangement. Minor dextral displacement of Fine-grained granite dike was also observed in one of the target structure.

Minerology

Major constituent minerals of filling/coating of faults and fractures on sidewalls are chlorite, calcite, epidote and clay minerals. There are seven assemblages of these minerals including the "no mineral" (Table 3-1). Assemblages of the target structures contain more than three minerals while those of the other fractures are simple, and those of the other faults are in between. This implies the abundant hydrothermal events in the target structures compared to the other faults and fractures. A clear tendency is not found in the orientation of filling/coating mineral assemblages on the stereo plot (Figure 3-4).

Hydrogeology

Majority of rock surface in the site is moist to wet while northwest area is relatively dry. Flowing of groundwater occurs only one spot on fracture plane at 1554 m. Drop and wet spots occur on fracture plane and often at intersection with other structures and branched part.

Structures on the ceiling are divided tentatively into wet structures where the wet % (percentage of total length of wet area on fracture against its whole trace) are more than 50, and dry structures where the wet % are less than 50. The NNE trending steep structures, in addition to the WNW sets, are emphasised in the dry structures compared to the wet ones on the stereo plot (Figure 3-5).

Characterisation of target structures:

Structure 1555 m (ceiling: No. 14, sidewall 1545A: No.1, 3, 6, and sidewall 1561B: No. 1)

Host rock

The structure is in most part hosted by Äspö diorite, it locally cuts Fine-grained granite dikes at the A (left) wall.

Geometry

The structure is very simple in geometry and comprises only of a single fault plane except the sidewall at 1545A where there are other two parallel faults. Minor steps of fault plane occur on the ceiling. There are sets of parallel steep fractures with no or minor filling/coating minerals, extending oblique to the fault. Given the strike slip displacement of the fault suggested by sub-horizontal striations, such structures are tentatively interpreted as splay cracks without any confirmation. There are 7 possible splay cracks, five imply dextral and two imply sinistral displacement along the fault. This structure is interpreted as the "type 1" structure according to the classification scheme in the FCC study (Mazurek, et al., 1996). The structure is trending NNW, strikes 334 and dips 78 degrees in average. Trace length in the tunnel is 19 m.

Ductile and brittle structure

No mylonite is observed along the fault on sidewalls, and probably not on the ceiling. Cataclasite where a fault breccia had been healed by later epidote alteration is ambiguously observed along fault plane on sidewall to ceiling at 1561B with maximum thickness of 3 cm (Photo 2). Fault crush or breccia partly occurs at intersection with other fractures, stepped part and near Fine-grained granite dike with maximum thickness of 20 cm. Fault gouge comprises clay minerals and ground pre-existing filling minerals, and exist all over the fault plane on sidewalls with maximum thickness of 2 mm. Striations displayed by stretched growth of chlorite and asymmetric growth of calcite on groove are observed on fault plane. Steps on such striations are considered as accretion steps, and senses of slip can be estimated (Photos 1 and 2). Most of them display sub-horizontal sinistral sense except a dextral sense in a minor converging fault. However, a possible reverse fault component is also suggested by the displaced Fine-grained granite dike on sidewall at 1561B.

Mineralogy and alteration

Epidote, chlorite, calcite and clay (gouge) fill the aperture of 0.5 to 2 mm thick, from rim to centre in this order (Photo 1). Epidote is sometimes missing and often postdates chlorite. Oxidation (redening) of feldspar occurs along fault with 3 cm thick, and local epidote alteration is ambiguously observed on sidewall at 1545A. White (clay?) alteration is observed at crushed part on the ceiling.

Hydrogeology

Types of water discharge from the structure are heterogeneously distributed. Drop and moist spots occur on fracture plane and intersection with other fracture. Drop spot is relatively increased near intersection with the structure 1558 m.

Structure 1558 m (ceiling: No. 23, 24, 40, sidewall 1553B: No. 1, 2, 3, sidewall 1566A: No.1)

Host rock

The structure is in most part hosted by Äspö diorite, it cuts Fine-grained granite dikes at the B (right side) wall.

Geometry

The structure is in between simple and complex in geometry. It comprises several discontinuous fault planes and their overlapped or paralleled parts are small relative to the total length. There are two major clockwise steps of fault planes. Fault planes are branched, paralleled and discontinued near and on sidewalls. There are several possible splay cracks, all imply dextral displacement along the fault. This structure is interpreted as rather belong to the "type 3" structure. The structure is trending WNW, strikes 113 and dips 84 degrees in average. Trace length in the tunnel is 9 m.

Ductile and brittle structure

No mylonite is observed along the faults on sidewalls, and probably not on the ceiling. Possible cataclasites are observed partly along the fault planes, in some place deviating 5 cm from the plane, on sidewalls and ceiling with maximum thickness of 3 cm (Photo 3). Fault crush or breccia locally occurs at stepped parts and along fault plane with maximum thickness of 30 cm. The fractured/crushed part near the centre of the ceiling at 1560 m may have been caused by blasting because a blast hole exists on the part (X on Map 1). Fault gouge exists in most part of fault planes on the sidewalls with maximum thickness of 1 mm. Striations displayed by stretched growth of chlorite and epidote, and asymmetric growth of calcite on groove are observed. Steps and asymmetric growths of minerals display sub-horizontal dextral displacement dipping to SE in most planes (Photo 4). It is noted that a weak sub-horizontal NW dipping striation with no indication of sense coexist with the SE dipping striation on a plane at 1566A.

Mineralogy and alteration

Filling/coating minerals differ significantly within each fault on sidewalls. Common minerals are epidote, chlorite, calcite and clay (gouge) with minor sulphide, from rim to centre in this order, filling the aperture of 0.5 to 2 mm thick (Photo 3). Epidote is sometimes missing and often postdates chlorite. Two successive types are recognised in calcite, the older grey layers and the younger local white patches. Moderate to weak oxidation (red alteration) of feldspars occur along fault on the sidewalls in irregular shape and width ranging from 5 to 50 cm.

Hydrogeology

Types of water discharge from the structure are heterogeneously distributed. Drop and moist spots occur on fracture plane and intersection with other fracture. Increase of drop spots near intersection is not distinct on the fault plane, but rather at nearby minor fractures excluding the possible blasting damage zone. Only a single flowing spot occurs on a fracture sub-parallel to the fault on the ceiling at 1554 m.

Structure 1570 m (ceiling: No. 50, sidewall 1573A: No. 1, 2)

Host rock

The structure is in most part hosted by Äspö diorite. Only a small portion of a Fine-grained granite dike is cut by this structure.

Geometry

The structure is in many parts complex and some simple in geometry. It comprises basically two parallel faults merging at ESE side on the ceiling. It terminates at ESE side on the ceiling and does not intersect the structure 1555 m as expected. Many minor steps and branching occur on the ceiling and sidewall. There are several possible converging and diverging splay cracks on the ceiling but interpretation of displacement sense is difficult due to their angles nearly perpendicular to the fault planes. This structure is interpreted as rather belong to the "type 3" structure. The structure is WNW trending, strikes 110 and dips 86 degrees in average. Trace length in the tunnel is 12 m.

Ductile and brittle structure

No mylonite or cataclasite is observed along the faults on sidewalls, and probably not on the ceiling. Fault crush or breccia locally occurs with maximum thickness of 40 cm at merged and minor stepped parts, and intersection with other fracture. Minor dextral displacement less than 1 cm of Fine-grained granite dike is observed on the ceiling at 1565 m. Fault gouge only locally exists in one of the major fault planes on the sidewall with small amount and thickness less than 0.5 mm. No striation is visible on smooth to rough fault planes.

Mineralogy and alteration

Filling/coating minerals differ significantly within each fault on sidewalls. Calcite is the only common mineral, and epidote, chlorite and clay (gouge) locally exist in any of faults on the sidewall, filling the aperture up to 2 mm thick. Alteration of wall rock along the structure is not obvious due to bad exposure.

Hydrogeology

Types of water discharge from the structure are heterogeneously distributed. The simple ESE side of the structure is relatively dry. Drop spots occur more at the stepped and paralleled part, and intersection with the possible splay cracks.

3.3.2 Site 2

Site: tunnel 2150 to 2170 m and niche 2156B

Structure: 2154 m , 2163 m

Site and mapping area:

The tunnel orients 192 degrees and dips 8 degrees continuously. The niche is horizontal. Mapping was performed for ceiling from 2152 to 2169 m of the tunnel and 0 to 6 m of the niche. Regarding sidewalls, because of the acute intersection angles of the target structures, and also of time constraints, only near intersections at 2151B in the tunnel and B-side of the niche were mapped. Borehole KA2048B runs sub-parallel to the tunnel and under the niche. Pre-grouting was performed from 2142 to 2151 m.

Characterisation of site:

Lithology

Äspö diorite dominates in the site. A distinctive E-W striking subvertical dike of foliated granite truncates the tunnel and extends to the niche. The foliation is probably a primary structure of the dike and not tectonic in origin judging from its texture. The southern margin grades into the Fine-grained granite. The mineral composition varies from granite as Småland granite to pegmatite. The grain size varies from fine to coarse grained. No other foliation or ductile deformation is observed in the site. A few Fine-grained granite dikes crosscut the diorite. Rock types of the Fine-grained granite vary from pegmatite to aplite.

Structure

There are two dominant orientations in 68 structures on the ceiling, sub-vertical NW and steep ENE (Figure 3-1). Faults and fractures form interconnected network on the ceiling. Number of faults including minor ones is much larger than the other sites. On sidewalls, the sub-vertical NW set is more predominant in faults than in the other fractures.

Average and mode trace length of all structures on the ceiling are 3.3 m and 2 m respectively (Figure 3-2).

Striations on fault plane were observed in 5 fault planes on sidewalls, of which 2 are from target structures (Figure 3-3). All of them plunge sub-horizontal suggesting strike slip displacement. Only one ambiguous dextral sense was estimated from step on coating at 2168A. There are 8 faults displacing the Fine-grained dikes. 7 faults including two of the structure 2163 m indicate dextral and one indicates sinistral displacements.

Minerology

Major constituent minerals of filling/coating of faults and fractures on sidewalls are chlorite, calcite, epidote and clay minerals. There are seven assemblages of these minerals including the "no mineral" (Table 3-1). Assemblages of the target structures contain four minerals while those of the other fractures are simple, and those of the other faults are in between. This implies the abundant hydrothermal events in the target structures compared to the other faults and fractures. A clear tendency is not found in the orientation of filling/coating mineral assemblages on the stereo plot (Figure 3-4).

Hydrology

Majority of rock surface in the site is moist to wet while southwest area is relatively dry. However, northern part of the site may have been partly influenced by the pre-grouting. Strong outflow occurs in two spots of the structure 2163 m on sidewall at 2166A and the niche wall. Another minor flow spot occurs on the structure 2154 m at 2151B. Drop and wet spots occur on fracture plane and often at intersection with other structures and branched part.

Subvertical NW structures and subordinate steep ENE structures dominate in the wet structure on the stereo plot while structures are rather scattered in the dry structure (Figure 3-5).

Characterisation of target structures:

Structure 2154 m (ceiling: No. 1, 18, sidewall: No. 1)

Host rock

The structure is entirely hosted by Äspö diorite.

Geometry

The structure is in between simple and complex in geometry with a few smaller parallel faults. The master fault branches and curves at the largest crush zone on the ceiling. The master fault and smaller faults are connected through other perpendicular faults and fractures. There are some diverging fractures, but it is not obvious whether they are splay cracks. This structure is interpreted as a complex variety within the "type 1" structure according to the classification scheme in the FCC study. The structure is trending NW, strikes 142 and dips 87 degrees in average. Trace length in the tunnel is 9 m.

Ductile and brittle structure

No mylonite is observed along the fault on sidewalls, and probably not on the ceiling. Possible cataclasite, a 3 cm thickness of strong epidote alteration zone with grain size reduction is observed along fault plane on sidewall at 2151B. Fault crush or breccia is very common along the master fault with maximum thickness of 40 cm. Fault gouge exists all over the fault plane on sidewalls with maximum thickness of 2 mm (Photo 5). No striation or displaced dike is observed.

Mineralogy and alteration

Epidote, chlorite, calcite and clay(gouge) fill the aperture of 0.5 to 3 mm thick, from rim to centre in this order (Photo 5). Grout or calcic precipitation (remobilised grout?) is locally observed at crush/breccia on the ceiling. Oxidation (red alteration) of feldspars with 10 cm thick, and weak epidote alteration with 0.5 m thick occur along the fault on sidewall at 2151B and 2159A.

Hydrogeology

Types of water discharge from the structure are heterogeneously distributed, but those must have been disrupted to some extent by grouting in addition to the excavation damage. Drop and moist spots occur on fracture plane, crush/breccia zone and intersections with other fractures. A minor flowing spot exists on the fault plane at the intersection of a minor fracture on the sidewall at 2151B.

Structure 2163 m (ceiling: No. 40, sidewall: No. 40)

Host rock

The structure is hosted by Äspö diorite, the foliated granite and Fine-grained granite dikes. It cuts all these rocks.

Geometry

The structure is again in between simple and complex in geometry with many parallel/sub-parallel faults of various sizes. The master fault steps, branches, parallels and curves in many parts on the ceiling, especially near the foliated granite. The other

faults are relatively straight compared to the master fault. Possible splay cracks of the master fault and of the structure No. 52 imply sinistral displacement on the tunnel ceiling while those of the master faults on the niche ceiling imply dextral. This structure has some characteristics of the rounded "type 4" structure, but still is interpreted as a complex variety within the "type 1" structure. The structure is trending NW, strikes 139 and dips 83 degrees in average. Trace length in the tunnel and niche is 16 m.

Ductile and brittle structure

No mylonite is observed along the fault on sidewalls, and probably not on the ceiling. Possible cataclasite, maximum 2 cm thickness of strong epidote alteration zone with grain size reduction is observed along fault plane on sidewalls at the niche 2156B and 2166A in the tunnel (Photo 6). Fault crush or breccia is very common along the master fault with maximum thickness of 40 cm. Fault gouge exists all over the fault plane on sidewalls with maximum thickness of 2 mm. Striation shallowly plunging to NW is recognized on the master fault planes without indications of slip sense.

The master fault displaces the foliated granite 50 cm and Fine-grained granite 40 cm both in dextral sense. The other faults displace the Fine-grained granite dikes maximum 15 cm all in dextral sense except the structure No. 39 in sinistral.

Mineralogy and alteration

Filling/coating minerals differ significantly within the master fault on the two sidewalls. Epidote, chlorite, calcite, clay (gouge) and local grout fill the aperture of maximum 2 mm thick, from rim to centre in this order, along the master fault on the B wall of the niche 2156B (Photo 6). On the other sidewall at 2166A in the tunnel, only chlorite and minor amount of calcite patch exist. Weak oxidation (red alteration) of feldspars with maximum 10 cm thick is observed on both sidewalls while white-green (clay or epidote?) alteration with 40 cm thick occurs only on the sidewall at niche 2156B.

Hydrogeology

Types of water discharge from the structure are heterogeneously distributed. Influence of the grout seems to be limited to the B wall of the niche judging from its existence. Drop and moist spots occur on fracture plane, crush/breccia zone and intersections with other fractures. Strong flowing spots occur on both sidewalls. One is from the calcite coated fracture parallel and close to the master fault at the niche wall. Another is from the stepped edge of the master fault at 2166A in the tunnel.

3.3.3 Site 3

Site: tunnel 2194 to 2202 m and niche 2198A

Structure: 2198 m

Site and mapping area:

Origin of grid in this site is set at 2200 m on the centre line because the tunnel starts turning to NE. The longer axis is on the line of 2200 m where the lines radiate from inside to outside at the turning. The shorter axis deviates 10 degrees to the east from the north. The tunnel and niche is almost horizontal. Mapping was performed on ceiling

from 2194 to 2202 m of the tunnel and 13 m between the tunnel wall and niche wall. The mapped niche wall was formed by blasting to extend the entrance. It strikes 58 degrees to the east and vertical. Those sidewalls were also mapped within a few metres from the target structure. Borehole KA2048B runs beyond and under the sidewall 2198B.

Characterisation of site:

Lithology

Åspö diorite dominates in the site. A few Fine-grained granite dikes crosscut the diorite. Rock types of the Fine-grained granite vary from pegmatite to aplite. Half of the niche wall is occupied by a large lens of green stone about 1m thick with rim of Fine-grained granite 1 to 5 cm thick, striking 140 and dipping 85 degrees, oblique to the niche wall.

Structure

Two master faults of the target structure dominate the structures on the ceiling (Figure 3-1). On the stereo plot, there are two dominant orientations in 32 structures on the ceiling, subvertical NW and steep NE. Connection between these structures through other faults/fractures is limited compared to the other sites. The NW set is common in both faults and fractures while the NE set is dominant in fractures. On sidewalls, a sub-horizontal set of fractures is obvious in addition to the NW set.

Average and mode trace length of all structures on the ceiling are 2.9 m and 1 m respectively (Figure 3-2). It is noted that shape of histogram is different from those of the other sites.

Weak NW shallowly dipping striation without any indication of slip sense is observed only in a fault plane of the target structure (Figure 3-3). Four faults of the target structure displace Fine-grained dike and veins maximum 3 m all in dextral sense.

Minerology

Major constituent minerals of filling/coating of faults and fractures on sidewalls are chlorite, calcite, epidote, quartz and clay minerals. There are nine assemblages of these minerals including the "no mineral" (Table 3-1). Assemblages of the target structures contain four minerals while those of the other fractures are simple, and those of the other faults are in between. This implies the abundant hydrothermal events in the target structures compared to the other faults and fractures. A clear tendency is not found in the orientation of filling/coating mineral assemblages on the stereo plot (Figure 3-4).

Hydrogeology

Majority of rock surface within 1 m from the target structure in the tunnel is dry due to the successful grouting. On the other hand, fractures to the south in the tunnel and structures in the niche are not fully grouted, and are mostly wet. Several outflow spots exist on the niche wall, but damages of blasting cannot be wiped out considering the existence of blast holes. Further, a much stronger flow occurs at the rock bolt nearby but out of the mapping area. Therefore, the grouted section only represents the primary hydraulic condition.

Characterisation of target structure:

Structure 2198 m (ceiling and sidewalls No. 1, 25, 26, 27, 36)

Host rock

The target structure is dominantly hosted by Äspö diorite. It cuts the Fine-grained granite dike and vein on the ceiling. It cuts the green stone at the niche wall.

Geometry

The main master fault, No. 1, has complex geometry comprising many small parallel/sub-parallel faults in the tunnel, and branch out to three faults, No. 25, 26 and 27, and many parallel fractures in the niche. The main fault steps, branches, parallels and curves in small extent forming many distinct shear zones or lenses on the ceiling. The curves of the branched fault and smaller faults tend to turn to the south. The subordinate fault, No. 36, has simple geometry and merge to a branch of the master fault at the niche. This structure also turns to south at the south-eastern end. Although it is uncertain, there are two sets of possible splay cracks of the master faults implying opposite senses of displacement in each fault on the tunnel ceiling. This structure is interpreted as the "type 3" structure with some essence of the "type 4" structure. The structure is trending NW, strikes 295 and dips 81 degrees in average. Trace length in the tunnel and niche is 12 m.

Ductile and brittle structures

Mylonite is observed along the main faults on the tunnel sidewall, the niche ceiling and niche wall, but is uncertain on the tunnel ceiling. At the sidewall 2198B along the fault No. 1, mylonite with moderate relative intensity ranging is developed in 5 to 10 cm thick between weak mylonite up to 50 cm thick and undeformed Äspö diorite. This situation is common as observed in the other part of the Äspö HRL (e.g. Photo 12 and Mazurek, 1996). Shear planes and foliation are developed within the fine grained matrix in the moderate mylonite. These features are less prominent in the weak mylonite. The fault No. 1 on sidewall at 2198B has the maximum aperture of 8 mm filled with grout (Photo 8) while the other master faults have apertures 0.5 to 2 mm. On the niche ceiling, the moderate mylonite branches along the faults No. 25 and 27, and extend to the niche wall with thickness 3 cm and 5 cm respectively. The fault No. 27 on the niche wall basically follows the edge of precursors of mylonite, cataclasite and quartz-fluorite vein but locally crosscut them (Photo 9 and 11). It is noted that the mylonite along the fault No. 27 displaces the green stone in dextral sense causing complicated distribution of the diorite/green stone boundary on niche wall. Possible cataclasites with maximum 4 cm thick are locally observed along the faults No. 25 and 27 on the niche wall. Fault crush or breccia is very common along the master faults with maximum thickness of 50 cm. Fault gouge exists all over the fault plane on sidewalls with maximum thickness of 2 mm (Photo 10). Faint striation shallowly plunging to NW is recognized on the fault No. 27 without indications of slip sense.

Mineralogy and alteration

Filling/coating minerals differ within the master faults on the sidewall and niche wall. Epidote, chlorite, calcite, clay (gouge) and grout are common filling minerals/material outside to inside in this order (Photo 10). Epidote is sometimes missing or postdates chlorite. Two thin veins along the fault No. 27, a vein of fluorite with local quartz and a

later vein of epidote with local quartz, predates the chlorite, calcite and clay. Oxidation (red alteration) of feldspars is extensive on both sidewall and niche while epidote alteration is local and observed only on the sidewall at 2198B.

Hydrogeology

It was impossible to make detailed observation of the flow path indicated by the grout at sidewall 2198B because the leached and re-precipitated grout covers the surface of structure (Photo 8 and 9).

Two outflow spots occur at the master fault planes on the niche wall, but again they may have been influenced by blasting considering the vicinities of the blast holes (X on Map 6).

3.4 Summary of interpretations

Descriptions of the target structures are summarised in Table 3-2. Interpretation of results regarding the potential connecting structures, minor structures and intersection of minor structures are summarised in the following sections.

3.4.1 Potential connecting structures and minor structures

The results are interpreted in terms of geometry, mechanism and genesis, hydrology and transport of solutes.

Geometry

- It is impossible to discriminate between potential connecting structures and minor structures by the geometrical indices as the complexity and type.
- Geometry within a structure is highly heterogeneous and changes along its trace, i.e. in some parts it is simple as "type 1" or "type 2" structure and in other parts it is complex as the "type 3" or "type 4" structure. Therefore it is often difficult to determine the types of a structure.
- The structure 2198 m, with the highest potential for the connecting structure, differs from the other target structures in its longer history since the mylonite formation, the largest horizontal displacement of 3 m, and the largest maximum aperture of 8 mm filled with grout.

Mechanism and genesis

- All the target structures are faults, and most of which have reactivated pre-existing structure as cataclasite and /or mylonite.
- Plural activities of strike slip faults in different senses are suggested by the inconsistency of senses deduced from striation, arrangement of possible splay cracks and displaced dikes, and also by the two sets of possible splay cracks implying opposite senses, and further by the two sub-horizontal striations plunging to opposite trend on a fault plane.

- Slip senses of the structures in the Site 1 form a conjugate set, displayed by the sinistral NNW and dextral NW to WNW structures. Only the dextral NW sets are observed in the Site 2 and 3. If the sinistral sense is applied for the minor fracture zone NNW-4 near those sites, the condition is similar to the Site 1, and one of the study sites of SELECT project in the deeper level (Figure 3-6).
- Abundance of constituent minerals in the target structures suggests abundant hydrothermal events compared to the other faults and fractures.
- Majority of the target structures have common history that formed epidote, chlorite, calcite and clay in this order. However, the reversed order of epidote and chlorite, and plural precipitation events of calcite and quartz are observed. Detailed interpretation requires microscopic and mineralogical investigations.

Hydrogeology

- Examples of the block scale hydrological fracture network which comprise the target structures, other faults and fractures are observed in the tunnel.
- There are hydrological anisotropies in the Site 1 and 2 where the NW trending structures are more water-conductive than those of the other orientations.
- Distribution of water on the target structures are highly heterogeneous, but the drop and wet spots tend to occur more at the branched or stepped parts, also at the intersections with the other fracture.

Transport of solutes

- The fault gouge comprises clay minerals and fine fragments of the pre-existing coating minerals and/or the wall rock. All the target structures contain fault gouge. The consistency of gouge is estimated to be very high because gouge exists almost all along the target structures on the sidewalls. Retardation of radionuclide by sorption is expected in these structures.

3.4.2 Intersection of the minor structures

The following were observed at the intersection of the minor structures 1555 m and 1558 m in Site 1.

- In the structure 1555 m, there is little change in the geometry but a little increase of drop spots.
- In the structure 1558 m, the master faults split into minor water-conducting fractures, but more drop spots exist at the stepped part to the southeast. The only outflow spot lies on the fracture close to and parallel to the master fault, but 3 m away from the intersection.

It is concluded that fractures and discharge spots are increased to some amount but the increases are less than variability within the structures, therefore the significance of the FIZ is not positively suggested.

Table 3-1: Assemblages of constituent minerals of coating/filling material - sidewall observations -

Site 1

assemblage	target structure	other fault	other fracture
no mineral			2
chl			4
cal			3
chl, cal		1	5
epi, chl, cal	2	2	2
chl, cal, clay	1		
epi, chl, cal, clay	3	□	□
sum	6	3	16

Site 2

assemblage	target structure	other fault	other fracture
no mineral			1
chl		1	
cal			
chl, cal		3	2
epi, chl, cal		2	
chl, cal, clay			
epi, chl, cal, clay	2	□	□
sum	2	6	3

Site 3

assemblage	target structure	other fault	other fracture
no mineral			3
chl			8
epi, chl			2
chl, cal			6
epi, qtz		1	
epi, chl, cal	1		
epi, chl, cal, qtz			1
epi, chl, cal, clay	1	1	
epi, chl, cal, qtz, clay	1	1	□
sum	3	3	20

Table 3-2: Summary of detailed tunnel mapping observations

structure	1555m	1558m	1570m	2154m	2163m	2198m
structure type	minor	minor	minor	minor? connecting?	minor? connecting?	connecting?
No. on maps	14	23, 24, 40	50	1, 18	40	1, 25, 26, 27, 36
complexity (see Figure 1-4)	simple	simple-complex	simple-complex	simple-complex	simple-complex	complex
geometry type (see Figure 1-4)	1	3	3	1	1	3
mylonite (intensity, width cm)	no	no	no	no	no	mod, 10
cataclasite (existence, width cm)	±?, 3	±, 3	no	±, 3	+, 2	±, 4
crush/breccia (existence, width cm)	±, 20	±, 30	±, 40	+, 40	+, 40	+, 50
gouge (existence, width cm)	+, 0.2	+, 0.1	±	+, 0.2	+, 0.2	+, 0.2
orientation (strike, dip)	334, 78	113,84	110, 86	142, 87	139, 83	295,81
striation (strike, dip, sense)	335, 10, s	107, 9, d / ±275, 10, ?	no	no	±319, 15, ?	±300, 20, ?
dike displacement (sense, cm)	?	?	d, <1?	?	d, 40 - 50	d, 100-300
trace length in tunnel (m)	19	9	12	9	16	12
aperture (mm)	0.5 - 2	1 - 2	0.5 - 2	0.5 - 3	0.5 - 2	0.5 - 8
coating/filling rim to centre in order (amount, max width mm)	±epi<1, chl<1, cal <2, clay<2	±epi<0.5/ chl<1, cal<2, -py, ±clay<1	±epi<0.5, chl <0.5, cal <2, ±clay<0.5	epi<0.5, chl<1, cal<3, clay<2, ±grout<1	±epi<2, chl<0.5, ±cal<1, clay<2, -grout<0.5	±qtz/fluo<1, ±qtz/epi 1-2, ±epi<0.5 / chl<1, cal<1, ±clay<2, ±grout<8
order of T (m ² /s) in probe holes	?	(1.0E-8)	(1.0E-8)	(1.0E-5?)	1.0E-7,(1.0E-5?)	1.0E-5
water discharge type	d	d, (f)	d	±f	f	f
grout or calcic precipitation (existence)	no	no	no	±	-	+ / no
existence +: entirely along structure ±: partly along structure -: very locally along structure						<input type="checkbox"/>
sense d: dextral s: sinistral						<input type="checkbox"/>
amount no symbol: abundant ±: subordinate -: trace						<input type="checkbox"/>
water discharge type d: dripping f: continuous flow						<input type="checkbox"/>
() for T plural structures in the probe hole						<input type="checkbox"/> <input type="checkbox"/> <input type="checkbox"/> <input type="checkbox"/>

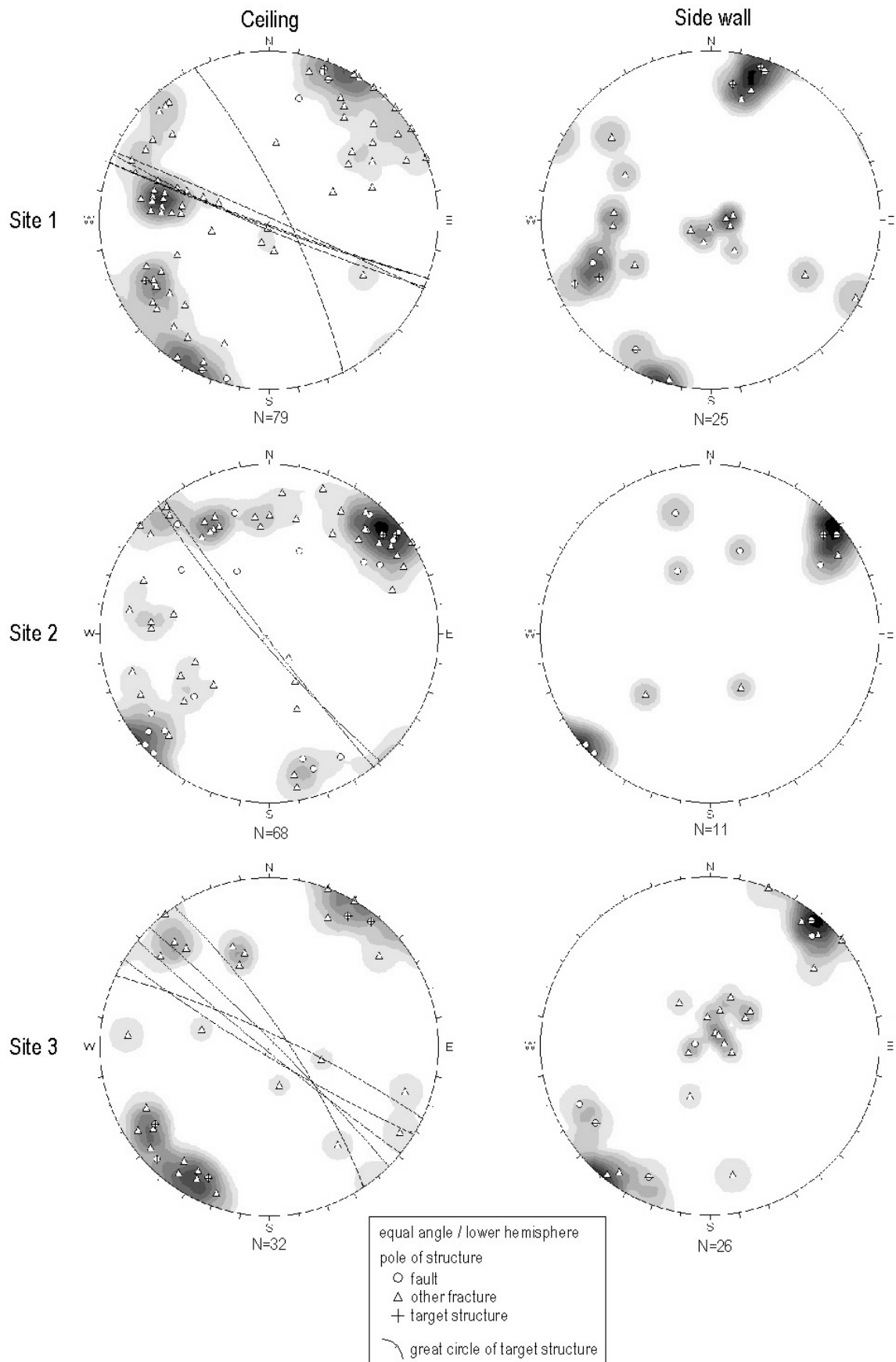


Figure 3-1. Orientation of structures on ceiling and sidewalls in each site

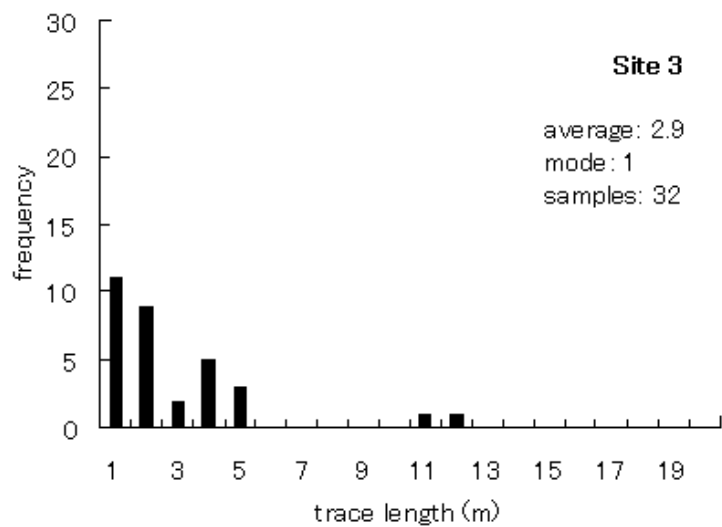
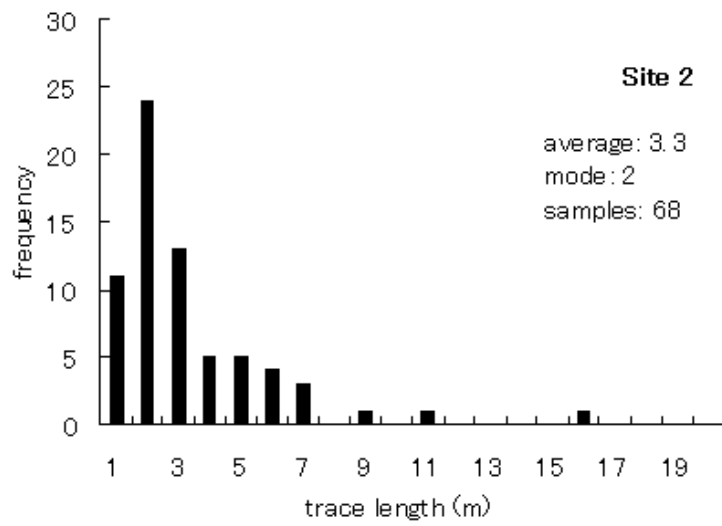
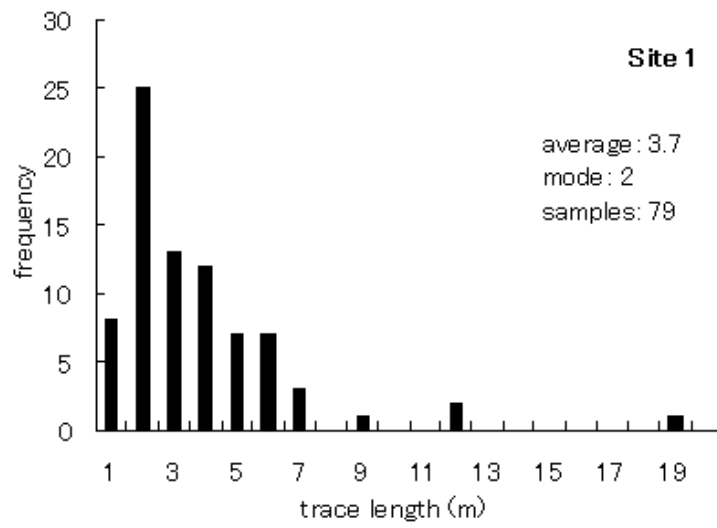


Figure 3-2. Histogram of trace length of structures on the ceiling

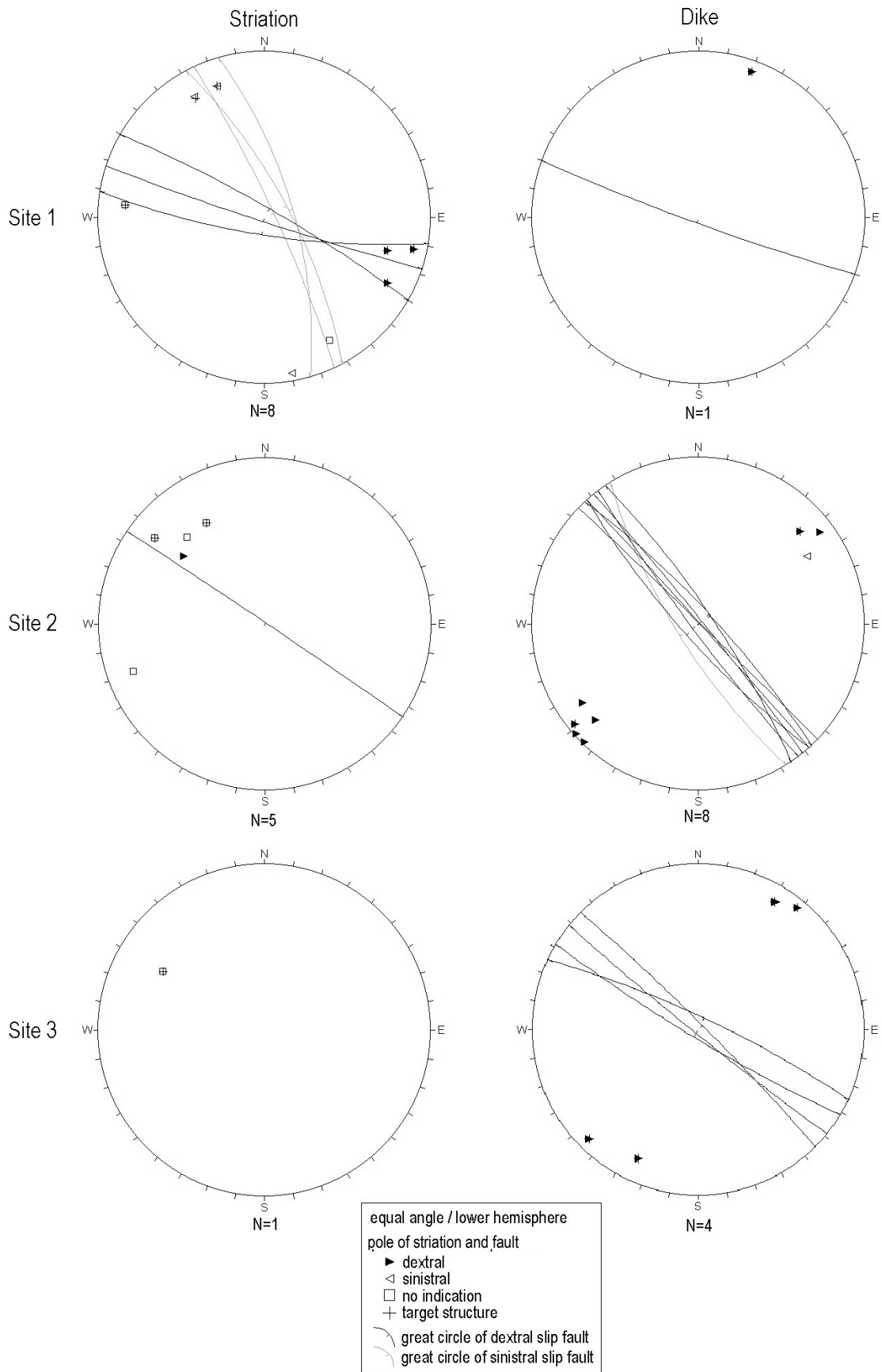


Figure 3-3. Orientation and slip sense of faults estimated from striation and displaced dike

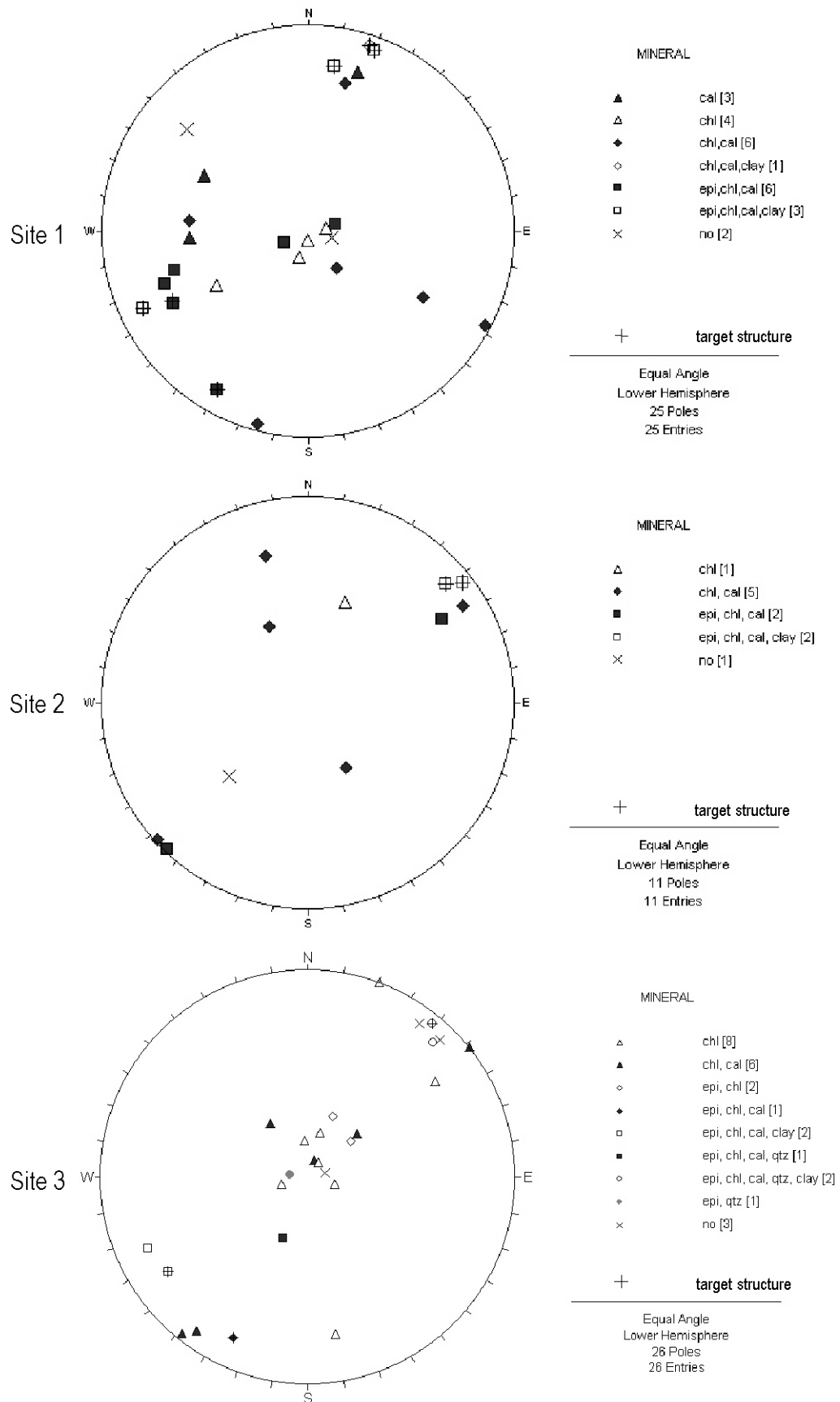


Figure 3-4. Orientation of structures with different filling/coating mineral assemblages

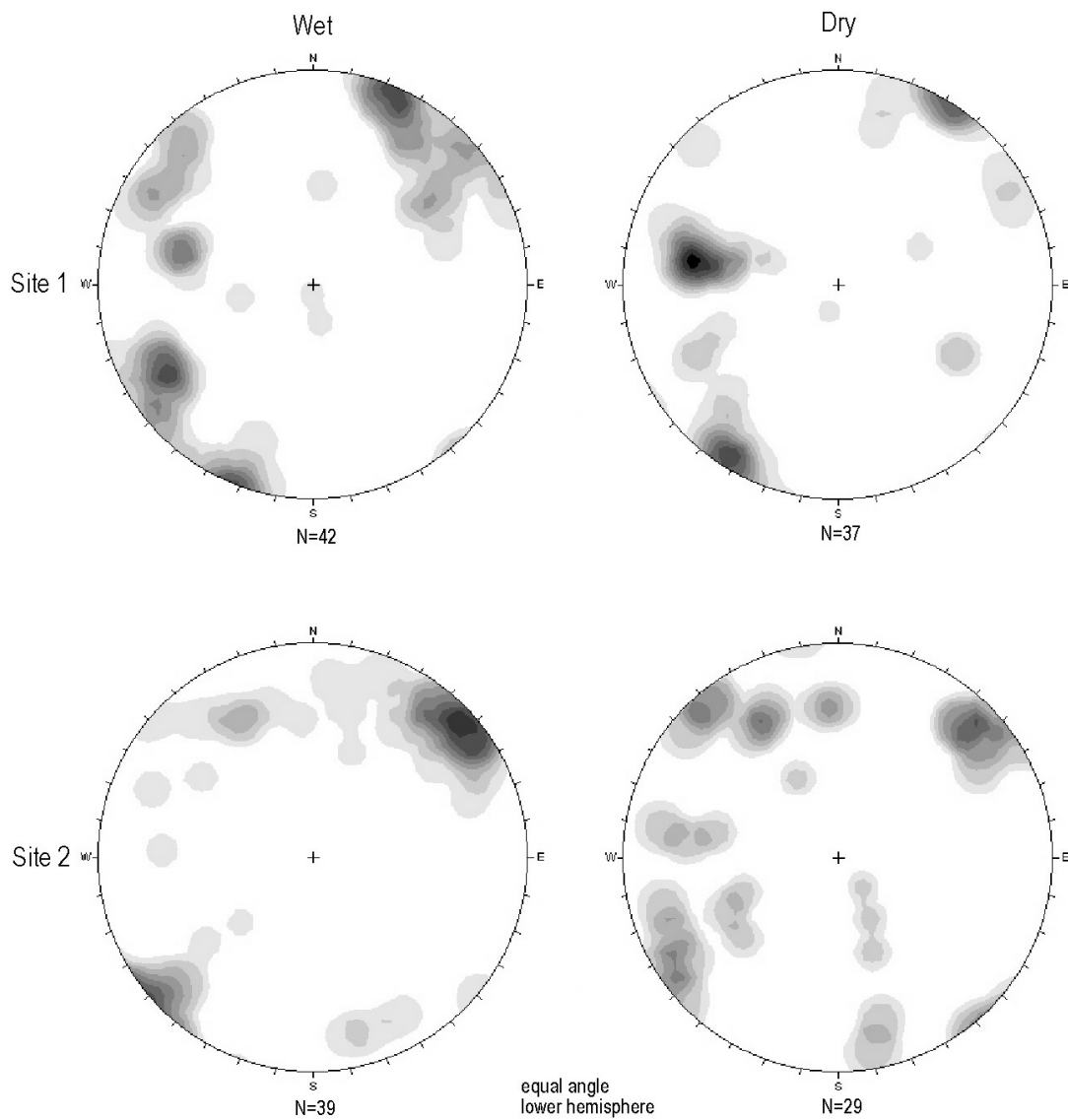


Figure 3-5. Orientation of wet structures (wet area more than 50%) and dry structures (less than 50%)

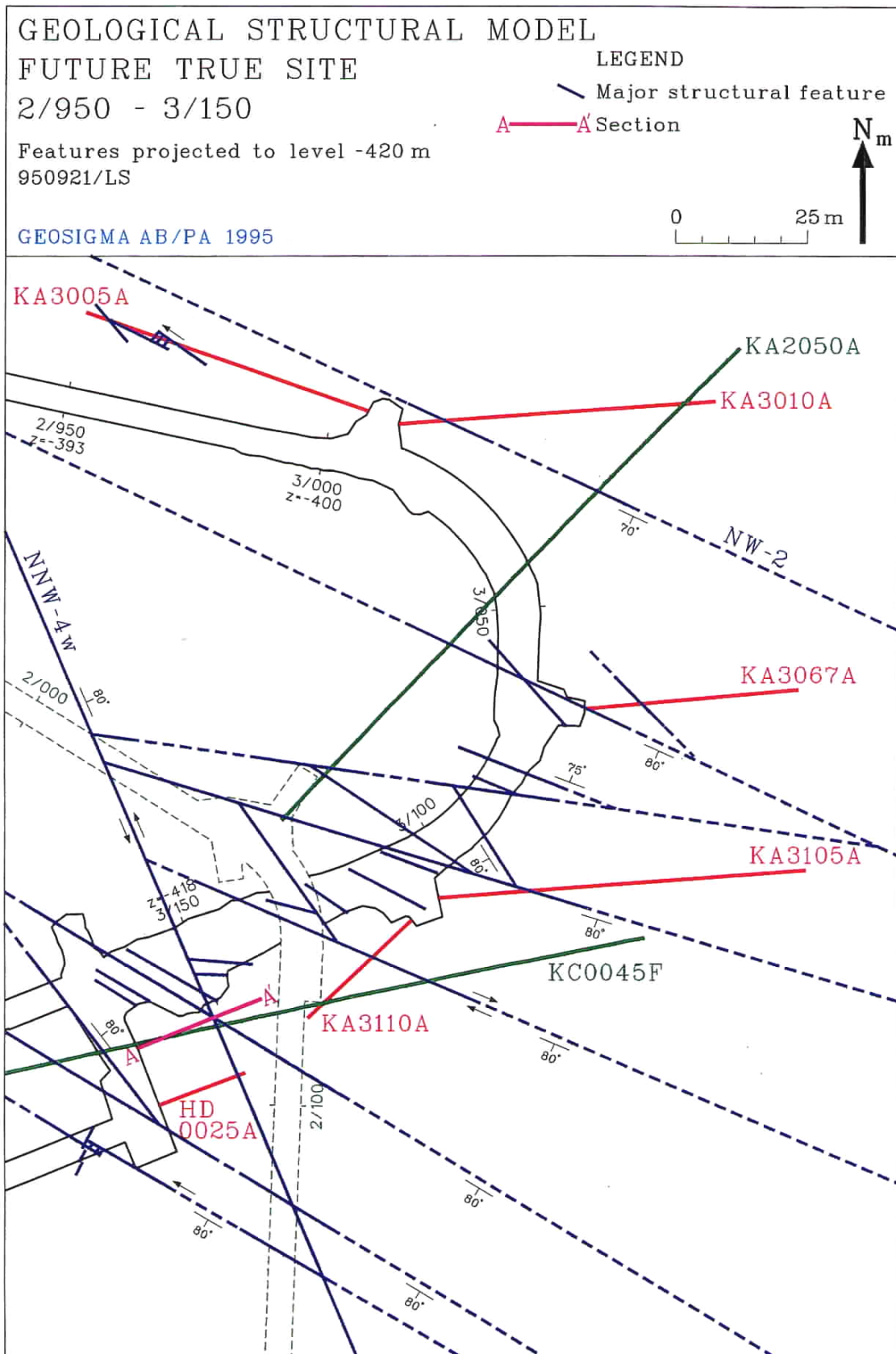


Figure 3-6. Structural setting at one of the site in the SELECT project
 (Winberg, et.al., 1996)

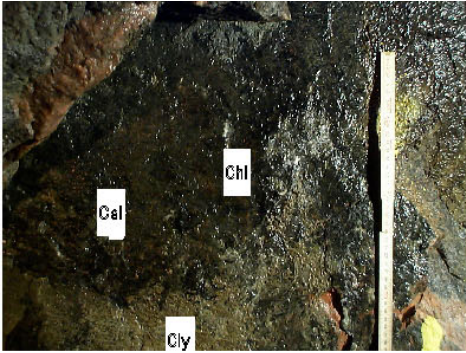


Photo 1: Structure1555m at 1545A (Site 1)
 Fault plane coated by chlorite(Chl), calcite(Cal) and clay/gouge(Cly). Steps and weak subhorizontal striations indicating sinistral strike-slip. Width of photo ca.60cm.

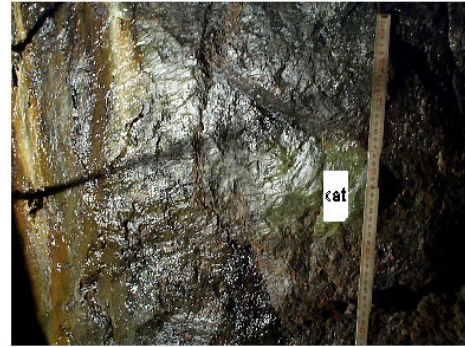


Photo 2: Structure1555m at 1561B (Site 1)
 Fault steps and subhorizontal striations indicating sinistral strike-slip. Epidotized cataclaste or vein (cat) along fault plane.Width of photo ca.60cm.

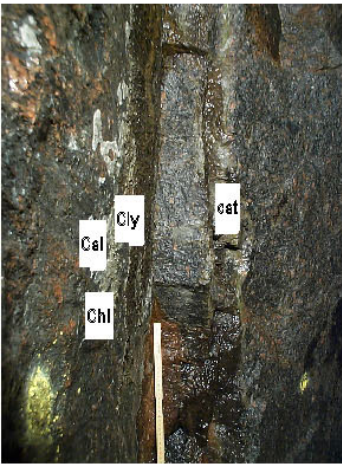


Photo 3: Structure1558m at 1566A (Site 1)
 Looking subparallel to fault plane. Fault plane (left side) coated by chlorite(Chl), calcite(Cal) and clay/gouge(Cly). Epidote-cataclaste(cat) along the parallel fault(middle-right). Width of photo ca.80cm.



Photo 4: Structure1558m at 1566A (Site 1)
 Looking normal to the same fault plane. Steps and subhorizontal striations indicating dextral strike-slip. Width of photo ca.90cm.

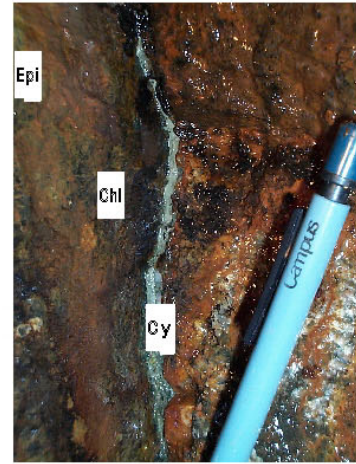


Photo 5: Structure2154m at 2151B (Site 2)
 Fault plane (left side) coated by chlorite(Chl), epidote(Epi), and filled by clay/gouge(Cly). Width of photo ca.10cm.

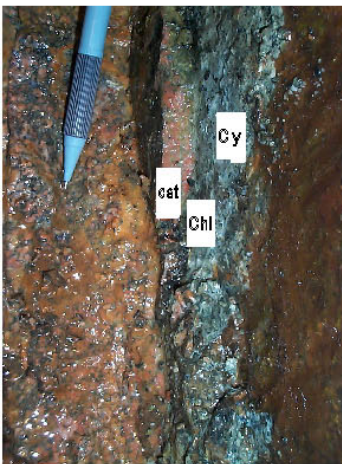


Photo 6: Structure2163m at Niche2156B (Site 2)
 Fault plane (right side) coated by chlorite(Chl) and clay/gouge(Cly). Epidote vein/cataclaste(cat) and red alteration along the fault. Width of photo ca.10cm.



Photo 7: Structure2198m at 2198B (Site 3)
 The structure comprises of several fault planes lying in a thin zone of moderate mylonite (centre) between weak mylonite (right) and undeformed diorite (left). White material is re-precipitated grout. Width of photo ca.15cm.



Photo 8: Structure 2198m at Niche 2198A (Site 3)
Grout (G; light orange colour) injected into the master fault No. 1 with maximum thickness of 8mm. White material is re-precipitated grout. Width of photo ca. 15 cm.

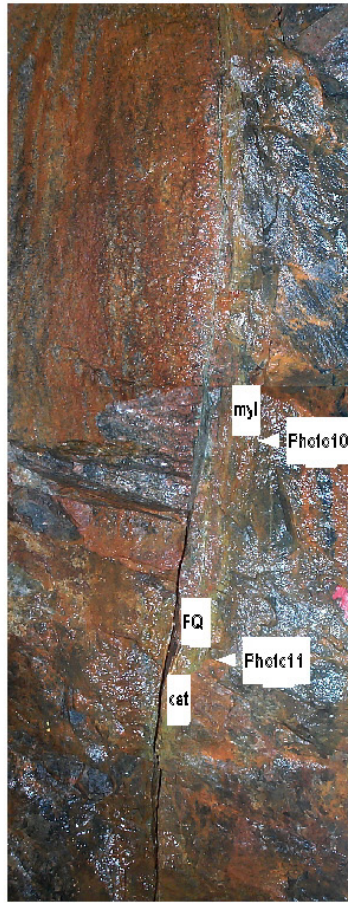


Photo 9: Structure 2198m at Niche 2198A (Site 3)
Niche-wall view. Master fault No. 27 (centre) basically follows the edge of precursors as mylonite (myl), cataclasite (cat) and fluorite-quartz vein (FQ) but locally crosscuts them. Width of photo ca. 1 m.

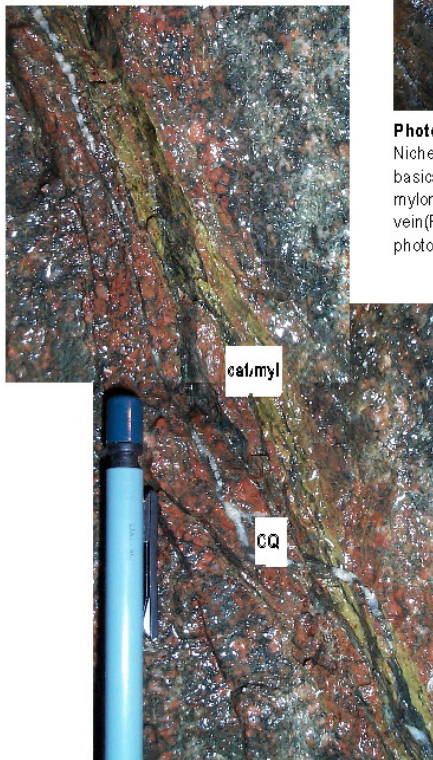


Photo 12: Structure at 3401m (TBM tunnel)
Example of reactivation of structure. Cataclasite/mylonite (cat/myl) is locally cut by chlorite-quartz filled fault (CQ) parallel to the structure. Red alteration halo along structure. Width of photo ca. 8 cm.

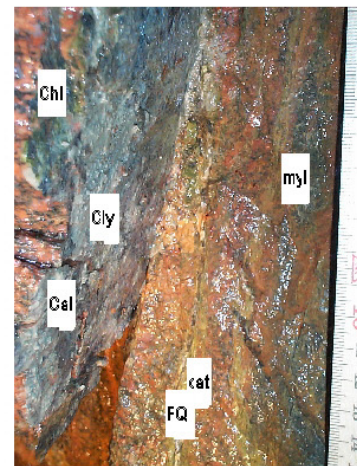


Photo 10: Close-up of fault No. 27 (Site 3)
Fault plane (left) coated by chlorite (Chl), calcite (Cal) clay/gouge (Cly). Mylonite (myl), cataclasite (cat) and fluorite-quartz vein (FQ) on the wall (right). Width of photo ca. 10 cm.

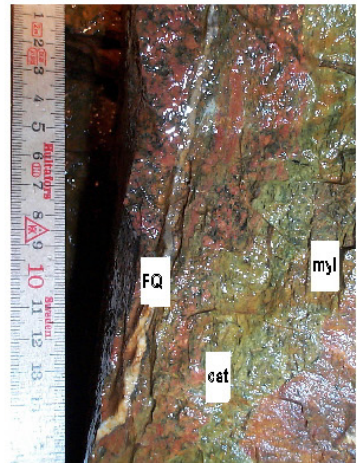


Photo 11: Close-up of fault No. 27 (Site 3)
Mylonite (myl), cataclasite (cat) and fluorite-quartz vein (FQ) are cut by the master fault. Width of photo ca. 12 cm.

4 Microscopic and mineralogical investigations

4.1 Objectives

Objectives of the microscopic and mineralogical studies are:

- to increase understanding of micro scale structures relevant to flow/transport within water-conducting structures in block scale.

The above objective is subdivided into the following:

- to investigate genesis and mechanisms of the mapped water-conducting structures through observation of micro-structures, and
- to qualify and quantify constituents of gouge/filling materials in the mapped water-conducting structures which are relevant for transport of groundwater and solutes.

4.2 Methods

4.2.1 Sampling

Oriented rock samples were collected from sidewalls and niche wall of the six mapped structures (Figure 4-1, Photo 13). The samples contain half side of the structure, i.e. wall rock and fault plane with fault gouge and filling/coating materials. The samples are collected carefully with the least use of hammer to minimize damage. Orientations of the ceiling and north were marked on the samples. The sampling points are indicated on the sidewall/niche maps (Maps 2, 4 and 6 in Appendix 2).

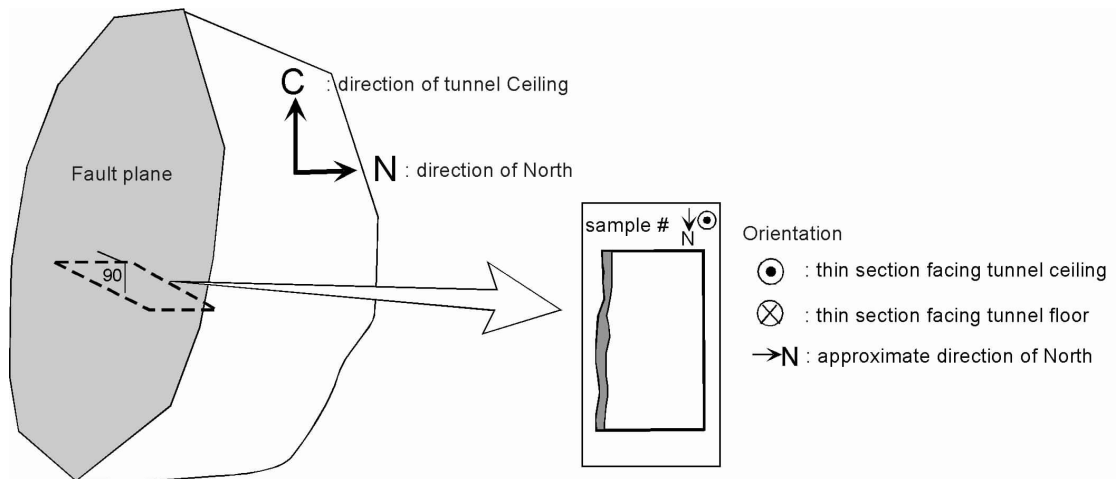


Figure 4-1. Schematic figure of oriented rock samples and thin sections

4.2.2 Microscopy

Oriented thin sections were prepared through Terralogica AB (Photo 14). The loose materials as gouge/filling materials on the fault planes, where thin sections were to be made, were fixed with resin. Rests of the loose materials were used for the XRD analysis. The thin sections are oriented parallel to the striations and normal to the fault planes, and include the best portion of fault planes with gouge/filling materials. Optical microscopic observations were performed both at Geovetarcentrum of the Göteborg University and at JNC Tono Geoscience Center. Emphasis was put on the textures and constituent minerals of both wall rock and gouge/filling materials upon observation. A thin section of a fresh undeformed Äspö diorite was also observed as a reference.

4.2.3 XRD

Preparation and analysis were made at the Geological Survey of Sweden, through Terralogica AB. Gouge/filling materials were sieved and separated into the clay fraction smaller than 2 micro meters and the fraction from 2 μm to 0.125 mm, then weight percent of both fractions were measured. Identification of mineral species and estimation of relative abundance were made in the preferred orientation method for both fractions. In addition to the natural specimens, ethyleneglycole treated specimens were analyzed to discriminate smectites from chlorites.

4.3 Results

4.3.1 Microscopic observation

Results of the observation are described in detail as below and summarised on Table 4-1. The orders of brittle deformations, coatings/fillings and alterations are estimated based on the crosscutting relations or covered/coated relations. The senses of fault displacement estimated from arrangements of fractures are based on the assumption that the fractures are the possible splay crack formed with the strike-slip displacement of faults.

1553B (structure 1558 m)

Asymmetric recrystallised quartz around K feldspars are observed. These are typical in the Äspö diorite and probably the product of early ductile deformation that formed primary foliation. Three brittle deformation events are presumed (Photo 15). 1) The first is formation of the parallel fractures filled either with quartz or fluorite, and micro fractures filled with quartz all over in a large K-feldspar. Dextral sense of the fault is assumed from fracture arrangement. 2) The second is the fracturing or faulting that cut fractures of 1). The fracture plane is locally coated with chlorite and calcite. Dextral sense of the fault is again assumed from fracture arrangement. 3) The third events resulted in the formation of gouge. It contains fragments of sub-angular quartz, K feldspar and minor fluorite grains within the matrix of very fine clay and minor chlorite. Fissures within the gouge are filled with calcite. The entire wall rock suffered chloritisation of biotite, saussurisation (very fine epidote and clay (sericite) inclusions in plagioclase due to decomposition) and minor epidote alteration, probably in the early stage of deformation/alteration history.

1561B (structure 1555 m)

This thin section is divided into two domains. The half consists of cataclasite facing the main fault plane, and another half, bounded by a smaller fault, comprise fractured and altered wall rock. No significant ductile texture is observed. Five brittle deformation events are presumed (Photo 16). 1) The first is formation of cataclasite or fault gouge, details of which is not obvious due to the subsequent epidote alteration. 2) In this epidote cataclasite, parallel micro fractures filled with calcite is observed that imply a sinistral displacement relative to the fault planes. 3) The set is cut by a calcite filled fracture that implies the opposite sense. 4) The above fractures are cut by the main and smaller fault. The fault planes are coated with drusy calcite (Photo 17), locally fluorite and probably thin chlorite. 5) Fault gouges are formed along the main and smaller fault planes. It contains fragments of sub-angular calcite, and minor K feldspar and quartz grains within the matrix of very fine clay minerals. An open fracture that is locally filled with the gouge implies the sinistral strike-slip displacement of the faults. Drusy calcite grows on the open fractures within and parallel to the fault gouges. In addition to the chloritisation and saussuritisation, red stains of very fine hematite spread in the feldspar grains and grain boundaries within the wall rock.

1575A (structure 1570 m)

No significant ductile texture is observed. Two brittle deformation events are presumed (Photo 18). 1) The first is formation of a fracture or fault plane that is subsequently coated with local chlorite, extensive fluorite and calcite layers in this order. 2) The second is the formation of the fault gouge. It contains fragments of sub-angular to angular K feldspar, plagioclase, quartz, epidote, calcite and fluorite in this order of abundance. The matrix comprises very fine clay minerals. The common chloritisation and saussuritisation are observed in the wall rock.

2151B (structure 2154 m)

No significant ductile texture is observed. Four brittle deformation events are presumed (Photo 19). 1) The first is formation of the parallel fractures filled with epidote, chlorite and local calcite. Their arrangement implies the sinistral displacement of the fault. 2) One of the above fractures is cut by several micro faults that display minor sinistral displacement of quartz and the epidote filled fracture. 3) The third is the fracturing or faulting along the present fault plane, and subsequent coating of chlorite, calcite and local Fe-oxy hydro-oxide. 4) Fault gouge is formed along the present fault plane. It contains fragments of sub-angular calcite, K feldspar and minor epidote grains within the matrix of very fine clay minerals. Two layers of coating materials are observed on the gouge (Photo 20). The first, adjacent to the gouge, comprises of calcite and local Fe-oxy hydro-oxide. The second, innermost of the coating/filling on the fault plane, has distinctive texture of the scattered small round fluorite within the matrix of very fine clay minerals. These two fillings are tentatively considered as the alteration products of the gouge, but subject of further investigation. The common chloritisation and saussuritisation are observed in the wall rock.

2156B (structure 2163 m)

Semi-ductile deformation texture, tentatively called as proto-mylonite, is observed in a small part near the fault plane (Photo 21). It comprise oriented and deformed plagioclase, recrystallised fine grained quartz and minor chlorite layers, and those display trace foliation oblique to the fault plane, implying sinistral shearing. It grades into the cataclasite without any ductile texture toward the wall rock. Three brittle deformation events are presumed, including the cataclasite. 1) The cataclasite is defined as a zone of weakly broken mineral grains and abundant epidote. 2) The second is the fracturing or faulting along the present fault plane, and subsequent coating of local epidote and more extensive chlorite. 3) Fault gouge is formed along the present fault plane. It suffered extensive alteration and only a small portion of calcite fragments are remained in the clay altered matrix. The scattered fluorite within the clay matrix similar to the previous sample is also observed at innermost of the filling materials. The chloritisation, saussuritisation and hematisation are observed only in the wall rock.

2198A (structure 2198 m)

Mylonite is developed in major part of this sample. It is defined as very fine grained and oriented recrystallised quartz and feldspars, and chlorite layers, forming weak foliation. The structure displayed by the asymmetric growths of fine grained quartz and chlorite around K feldspar grains implies the dextral shear of mylonitisation (Photo 22). It is noted that the mylonitisation is weaker toward the present fault plane and cataclasite exists near the fault plane. Five brittle deformation events are presumed, including the cataclasite (Photo 23). 1) The cataclasite is defined as a thin zone of broken mineral grains between the calcite vein and the fault gouge described later. There seems to be another possible cataclasite on the other side of the main fault displayed as an isolated piece of crushed and epidote altered rock at the rim. 2-3) A fracturing or faulting along the present fault plane occurred, and the plane was coated with epidote. Another fracture or fault lying sub-parallel and close to the present fault plane resulted in the formation of a 3 mm thick calcite vein. The wall rock side of the vein is decomposed to form a fluorite-clay layer. Order of these events is not obviously estimated. 4) Fault gouge is formed along the present fault plane. The fragments comprise epidote, plagioclase and pieces of mylonite. Major part of the matrix is altered possibly to Fe-oxy hydro-oxide. 5) A fracturing formed irregular wavy calcite filled fractures both along the fault side of the calcite vein 2) and cutting the altered fault gouge 3). 6) A new gouge is formed between the altered gouge and the possible epidote cataclasite on the other side. It contains fragments of angular to sub-angular calcite, quartz and minor epidote grains within the matrix of very fine clay minerals. The extensive alteration in the mylonite is chloritisation of biotite, epidotisation of plagioclase, and red stains of very fine hematite.

4.3.2 XRD analysis

Original report including charts of X-ray intensity is presented in Appendix 4. The translation is presented below. The results are summarised in Table 4-1.

1553B

fraction: <2 μ m (clay)

The mineral consists of chlorite and swelling mixed layer clay of correusite type (chlorite/vermiculite, chlorite/tri-octahedral smectite). The portion of mixed layer clay is considerable.

fraction: 2 μ m - 0.125mm

Chlorite, Fe-rich mica (illite), quartz, plagioclase, fluorite, calcite and possibly some rutile are identified.

1561B

fraction: <2 μ m (clay)

Chlorite and swelling mixed layer clay interpreted to be correusite are identified. Compared with 1553B, this sample has higher portion of chlorite and the mixed layer clay is less well crystallised.

fraction: 2 μ m - 0.125mm

Chlorite, less crystallised illite, quartz, plagioclase, calcite and probably epidote are identified.

1575A

fraction: <2 μ m (clay)

The major part of the sample consists of mixed layer clay of correusite type. Chlorite, calcite and fluorite are found in minor amounts.

fraction: 2 μ m - 0.125mm

Mixed layer clay, chlorite, illite, quartz, plagioclase, calcite, fluorite and some rutile are identified.

2151B

fraction: <2 μ m (clay)

Chlorite and minor amount of mixed layer clay and traces of calcite and quartz are identified.

fraction: 2 μ m - 0.125mm

Chlorite, quartz, plagioclase, (lots of) calcite and fluorite are identified.

2156B

fraction: <2 μ m (clay)

Mixed layer clay of correusite type dominates. Additionally, chlorite is present.

fraction: 2 μ m - 0.125mm

Mixed layer clay, chlorite, quartz, fluorite, plagioclase, calcite and possibly some rutile are identified.

2198A

fraction: <2 μ m (clay)

Chlorite is the dominant clay mineral. Minor amount of mixed layer clay (correusite type) is also found.

fraction: 2 μ m - 0.125mm

Chlorite, quartz, plagioclase, calcite, fluorite and epidote are identified.

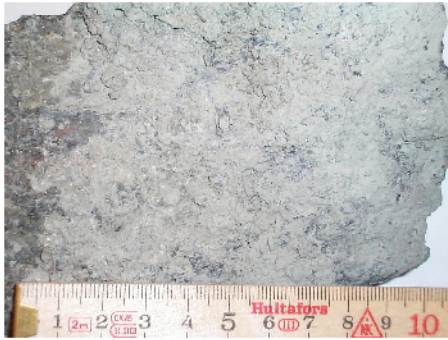
4.4 Summary of interpretations

The interpretations of results are summarised as follows.

- All the samples from the target structures have micro structures that suggest reactivation of pre-existing structures. They have common brittle reactivation events, the older faults or fractures that formed gouges or mineral coatings and the younger faults that formed gouges. Some of those have preceding structures as mylonite and cataclasite.
- Each structure suggests different history of ductile/brittle deformations, coating/filling minerals, alterations of wall rock and fillings. It is impossible to discriminate clearly the minor structures and potential connecting structures in the micro scale observations. However, the most potential connecting structure 2198A has the longest and the most abundant deformation history. Only one sample displays the sense of displacement of the latest brittle deformation, which matches with the tunnel observation. There are senses of displacement of the preceding structures that may explain the inconsistency among senses estimated from dike displacements, splay cracks and striations in the tunnel.
- There is not much difference in species but in relative amount of constituent minerals of the clay and larger fractions between the samples. The clay contents vary from 13 to 50 % of the total amount of the filling/coating including gouge. The dominant clay mineral is either chlorite or chlorite-smectite mixed layer, depending on the samples.

Table 4-1: Summary of results of microscopic and mineralogical studies

sample	Microscopy				XRD				
	structure	ductile event	brittle event	gouge fragment	gouge matrix	coating/filling mineral	wall rock alteration	< 2µm (clay)	2µm - 0.125mm
1553B	1558m	no	1) // qtz filled fracture and qtz filled micro fractures in Kfs (sinistral), 2) coating, 3) gouge	qtz, Kfs, ±fluo	clay, ±chl	(±chl, ±cal)coating, cal filling in fissure in gouge	ch(bi), saus(pl), epi	wt% minerals 27 ++chl/smec mixed layer, ±chl	wt% minerals 73 chl, ill, qtz, pl, fluo, cal, ±rut
1561B	1555m	no	1) cataclasisite (epi altered), 2) cal filled // micro fractures (sinistral), 3) cal filled fracture (dextral?), 4) coating, 5) gouge filled fracture (sinistral)	cal, ±Kfs, ±qtz	clay	(cal, ±fluo, chl?)coating, drusy cal in fracture in gouge	chl(bi), saus(pl), epi, very fine hematite	30 chl, chl/smec mixed layer	70 chl, ill, qtz, pl, cal, ±epi
1575A	1570m	no	1) coating, 2) gouge.	Kfs, pl, qtz, epi, cal, fluo	clay	(±chl, fluo, cal)coating	ch(bi), saus(pl)	13 ++chl/smec mixed layer, ±chl, ±cal, ±fluo	87 chl/smec mixed layer, chl, ill, qtz, pl, cal, fluo, ±rut
2151B	2154m	no	1) epi, chl, ±cal filled fracture (sinistral), 2) cal filled // micro faults (sinistral), 3) coating, 4) gouge.	cal, Kfs, ±epi	clay	(chl, cal, ±FeOOH)coating, (chl, ±FeOOH)filling, (fluo in clay matrix)filling	ch(bi), saus(pl)	38 chl, ±chl/smec mixed layer, -cal, -qtz	62 ++cal, chl, qtz, pl, fluo
2156B	2163m	local proto-mylonite (sinistral trace foliation)	1) cataclasisite, 2) coating, 3) gouge.	cal (almost altered)	clay? (almost altered)	(±epi, cal)coating, (fluo in chl-clay matrix)filling	ch(bi), saus(pl), epi, very fine hematite	50 ++chl/smec mixed layer, ±chl	chl/smec mixed layer, chl, qtz, fluo, pl, cal, ±rut
2198A	2198m	mylonite (dextral weak foliation, dextral σ structure)	1) cataclasisite, 2-3) coating and cal-fluo vein, 4) altered gouge (dextral?), 5) wavy cal fracture, 6) new gouge	epi, pl, ±mylonite (altered gouge), cal, qtz, ±epi (new gouge).	clay altered to FeOOH-chl? (altered gouge), clay (new gouge).	epidote coating, (cal-fluo vein, wavy cal fracture, FeOOH-chl) coating/filling	ch(bi), epi(pl), very fine hematite	35 ++chl, ±chl/smec mixed layer	65 chl, qtz, pl, cal, fluo, epi
<p>1), 2), □□□: order of events deduced from</p> <p>crosscutting relations.</p> <p>qtz: quartz pl: plagioclase Kfs: K feldspar bi: biotite chl: chlorite epi: epidote cal: calcite fluo: fluorite rut: rutile saus: saussurite (mixture of epidote and sericite in plagioclase) FeOOH: Fe-oxy hydro-oxide smec: smectite ill: illite</p> <p>Relative amount</p> <p>++: abundant (no symbol): common ±: minor -: trace</p>									



1553B
 C (ceiling)
 ↗ N (north)



1561B
 C
 ↗ N



1575A
 N
 ↗ C



2151B
 N
 ↗ C



2156B
 C
 ↗ N



2198A
 C
 ↗ N

Photo 13: Oriented samples of fault plane for microscopy and XRD
 See Figure 4-1 for explanation of orientation.

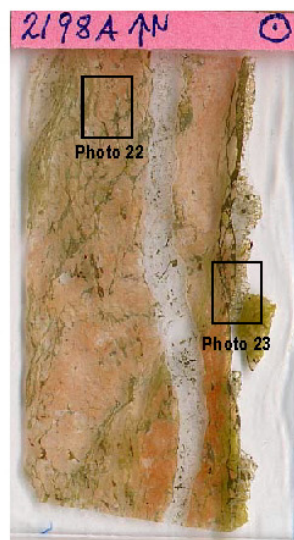


Photo 14: Prepared thin sections and location of microscopic photos
 See Figure 4-1 for explanation of orientation. Longer side of thin sections 45mm.

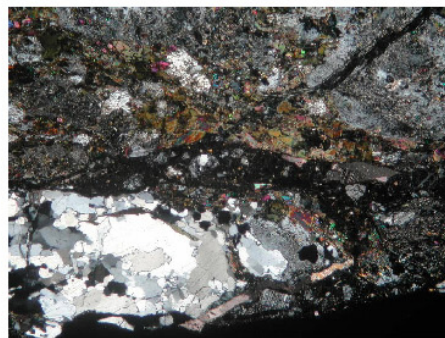
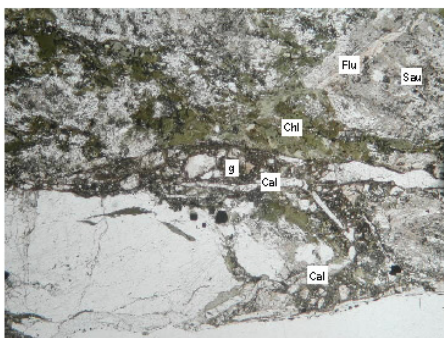


Photo 15: 1553B (width of photo ca. 5mm)
 Fluorite vein (Flu) is cut by the fault with gouge (g). Wall rock near the fault plane is deformed and altered (chloritisation (Chi) of biotite and saussuritisation (Sau) of plagioclase). Calcite (Cal) fills the fissure in the gouge.

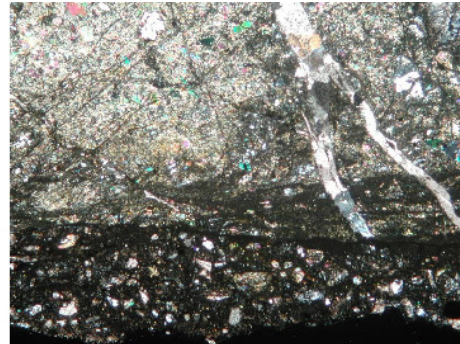
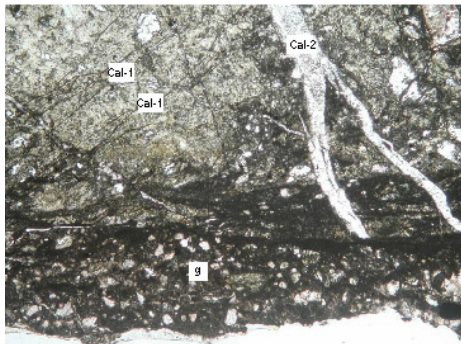


Photo 16: 1561B (width of photo ca. 5mm)
The older calcite-filled parallel micro fractures (Cal-1) in the epidote-cataclasite matrix are cut by the younger calcite-filled veins (Cal-2). These are then cut by the fault gouge (g).



Photo 17: 1561B (width of photo ca. 5mm)
Epidote vein (Epi) in the weakly crushed matrix is cut by the open fracture coated with fine drusy calcite (Cal).

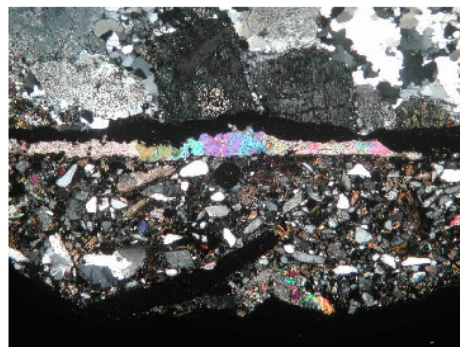
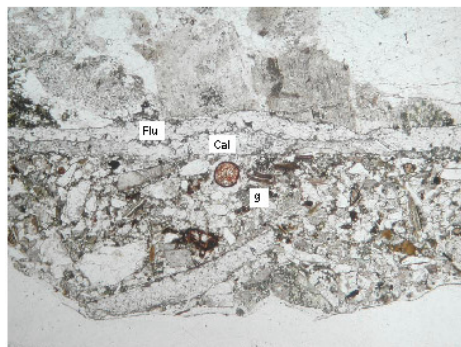


Photo 18: 1575A (width of photo ca. 5mm)
Coating of fluorite (Flu: dark in cross nicole) and calcite (Cal), and fault gouge (g) with fragments of quartz, K-feldspar, plagioclase, calcite, epidote and fluorite in the matrix of very fine clay minerals.

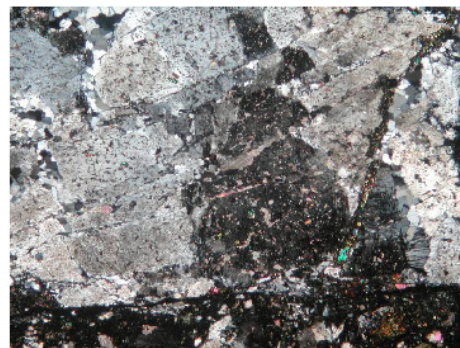
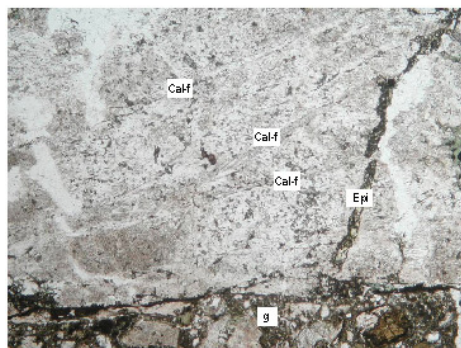


Photo 19: 2151B (width of photo ca. 5mm)
Epidote vein (Epi) is cut by micro faults filled with calcite (Cal-f). These are then cut by the fault gouge (g).

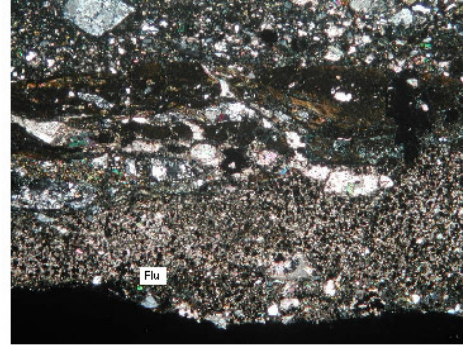
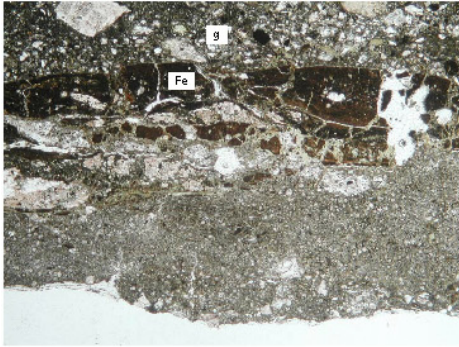


Photo 20: 2151B (width of photo ca. 5mm)
Two layers of coating material on fault gouge (g), possibly alteration products. Layer of Fe oxy hydro-oxide (Fe) and calcite (Ca), and layer of scattered fine round fluorite (Flu; dark in cross nicole) in very fine clay matrix.

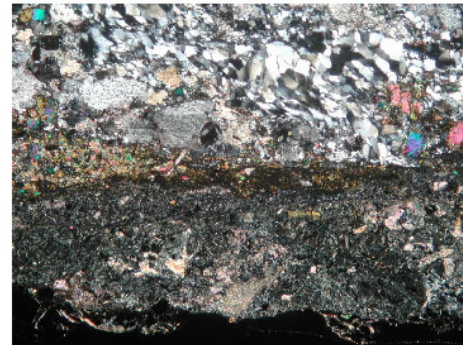
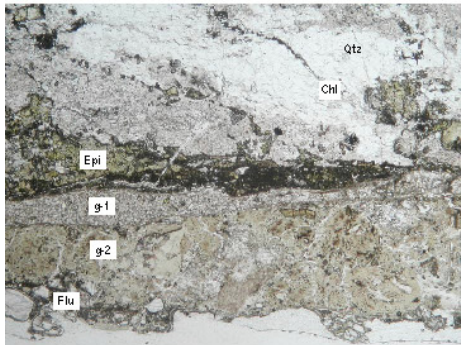


Photo 21: 2156B (width of photo ca. 5mm)
Top: proto-mylonite with recrystallised quartz (Qtz) and chlorite layers (Chl), displaying weak foliation. Bottom: epidote coating (Epi) on fault plane, and subsequent unaltered (g-1) and altered gouge (g-2). Idiomorphic fluorite (flu) at innermost layer of gouge.

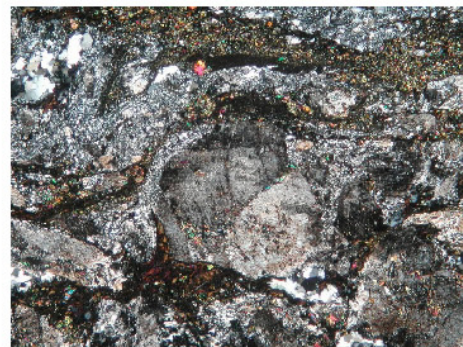
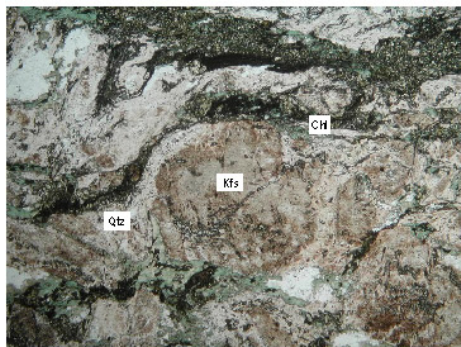


Photo 22: 2198A (width of photo ca. 5mm)
 σ structure displayed by asymmetric growths of fine grained quartz (Qtz) and chlorite (Chl) around K feldspar (Kfs) implying dextral shear of mylonite.

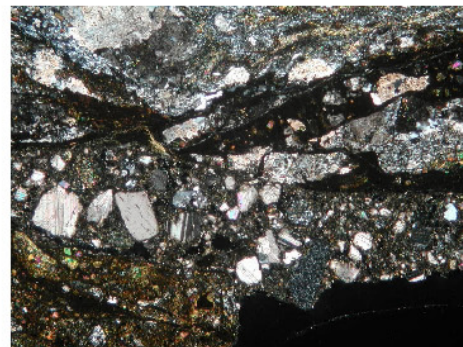
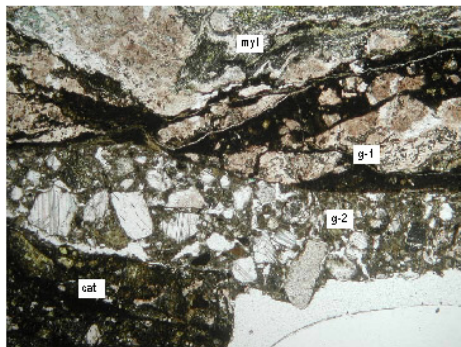


Photo 23: 2198A (width of photo ca. 5mm)
Different wall rocks of fault planes, mylonite (myl) on one side and cataclasite (cat) on the other side. Older altered fault gouge (g-1) with layer of Fe oxy hydro-oxide and younger fault gouge (g-2). Red stain in feldspars only in mylonite and older fault gouge.

5 Core Mapping

5.1 Objectives

The objective of the core mapping is,

- to correlate the mapped target structures in the tunnel with those on the drill core to assess consistency of characteristics.

5.2 Methods

Borehole KA2048B, which was drilled parallel to the tunnel prior to excavation, was selected for core mapping (Figure 5-1). Although it is too close to the tunnel, it was the only suitable borehole for the objectives. The mapped water-conducting structures in the Site 2 and Site 3 are expected to intersect in this borehole. The study was performed in the following procedure.

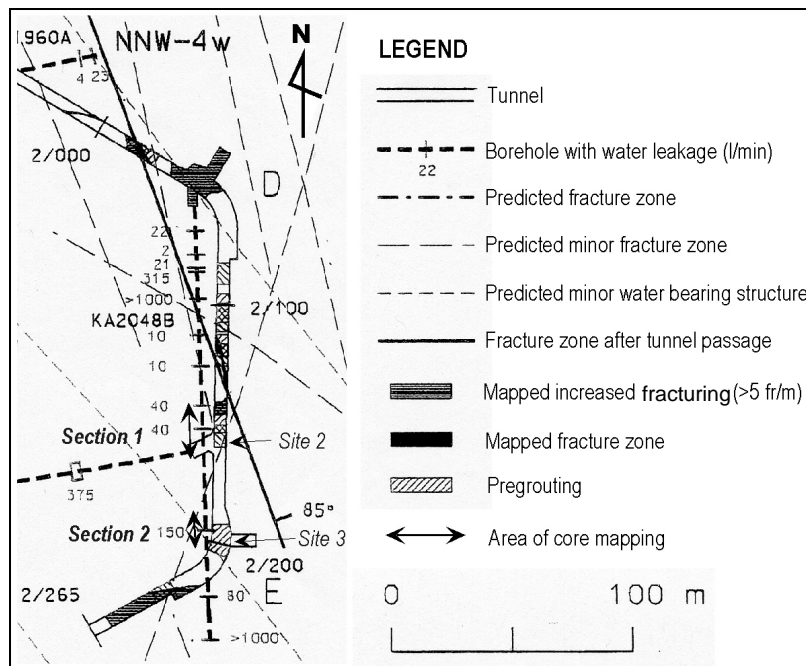


Figure 5-1. Area of core mapping and structural/hydrogeological information (modified from Rhén, et.al., 1994)

1) Evaluation of existing data and selection of mapping intervals

Approximate locations of the mapped target structures in the borehole were estimated, and compared with the relevant features in the borehole. The following information was available.

- drill core in 56 mm diameter,
- data on the Petrocore mapping system through the SICADA database (lithology, fracture, alteration, RQD, etc.) and interpretation (SKB, 1994)
- radar reflection survey (SKB, 1994)
- inflow monitoring during drilling (Rhén, et.al., 1994)

No borehole TV, flow logging and hydraulic test for a certain section was performed. Therefore orientation and transmissivity data of the structures are not available.

2) Core mapping

Sketch (scale 1/5), description of fractures (type, host rock, ductile/brittle features, orientation, lineation, aperture, fitness, roughness, filling/coating (see Appendix 5 and 6 for details), and photographing were performed in the core storage on the ground level.

5.3 Results

1) Evaluation of existing data and selection of mapping intervals

The estimated location in the borehole and distance between the borehole intersections and tunnel outcrops are presented on Table 5-1.

Table 5-1: Estimated location of structures and distance between the borehole and tunnel intersections

structure	depth (m)	distance(m)
2154 m	86.1	10.6
2163 m	98.3	3.0
2198 m	138.0	5.4

Information near the above intersections is described on Table 5-2. It is assumed that the structure 2154 m correspond to the conductive fractured part at 85 m, and the structure 2198 m to the conductive fracture on mylonite at 138 m.

Table 5-2: Hydrogeological, geological and geophysical information around the estimated intersections

depth (m)	inflow (l/min)	core description	radar reflector (strike/dip, magnitude)
85	40		
85.1-86.2		fractured	
88			129/76, moderate
95	40		
101			216/84, very weak
135			245/49, very weak
138	150		
138.3-138.4		mylonite	
140			253/80, very weak

Based on the above information, two intervals for the core mapping were determined.

Section 1: 83 to 103 m

Section 2: 135 to 142 m

2) Core mapping

39 fractures in Section 1 and 7 fractures in Section 2 are mapped and described (Appendices 5 and 6).

Section 1 (Photo 24)

There is a zone of higher fracture density between 85.2 and 86.1m where the intersection of the structure 2154 m is estimated nearby. There are 14 fractures in this zone and many of which have similar orientations (Photos 25). 5 fractures are open where fracture planes do not fit or partly fit, and may cause the inflow (Photos 26). No ductile deformation or fault rock but a 40 cm of red alteration with epidotic network veins exists. It is impossible to determine that this zone is the extension of structure 2154 m because characteristics of fractures in this zone are not identical with the structure. It is noted that the lithology is dominantly Småland granite that has more tendency to exhibit parallel fractures than Äspö diorite.

An identical structure with 2163 m was observed at 98.9 m, where open fractures No. 34 and 35 in re-activated cataclasite with similar red alteration halo and fracture mineralogy (Photo 28). However, no inflow was reported during drilling.

There is a tight or slightly open fracture, No. 32, with epidote vein and thin calcite coating at 95.6 m where inflow was reported at 95 m (Photo 27). This fracture is estimated to strike NE given the orientation of No. 34 and 35 are identical with the structure 2163 m. Also there is no water-conducting structure between 2154 m and 2163 m in the tunnel.

A fracture zone from 85.2 to 86.1 m is the only possible explanation for the moderate radar reflection at 88 m considering the density and orientation of fractures. The reflection at 101 m is not explained on the core.

Section 2 (Photo 29)

An identical structure with 2198 m was observed at 138.2 m, where an open fracture No. 7 occurs at the rim of distinct mylonite with similar alteration halo and fracture mineralogy (Photos 30 and 31). Occurrence of the fracture at the rim of the mylonite is consistent with the observations in the tunnel mapping and microscopy, and implies its preferred location where a contrast in physical property occurs. An extreme inflow of 150 l/min at 138 m is also consistent with the existence of this structure.

The very weak radar reflection at 135 m may represent the altered and fractured zone from 131.6 to 133.0 m, outside of the observed section. The reflection at 101 m differs in the orientation of structure 2198 m, and is not explained on the core.

5.4 Summary of interpretations

- Consistency of geological features as mylonite, cataclasite and hydrothermal alteration associated with the target structures are confirmed at the distance up to 5 m from the tunnel wall. Therefore these geological features are consistent nearly 20 m along strike and can be used as an indicators of the block scale water-conducting structures.
- It is difficult to locate and assume extensions of water-conducting structures only by inflow monitoring, radar survey and core mapping. As the current investigations, flow logging and borehole TV are necessary to precisely locate and orient the water-conducting structures. In addition, radar reflections seem to represent zones of increased fracture frequency (i.e. decreased density) irrespective of hydraulic conductivity rather than single open highly water-conducting fractures.

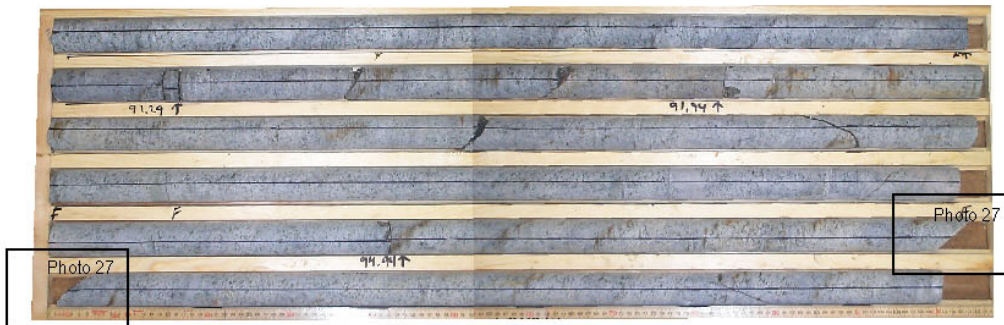
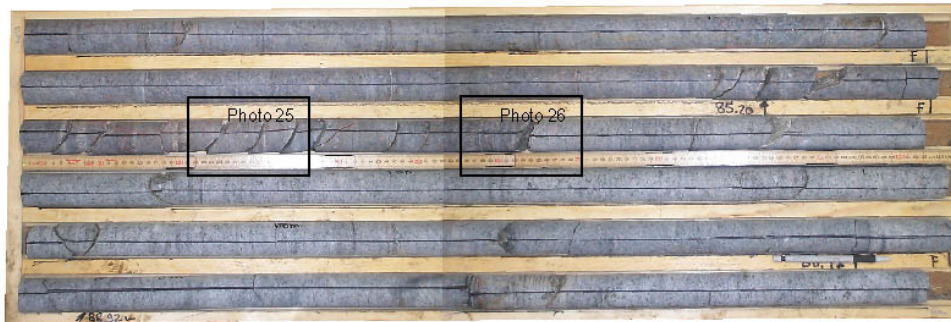


Photo 24: Section 1 whole view
Length of box = 120cm.



Photo 25: Section 1 No.9, No.10 and No.11
Parallel open fractures and random network veins of epidote.



Photo 26: Section 1 No. 16
An open fracture with clay coating, no visible alteration and ductile deformation.



Photo 27: Section 1 No.32
A slightly open fracture along epidote vein with calcite coating.



Photo 28: Section 1 No.34 and No.35
Open fractures along epidote-cataclasite with red alteration halo.



Photo 29: Section 2 whole view
Length of box = 120cm.



Photo 30: Section 2 No.7(left) and No.8 (right)
Fractures at the rim of mylonite.



Photo 31: Section 2 No.7
Fracture surfaces and fragments.

6 Conclusions

A certain connecting structure was not found in the area of target selection below 1500 m of the main tunnel, drifts and niches. The interconnected minor structures and the potential connecting structures were then selected and studied as target structures. Implications for the conceptual modelling of the block scale water-conducting structures are summarised in terms of structural geology, hydrology and transport of solutes.

structural geology

- All the target structures are faults. Plural activities of strike slip faults in different senses are suggested by the inconsistency of senses deduced from sub-horizontal striation, arrangement of possible splay cracks and displaced dikes on the tunnel outcrops. The target structures have more constituent coating/filling minerals than the other minor faults and fractures, reflecting their abundant hydrothermal events. In micro scale, at least two brittle events are recognised in all the target structures; 1) faults or fractures that formed mineral coatings/fillings or gouges, and 2) faults that cut 1) and formed gouges. Some structures follow preceding structures as mylonite and cataclasite.
- Internal geometry within each structure is highly heterogeneous and changes along its trace on the tunnel outcrops. It is impossible to discriminate between the potential connecting structures and minor structures by the geometrical indices as the complexity and type. The only possible discrimination is made for the most potential connecting structure in its longest history since the mylonite formation, the largest horizontal displacement and the largest maximum aperture compared to the other structures.
- Formation of the conjugate sinistral NNW and dextral NW to WNW structures is potentially proposed at the studied sites as well as one of the study sites of the SELECT project in the deeper level.
- Geological features as mylonite, cataclasite and hydrothermal alteration associated with the target structures are consistent nearly 20 m along strike, and can be potential indicators of the block scale water-conducting structures in boreholes.

hydrogeology

- There are hydrological anisotropies in the Site 1 and 2 where the NW trending structures are more water-conductive than those of the other orientations.
- Distribution of water on the target structures are highly heterogeneous, but the drop and wet spots tend to occur more at the branched or stepped parts, also at the intersections with the other fracture.
- Fractures and discharge spots are increased to some amount but the increases are less than variability within the structures, therefore the significance of the FIZ is not positively suggested.

transport of solutes

- All the target structures contain gouge in various amount and extent on their fault planes. The gouge consists of clay minerals and fine fragments of the pre-existing fracture coating and/or the wall rock. The clay minerals occupy 13 to 50% of the total amount of the gouge, and the dominant facie is either chlorite or chlorite-smectite mixed layer depending on the samples. Retardation of radionuclide by sorption on the clay minerals is expected in these structures.

Acknowledgements

The author thanks A Winberg of Conterra AB, M Uchida of JNC, L Stenberg of SKB, T Doe and J Hermanson of Golder Associates Inc., and E-L Tullborg of Terralogica AB for advices on the study plan, also M Mazurek of University of Bern and E-L Tullborg for comments on the results. The author also thanks SKB staff, L Stenberg for the field/underground guidance and all the logistics, T Hugo-Persson for preparation in the tunnel, E Eriksson and M Ohlsson for introducing database and visualisation systems. Finally, the author would like to express great thanks for the opportunity and encouragement for the study at Äspö HRL.

References

- Bäckblom, G. and Olsson, O., 1994:** Program for Tracer Retention Understanding Experiments. SKB Äspö Hard Rock Laboratory Progress Report, PR 25-94-24.
- Bossart, P., Hermanson, J. and Mazurek, M., 2001:** Analysis of fracture networks based on the integration of structural and hydrogeological observations on different scales. SKB Technical Report, TR-01-21.
- Eiben, T., Dershowitz, W., Takeuchi, S. and Uchida, M., 1999:** TRUE Block Scale project. Pathways analysis for fracture intersection zone effects on tracer test design. SKB Äspö Hard Rock Laboratory International Technical Document, ITD-99-21.
- Hermanson, J., 1995:** Structural geology of water-bearing fractures. SKB Äspö Hard Rock Laboratory Progress Report, PR 25-95-23.
- Hermanson, J. and Doe, T., 2000:** TRUE Block Scale Project. Traser test stage. March '00 structural and hydraulic model based on borehole data from KI0025F03. SKB Äspö Hard Rock Laboratory International Progress Report, IPR-00-34.
- Markström, I. and Erlström, M., 1996:** Overview of documentation of tunnel, niches and core boreholes. SKB Äspö Hard Rock Laboratory Progress Report, HRL-96-19.
- Mazurek, M., Bossart, P. and Eliasson, T., 1996:** Classification and characterization of water-conducting features at Äspö: Results of investigations on the outcrop scale. SKB Äspö Hard Rock Laboratory International Cooperation Report, ICR 97-01.
- Munier, R., 1995:** Studies of geological structures at Äspö. Comprehensive summary of results. SKB Äspö Hard Rock Laboratory Progress Report, PR 25-95-21.
- Morosini, M., 2001:** Äspö Task Force on modelling of ground water flow and transport of solutes. Proceedings from the 14th Task Force meeting at Säröhus, Sweden, November 14-16, 2000. SKB Äspö Hard Rock Laboratory International Progress Report, IPR-01-30.
- Rhén, I. and Forsmark, T., 2000:** High-permeability features (HPF). SKB Äspö Hard Rock Laboratory International Progress Report, IPR-00-02.
- Rhén, I., Danielsson, P., Forsmark, T., Gustavsson, G., and Liedholm, M., et al., 1994:** Geohydrological evaluation of the data from section 1475-2265 m. SKB Äspö Hard Rock Laboratory Progress Report, PR 25-93-11.
- Rhén, I., Gustafson, G., Stanfors R. and Wikberg P., 1997:** Äspö HRL - Geoscientific evaluation 1997/5. Models based on site characterization 1986-1995. SKB Technical Report, TR 97-06.
- Stanfors, R., Erlström, M. and Markström, I., 1997:** Äspö HRL - Geoscientific evaluation 1997/1. Overview of site characterization 1986-1995. SKB Technical Report, TR 97-02.
- SKB, 1994:** Supplementary investigations of fracture zones in the tunnel, core mapping data and radar measurement. Compilation of Technical Notes. Measurements performed during construction of section 1475-2265 m. SKB Äspö Hard Rock Laboratory Progress Report, PR 25-94-01
- Winberg, A., Andersson, P., Hermanson, J. and Stenberg, L., 1996:** Results of the SELECT Project. Investigation programme for selection of experimental sites for the operational phase. SKB Äspö Hard Rock Laboratory Progress Report, HRL-96-01.

Winberg, A., 1997: Tracer Retention Understanding Experiments (TRUE). Test plan for the TURE Block Scale Experiment. SKB Äspö Hard Rock Laboratory International Cooperation Report, ICR 97-02.

Winberg, A., Andersson, P., Hermanson, J., Byegord, J., Cvetkovic, V. and Birgersson, L., 2000: Final report of the first stage of the tracer retention understanding experiments. SKB Äspö Hard Rock Laboratory Technical Report, TR-00-07.

Winberg, A. (editor), 2000: TRUE Block Scale Project. Final report of the detailed characterisation stage. Compilation of premises and outline of programme for tracer tests in the block scale. SKB Äspö Hard Rock Laboratory International Progress Report, IPR-00-26.

Appendix 1

Table of description for the target selection

Appendix 1

Target Selection

location (m)	exist	FCC	HRL map	JH map	HPF	lithology	strike	dip	lineation	str type	duct def.	fault rock	coating/filling	T (m2/s)	Q (l/min)	wet%	water discharge	water discharge description	grout / s.c.	outcrop condition	nearby borehole	B	R	H	F	FCC investigations	remarks	1st select	2nd select	final select
1537	x	x	x	x		A, ±pm, F	20	80	?	2	?	?	chl?, cal?		0,0	100	d	d from fine splays on roof		strong precipitation								c		
1555	x	x	x	x		A, ±ap	338	80	338	10	1	±b	chl, epi, qtz			80	d	d from plane, splay										a	A	Site 1
1558	x	x	?	x		A	115	90	308	15	3		(not observed)	1,8E-08	0,1	100	f	f from master fault, many d from splays at step		strong precipitation (A)								a	A	Site 1
1570	x	?	x	x		A, ±me	115	85		1			(not observed)			100	d	d from plane and fine splays									a	A	Site 1	
1587	-		x	x		A	353						(not observed)	7,8E-08	0,3	0		dry		dry							d			
1594	-	x			?	A, ±G	0	80		3	?		(not observed)		27,6	0		dry		dry							d			
1602	x	x				A, ±F, ±G	30	70		1	m-s	b	(not observed)	2,9E-07	0,9	50	±f	dry A		partly sheeted					M		c			
1643	c	x	x	x										5,3E-07	2,7				s	completely covered							d			
1669	x	x	x	x		A	110	75		3			(not observed)	1,0E-11	0,0	60	±d	d at intersection with splays and other fracture							M		b			
1691	x	x	x	x	x	S, G	310	85		5			chl	2,9E-05	66,6	100	±f+d			roof sheeted, strong precipitation								b		
1695	x		x	x		S	310	90		2			clay?	2,9E-05	66,6	100	w	only wet									c			
1699	x	x	x	x		S, ±G	310	85		5			chl, epi, cal, clay	8,6E-08	0,1	100	d	d at intersection with splays		strong precipitation (A)								b		
1729	x		x	x		S	342	80		4?			chl?	9,6E-06	5,2	100	d	d at finely split ends									c			
1731	x	x	?			S, ±F	290	80		2			chl?	1,3E-05	8,9	100	d	d at ends of fracture/splay	g?								c			
1736,5	c	x			x	S, ±F	285	85					chl		3,0	100	f+d			most part sheeted							c			
1750	?		x	x																							d			
1763	c	x	x																	s	completely covered							d		
1842	x		x	x		S	10	80		3			chl		8,3	15	w	w at finely fractured part									c			
1845	x	x	x	x		A, S	20	70		3	w-m	c-b	qtz, ±chl		8,3	70	±d											c		
1853	x	x	?		x	A, ±F	142	85	?	3			chl	1,5E-05	31,3	100	d+f	d at intersection and end of splays, f spot at B floor										a	C	
1872	x	x	x	x	x	A, ±F	100	80	?	1	?	c-b	chl?	3,9E-05	102,0	80	d	d from plane		g	roof partly metal plate				M, Hg			b		
1876	x	x	x	x	x	A, ±F	105	85	?	3	w-m	c-b	cal?, chl	3,9E-05	102,0	100	f?	f? (covered)		±g	partly strong precipitation and metal plate				(LC?)			a	C	
1907	x						342	75	342	10	1		cal(in)-epi-chl			100	d	d from plane and splay intersection									b			
1924	x		x		x	A, ±F	340	80	340	40	1		chl, epi, cal			75	d	d at splay end and intersection with fractures, dry B		g							a	C		
1988	x		x			A	13	75	13	10	1		chl, clay			100?	±d	minor d at roof and side walls		±s	roof partly sheeted						c			
1990	x	x	x	x		A, S, ±F	290	90	285	10	4	?	c-b	chl, epi, cal		2,0	100	f	strong flow		roof sheeted	KA2050A	x	x	x	DM, M, Hg		b		
2012	?		x	x	x									1,1E-04	57,0						not exist						d			
2020	c	x	x	x	x	S, A, F	325	75		5?			epi?	2,2E-08	0,2	100?	?			s	roof-sides shotcreted, strong precipitation	KA2048B	x	x				c		
2028	?		x	x	x									2,1E-04	20,2						roof sheeted							d		
2059	x		x	x	x	A	300	70		1-3			chl?			90	d	d intersection with conjugate fracture(210/75)									c			
2062	x	x	x			A, S, ±F	300	90	?	1			chl			90	d	d from plane		±s								c		
2075	-		x	x		S	82	60					(not observed)			0		dry		dry								c		
2090	x	x	x	x	x	S, ±F	114	90		2			cal, ±chl?	1,5E-03	500,0	100	w	wet along plane and splays		±g								a	B	
2098	-		x	x	x	S	310	75					(not observed)	7,0E-04	291,0	0		dry		±g	dry							c		
2120	c		x	x	x											43,0				s	completely covered	KA2048B	x	x				d		
2150	x	x	x	x	x	A, ±F	120	90		1			chl?	2,9E-05	4,0	90	d	d from fine fracture/ress between planes		g								c		
2154	x	x	x	x	x	A	140	85		1	c-b	chl, cal	7,6E-05	5,9	100	f	f from plane(B), intersection with splays		g	strong precipitation	KA2048B	x	x					a	B	Site 2
2155	x		x	x		A	130	80		1			(not observed)	7,6E-05	5,9	100	d	local d from plane										c		
2163	x	x	x	x	?	A	140	90		1	±c		(not observed)	2,9E-07	0,1	100	f	strong f from walls at A and niche			KA2048B	x	x					a	A	Site 2
2178	-		x	x		A, ±F	300	75					(not observed)	6,9E-09	0,0	0		dry		dry								c		
2198	x	x	x	x	x	A, ±F, ±G	115	90		3	w-m	c-b	chl	3,4E-05	3,0	50	f	dry roof, strong flow at A, only wet at B		g		KA2048B, KA2162B	x	x	x			a	A	Site 3
2208	x		x	x		A, ±G	281	85		1			chl		0,2	90	d	d at intersection with fracture, plane										b		
2209	x		x	x		A, ±G	305	90					(not observed)		0,2	100	d	d at intersection with fracture, splays, plane			strong Mn precipitation							b		
2220	x	x	x	x		A, ±F	115	90	?	3	?	±c	chl?		0,2	90	d	d at plane, splays			extensive Mn precipitation	KA2048B	x	x				b		
2230	x	x	x	x	x	F, A	316	85		5	w	b	chl	3,4E-05	54,2	70	d	d at fine splay fracture		g	strong precipitation							c		
2282	x	x	x	x	x	F, A	142	80	135	10	3	w	±c	chl, ±chl	0,3	90	d	d at plane, splays		g	roof partly metal plate, A strong precipitation							c		
2291	?	x	?	x		A, F	292	70		1			(not observed)		0,2	100	d	d at plane, split end(fine fracture) on roof			entire precipitation							d		
2295	x		x	x		A, ±F	178	70		1			(not observed)		0,2	20	±d	minor d at splays, split end(fine fracture)										c		
2298	x		x	x		A, ±F	310	80		2			(not observed)		0,2	90	d	d from plane, splays										c		
2301	x	x	x	x		A	0	70	?	1		±b,c,g	chl, clay 1cm		0,4	100	d	d from plane, splay intersection										c		
2305	x	x	x	x	x	A, ±F, ±me	140	80	140	0	4	?	b-g	chl, cal		0,2	60	d	d from plane, A wet, B relatively dry		g							a	C	
2311	x	x	x	x		A, ±F	315	80	88	5	1		chl?	2,1E-07	0,9	100	f+d			strong precipitation, roof-side sheeted								c		
2338	x	x	x	x		A, ±F, ±G	315	80	?	3	?	?	chl, clay?	5,6E-07	0,3	90	d	d at fine splays, plane			strong precipitation and dust							c		
2351	?	x	x	x		A, ±F							(not observed)	5,6E-07	0,3												d			
2369	x	x	x	x		A, ±me, ±F	310	80		1	±c,b	chl, epi	6,7E-06	3,5	100	d	d at fine plane, splays (more at fine fracture in f)		g	entire precipitation of Mn	KA2048B	x	x					b		
2430	x	x	x	x		A, ±me, ±F	345	88	333	7,5	1	b±g	cal, epi, chl	1,0E-07	0,0	80	d	d at intersection with splays (fine fracture), dry A										b		
2460	-		x	x		A, G, ±pg	188	50		1			chl, clay			15	w	w at intersection with minor steep //fractures // to tunnel										d		
2477	c	x	x	x		F, A, G, M	25	70																						

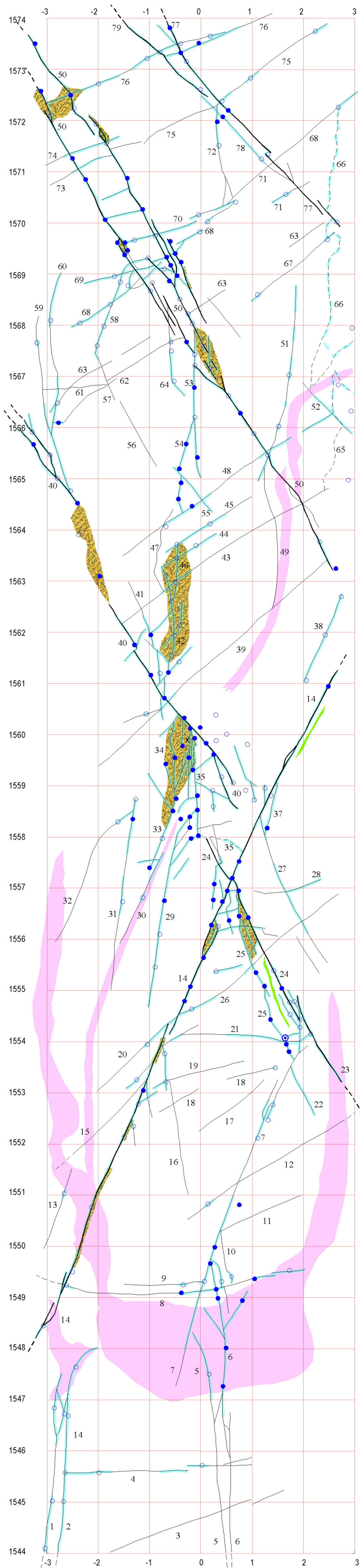
Appendix 1

Target Selection

Location (m)	exist	FCC	HRL map	JH map	HPF	lithology	strike	dip	lineation	str type	duct def.	fault rock	coating/filling	T (m2/s)	Q (l/min)	wet%	water discharge	water discharge description	grout / s.c.	outcrop condition	nearby borehole	B	R	H	F	FCC investigations	remarks	1st select	2nd select	final select
2849	x	x	x			A, ±S	355	80		1			chl, cal	3,6E-08	0,3	80	±d	minor d from plane			KA2858A	x	x				sinistral groove on plane (A)	c		
2860	x	x	x			M	350	45	105?	50?	1	s	c-b			70	d	d at fine fractures near plane and plane itself	±s							ductile(mylo) zone 20cm, trace striation - thrust?, 1 diverging wc-fracture (115/80)	a	B		
2862	x	x	?			A, ±S	20	75		1			chl	-	0,0	100	d	d at fine fracture along plane, intersection with other fracture								cross-cut the diverging fracture, merge to 2660 at B, end at A roof	a	B		
2877	x	x	x			A, F	5	80		1			qtz(jn)-cal-chl 2mm			40	±d	minor d from plane, wet roof, dry B								trace 6m, end at A roof	c			
2914	?					A								1,8E-04	400,0				S	not exist						fracture zone(NW-3, NNW-4w) boundary, no NNW fracture	d			
2929	?					A								-	73,2				S	not exist						fracture zone(NW-3, NNW-4w) boundary, no NNW fracture	d			
2935	x	x				A, ±F	140	90	320	15	3		cal, chl	2,5E-09	0,0	40	d	d finely fractured plane near WNW structure	±g, ±s							end in shotcreeet at A roof	b			
2940	x						310	80	140	10	1		chl?, cal?			40	d	d plane, intersection with fine splays								sinistral striation?/groove on plane (B)	b			
3058	x	x	x			S,A	135	80	315	15	1	w	±c			10	d	d at intersection with 3059m, discontinuous extension to niche			KA2050A	x	x	x		almost dry feature merging to 3059, extension?(145/80) intersect E-W wc-fracture at niche	a	B		
3059	x	x	x			S,A	120	75		3or4	m	c-b	chl	-	0,0	100	d	d at fine fracture at branch and intersection with 3058m			KA2050A	x	x	x		NW-3(?), ductile prec. breccia 5-1m, roof D-shape branching, extension to niche 3058A (LTDE)	a	A		
3083	x	x	x			A,G	295	80		3?	m	c-b	chl	1,9E-08	0,0	90	d±f	d from finely fractured splays, f ?(covered)			KA3105A, KA2050A	x	x	x		ductile zone 0.3m, crush/breccia, long splays B, G at A(relatedly dry)	b			
3085	x	x				A,M	135	85	320	10	2		chl, cal, epi 1mm	1,9E-08	0,0	60	d+f	d from plane, intersection splays, f from sub// fracture(130/80)			KA3105A, KA2050A	x	x	x		ductile precursor mylo 10-20cm, chl-cal-py(euhedral) filling 5mm (B)	a	C		
3089	x	x	x			A	140	80		3?	m	c-b	chl?			100?	f	f from splay near main fracture			KA3105A, KC0045F, KA2050A	x	x	x		not well observed	b			
3095	x	x				S	105	70		1			chl, clay?			70	d	d intersection other fracture and fine splays, plane			KA3105A?	x	x	x		curved, not reach to B - minor, trace 7m	b			
3102	x	x	x			A	300	80	?	1			chl, clay, cal, epi, fluo	-	0,7	55	d	d from plane, splay			KA3105A, KC0045F	x	x	x		ductile, breccia/crush 0.5m, follow epi-fluo vein, conjugate wc-fracture(100/75), B-roof dry	a	B		
3109	x	x				A	120	90	120	5	1		chl, cal(5mm), ±clay, ±ep	-	0,7	95	d	d at split ends, fine splays, plane			KA3105A, KC0045F?	x	x	x		trace >10m, sinistral striation on //fracture at niche(split close to end), meet KA3105A at 1-2m?	b			
3124	c	x	x											3,4E-04	67,2				s	completely covered	KA3110A, KC0045F	x	x		DM,M.P,Hg,LC					
3132	c																		s	completely covered	KA3110A, KC0045F	x	x							
3136	c																		s	completely covered	KA3110A, KC0045F	x	x							
3152	c																		s	completely covered	KA3110A, KC0045F	x	x							
3164	c																		s	completely covered	KC0045F	x	x							
3195	x	x	x			A, ±F	116	75		1			(not observed)			100	d	d from splays	g	precipitation	KC0045F, KXZC1-7	x	x	x		extension at ZEDEX side	b			
3204	x	x	x			A	108	90		1			(not observed)			60	±d	minor d from plane	g	precipitation	KC0045F, KXZC1-7	x	x	x		minor, B not distinct(end at B roof), extension at ZEDEX(LC)	b			
3230	x	x	x			A,M	30	70		1	s	g	chl, epi-qtz 4-5cm			70	d	d intersection with splays			KC0045F	x	x		M, P, Hg, LC	10cm mylonite zone, open one side of epi-qtz vein(LC), many discontinuous branches B	c			
3234	x	x	x			A,M	20	80		1	s		chl?			0,0	100	d±f	d at splay and intersection with fracture, ±f intersection with subhoriz fracture			KC0045F	x	x		mylonite zone // to 3230	c			
3275	x	x	x			A	115	75		1	w	±b	chl?			100	f	strong f at intersection with fractures on A, d from plane, intersection with diverg wc-fracture	g	strong Fe precipitation	KC0045F	x	x			connected minor fractures, 115/75(A) to 85/80(B), diverging wc-fracture(85/80, d, 100%)	b			
3278	x	x	x			A	110	90		1	w	±b	(not observed)			100	f	f ?(covered)			KC0045F	x	x			entire precipitation, roof-side sheeted	c			
3279	x	x	x			A	120	90		1			(not observed)			0,1	90	d	d from plane			KC0045F	x	x		B foot not obvious (precip from 3278m), weaker than 3278m	c			
3283	?					A										100	d	many d from minor fracture <3m			KC0045F	x	x			strong and entire precipitation	d			
3287	x	x	x			A	75	85		1						80	±d	minor d from plane, intersection with subhorizontal wc-fracture	g	strong shotcreeetprecipitation	KC0045F	x	x			minor, trace 4m, end at subhorizontal fracture on B	c			
3291	x	x	x			A	130	90		1						100	d	d from plane, f from minor fracture(1m) on B			KC0045F	x	x			Fe precipitation	c			
3297	x	x	x			A	120	90		1			chl?			0,0	100	d	no flow, d from plane	g	Fe precipitation	KC0045F	x	x			Fe precipitation	c		
3307	x	x	x			A	120	80		1	m		chl?			0,0	100	d	d from plane on roof			KC0045F	x	x			precipitation	b		
3313	x	x	x			A	125	90		1	w		(not observed)			0,0	100	d±f	f/d from plane			KC0045F	x	x			precipitation	b		
3314	x	x	x			A	90	90		1			(not observed)			100	f	f spot on plane (A)			KC0045F	x	x			strong and entire precipitation	c			
3362	c					A	115	90		1?			(not observed)			?	d		±s	blasted, roof shotcreeet and sheeted						minor, not reach to B, exposed niche only, not well observed	d			
3363	c					A	305	85		1?			(not observed)			?	d		±s	blasted, roof shotcreeet and sheeted						minor, end at B roof (split), exposed niche only, not well observed	d			
3393	x	x	x			A, ±F	310	75		1			chl, cal 2mm	4,8E-06	115,0	10	d	d from plane, dry A	g	blasted for door						relatively dry feature or grouted?	c			
3401	x	x	x			A	295	85		1	m	c	chl-epi-±qtz, cal	4,8E-06	115,0	90	±d	minor d from plane, f from nearby minor fracture with fine splays	g	cleaned						mylonite 2cm, shear/brittle 10-20cm, distinct flowpath by cal vein, extension N3384A?	c			
3405	x	x	x			A	105	90		1			chl, epi, cal	4,8E-06	115,0	90	w	wet on plane	g	cleaned	KA3385A	x	x	x		minor, trace 3m, end at B roof, grouted?	c			
3416	x					A	130	80		4?	w?	c?	qtz, epi, chl			80	d	d from planes, dry B	g	extend to niche 3419B						discontinuous fracture following epi? vein, many branches, end at A	b			
3430	x	x	x			A, ±F	290	80		1	w		chl, ±cal			100	f+d	d from plane, f covered								branch out at A, 30cm ductile(mylo) zone	b			
3443	c					A	300?	85		1			chl	4,1E-06	22,1	100?	f	?	g	roof-side sheeted, strong precipitation						not well observed	c			
3446	x	x	x			A	295	80	285	10	1	w?	chl, epi, qtz, cal	4,1E-06	22,1	100	f	f from both sides of floor, plane and fine fractures on A	g	cleaned, still strong precipitation						interconnected minor fractures(290/80, 300/75), mylonite or qtz-epi vein 2cm, brittle 5cm, cal vein	b			
3460	x	x	x			A, ±F	123	90		1	w?		qtz-epi, chl	6,5E-07	0,5	100	d	d intersection with fracture on roof	g	precipitation B						branch out to two, split fine fracture zone 10-20cm	b			
3465	x					A	132	85		1	w	±c	epi-qtz?, cal	4,1E-08	0,2	100	d	d intersection with splay and other fracture	g							duct/brit zone 5cm, cal vein 1mm	b			
3467	x					A	123	90		1			epi-qtz?, cal	4,1E-08	0,2	100	d	d at splay, branch and plane	g							simple single fracture, cal vein 3mm,	b			
3468	x	x	x			A	116	90		1	m	±c	qtz-epi, chl, cal			100	d	no flow, d from branch and splays	g					5 / 10cm LC	mylonite / qtz-epi vein 3cm cut by cal, 10cm core sampled	b				
3482	c					A	140	80		1			(not observed)			100?	w	entirely wet								not well observed, minor, weaker split end on B	c			
3500	?	x	x			A, ±F	140	80		3			chl			70	d	d from plane, splays	g					M, P, Hg	minor fractures, trace 2-3m, not well observed	d				
3510	?					A, ±F	280	80		5			chl			50	d	d from fine fractures in F								trace 4m, complex with ±f, not well observed	d			
3538	x	x	x			A	160	90		1	g?		chl	1,7E-06	27,7	70	d	d at intersection with small shallow fracture			KA3510A?	x	x	x		PRP Sec 2 plugg excavation	c			
3540	x	x	x			A	115	90		1			(not observed)			95	±d	d intersection with minor fracture, plane								minor, trace 5m, one end at minor fracture other end extinct	c			
3545	x	x	x			A	110	85		1			(not observed)			60	w	w on plane			KA3510A?	x	x	x		minor, trace 5m, end at B (no extension to blasted part)				

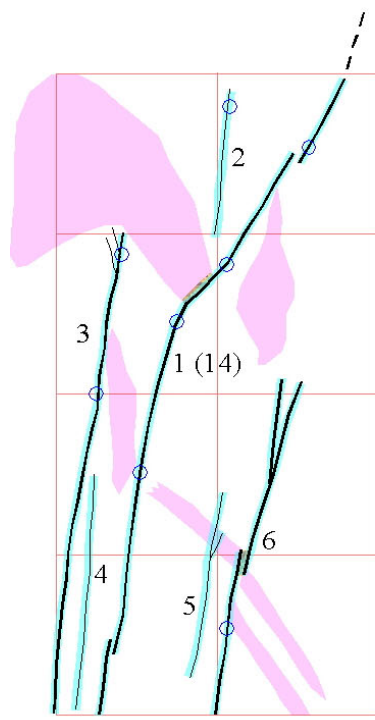
Appendix 2

Maps of the detailed tunnel mapping

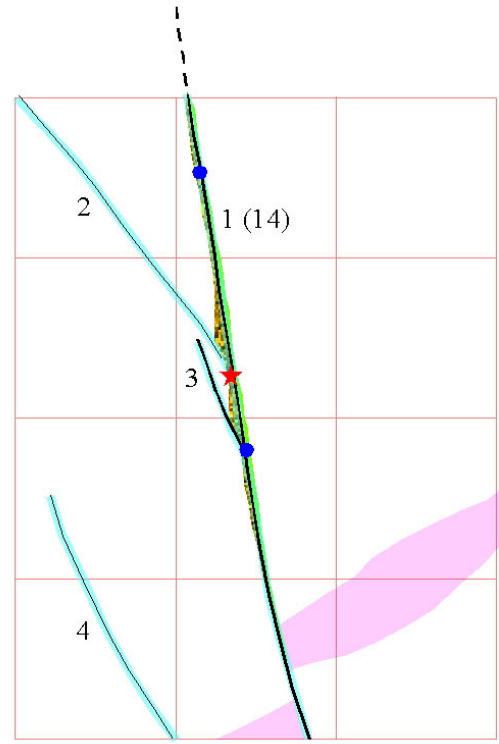


Detailed mapping
 Site 1 ceiling
 - projected to floor -
 Map 1

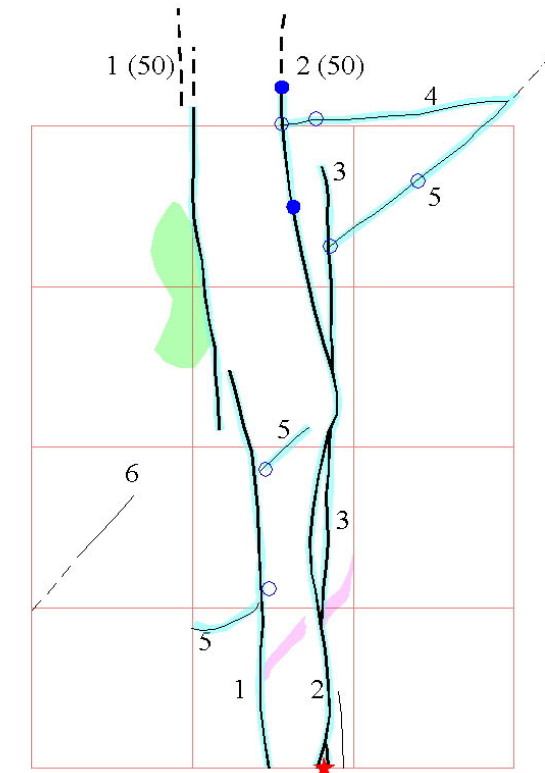
- Legend
- Aspö diorite
 - Fine-grained granite
 - cataclasite
 - crush breccia
 - fault
 - fracture
 - fracture (shallow dip)
 - blasting hole
 - flow
 - drop
 - moist
 - wet



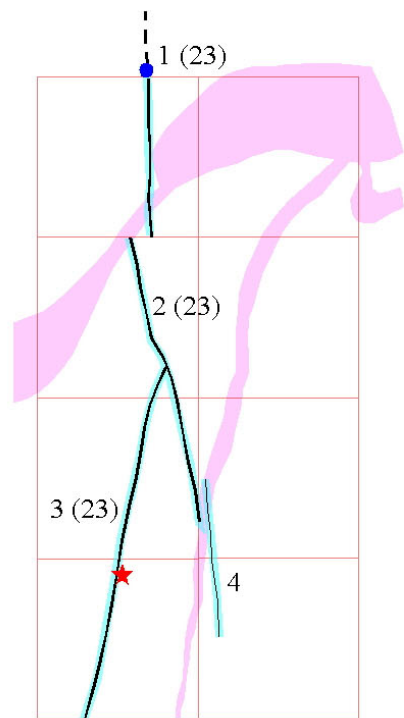
1545A



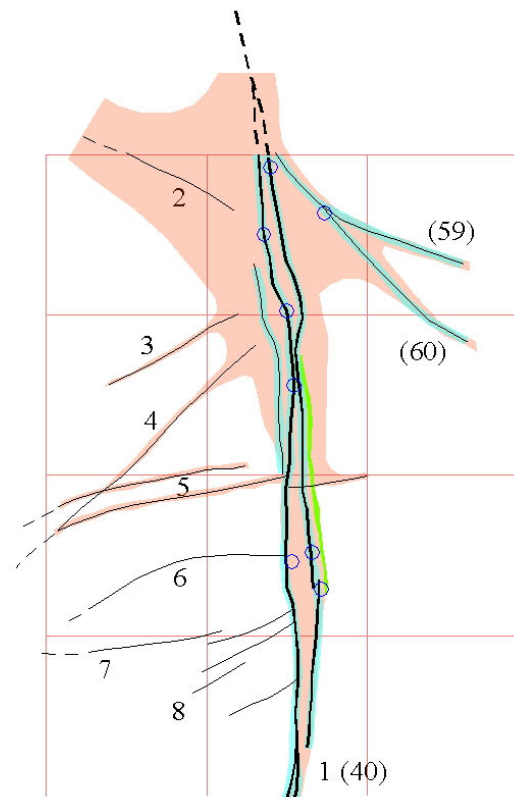
1561B



1573A



1553B

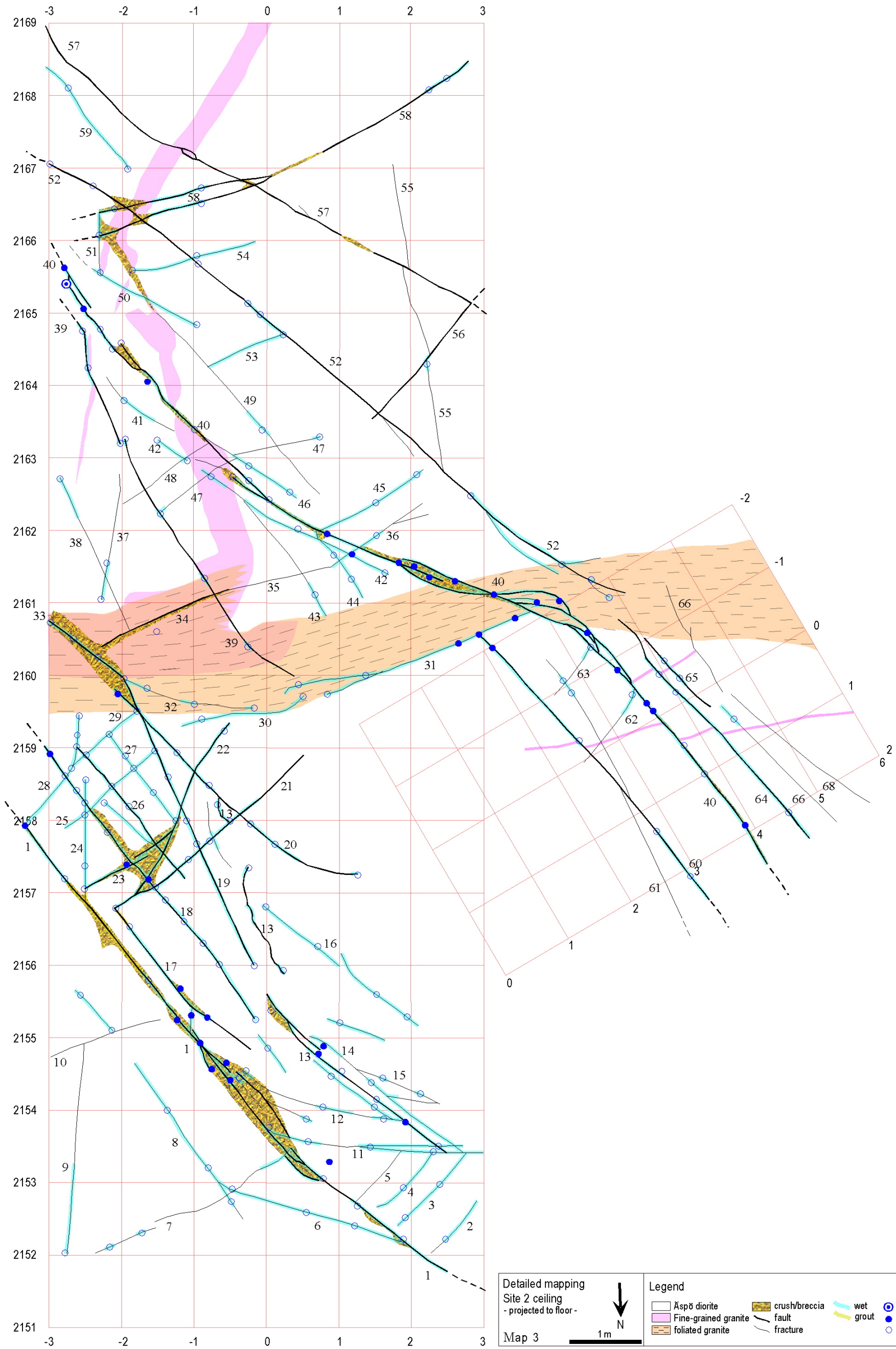


1566A

Detailed mapping
Site 1 sidewalls
- projected to plane normal to structure -
Map 2

Legend	
Åspö diorite	epidote-cataclasite
Fine-grained granite	crush/breccia
green stone	fault
hematite alteration*	other fracture
	sampling point
	flow drop
	moist
	wet

* 1566B only. Not well observed in other locations due to bad outcrop condition.



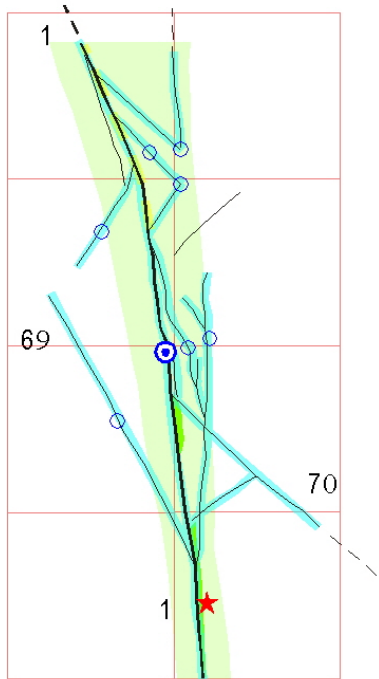
Detailed mapping
Site 2 ceiling
- projected to floor -

Map 3

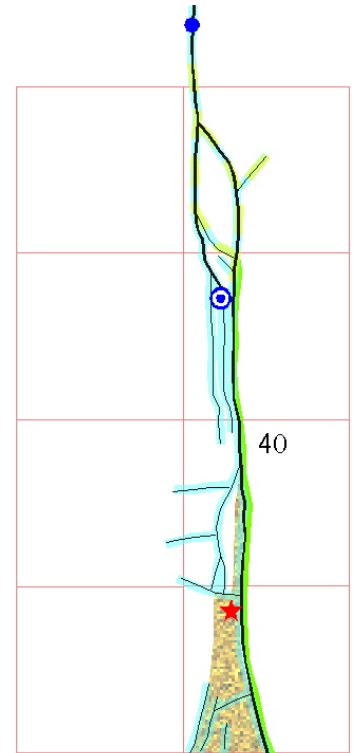
1 m

Legend

Äspö diorite	crush/breccia	wet grout	flow drop
Fine-grained granite	fault	grout	drop
foliated granite	fracture		moist

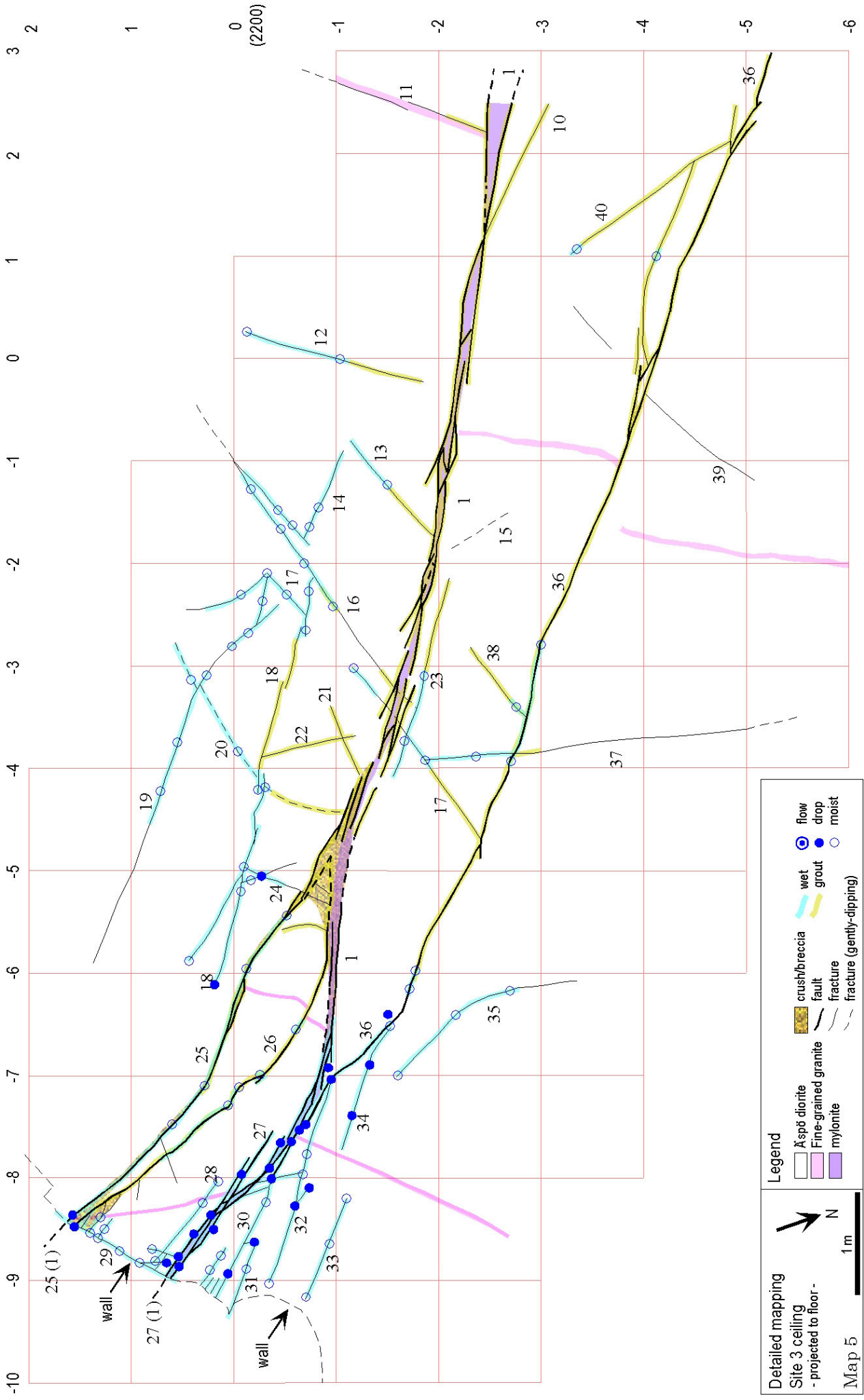


2151B



Niche 2156B

<p>Detailed mapping Site 2 sidewalls - projected to plane normal to structure -</p> <p>Map 4</p> <p style="text-align: right;">1 m</p>	<p>Legend</p>		
	<p>□ Åspö diorite</p> <p>□ Fine-grained granite</p> <p>□ epidote alteration</p> <p>□ epidote-cataclasite</p>	<p>■ crush/breccia</p> <p>— fault</p> <p>— other fracture</p> <p>★ sampling point</p>	<p>⊙ flow drop</p> <p>○ moist</p> <p>— wet grout</p> <p>— grout</p>



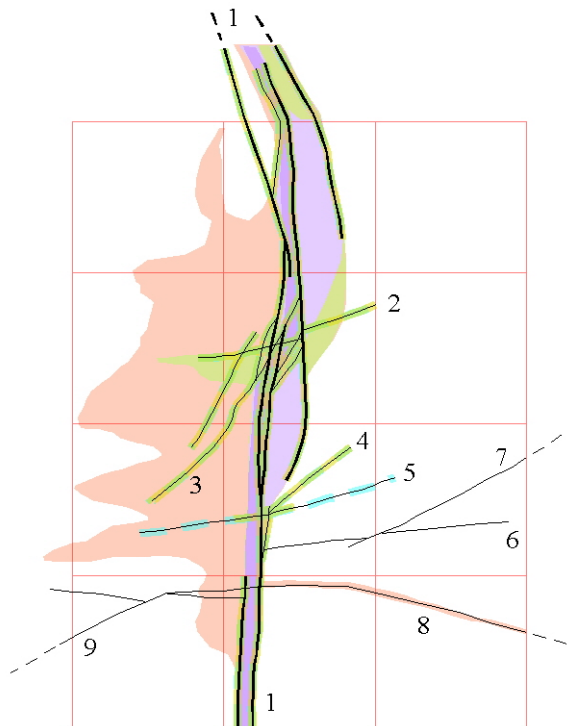
Detailed mapping
 Site 3 ceiling
 - projected to floor -

Map 5

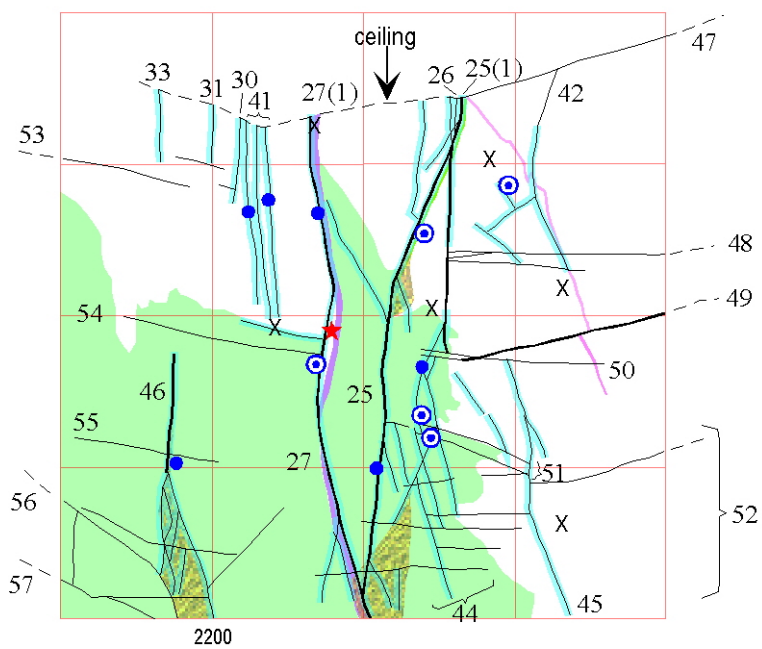
Legend

- Aspd diorite
- Fine-grained granite
- mylonite
- crush/breccia
- fault
- fracture
- fracture (gently-clipping)
- flow
- wet
- drop
- moist
- grout

N
 1 m



2198B



Niche 2198A
(wall orientation: 58/90)

Detailed mapping Site 3 sidewalls - normal to structure -		Legend	
Map 6	1 m	Åspö diorite	crush/breccia
		Fine-grained granite	fault
		green stone	other fracture
		mylonite(moderate/weak)	hematite alteration
		epidote-cataclasite	epidote alteration
			flow
			drop
			moist
			wet
			grout
			sampling point
			X blasting hole

Appendix 3

Tables of descriptions for the detailed mapping

Appendix 3: Detailed mapping description

LEGEND

No.	reference number in the map		
type	type of the feature		
	fr	fracture	displacement/slip along fracture is not obvious
	ft	fault	displacement/slip along fracture is observed or positively assumed
	sp	splay crack	tensile crack associated/connected with master fault
host	host rock		
	A	Aspö diorite	
	S	Småland grante	
	F	Fine-grained granite (including dikes/veins of leuco-granite and pegmatite)	
	G	green stone	(±: subordinate)
relation	relationship to the host rock		
	c	cutting	
	f	following	
ductile def.	intensity of ductile deformation (mylonitization) along the feature		
	w	weak	
	m	moderate	
	s	strong	
fault rock	cohesive and incohesive fault rock		
	cat	cataclasite	lithified fault breccia
	c	fault crush	fragments>90% matrix <10%
	b	fault breccia	fragments 90-30% matrix 10-70%
	g	fault gouge	fragments<10% matrix >90%
			(±: subordinate)
strike, dip	More than one value are put if orientation changes or if the feature has plural planes. Italic means orientation of the feature as a whole.		
lineation	orientation of slicken line and sense of slip		
	d	dextral	
	s	sinistral	
length	trace length		
	Italic means the feature extends beyond tunnel wall.		
width/apert.	range of aperture and width of fault rock(z)		
rough	shape along strike		/ surface condition
	s	stepped	r rough
	u	undulating	s smooth
	p	planar	p polished
filling/coating	nature and thickness of fracture filling/coating materials, ordered from outer to inner		
	cal	calcite	
	chl	chlorite	
	clay	clay minerals	
	epi	epidote	
	py	pyrite	
	grout	grout cement	(±: subordinate)
f/c%	approximate area filled/coated in a feature		
alteration	nature and width of alteration halo along strike		
wet%	approximate wet area an a feature		
seep.	type of seepage		
	m	moist	wet but little dripping(within c.a. 30 sec.)
	d	drop	dripping
	f	flow	continuouse flow
			(±: subordinate)

Appendix 3

Detailed Mapping - Site 1

No.	type	host	relation	ductile def.	fault rock (cm)	strike (deg)	dip	lineation	length (m)	aperture (mm)	roughness	coating / filling (mm)	f/c%	alteration (cm)	wet%	disch. type	discharge description	remarks		
1	fr	A, F	c	no	no	325	80		5	?	p-u/s	chl? <0.5	100?	no	60	w	plane	F: leuco-granite		
2	fr	A, F	c	no	no	330	75		5	?	p/p	chl <0.5	100	no	100	±d	plane	Mn precip., F: leuco-granite		
3	fr	A	c	?	?	10	75		4	?	p/s-p	chl	100	no	0					
4	fr	A	c	?	?	45	85		5	?	p/s-p	chl?	100?	no	30	w	int. minor fracture	cut by No. 2		
5	fr	A, F	c	?	?	305	80		6	?	?	?	?	?	10	w	wheather fracture near N end in FGG			
6	fr	A, F	c	?	?	128	90		7	?	p-u/s	chl?	?	?	40	d	plane, splay? in FGG, int. No. 8			
7	fr	A, F	c	?	?	158	90		7	?	p/s	chl?(local)	?	fsp red?	50	±d	plane			
8	fr	A, F	c, f	no	no	210	65		5	1-2	p/s	chl 1-2, cal 0.2	100?	no	30	±d	plane, int. No. 7	reactivated vein boundary		
9	fr	A	c	?	?	210	65		2	?	?	?	?	?	30	w	plane, int. No. 7	// to No. 8		
10	fr	A	c	?	?	120	90		1	?	?	?	?	?	30	w	matrix near fracture?	area entirely wet		
11	fr	A	c	?	?	5	70		2	?	p/s	chl, cal?	100?	no	0					
12	fr	A, F	c	no	no	12	65		4	?	p/s	±chl?, ±cal?	?	no	3	±d	int. minor fracture			
13	fr	A, F	c	?	?	335	70		4	?	p/s	chl, epi	?	no	5	w	near int. FGG dike			
14	FT	A, ±F	c	no	±cat?<3, ±c<20, g<0.2	334	78	335	10	s	19	0.5-2	p-u/s-p	±epi <1, chl <1, cal <2, clay<2	100	white at crush, local epi, mod red<3	95	d	plane, fracture int.	at 1545A: slicken by chl stretch. at 1560m: epi vein or cataclasite? at 1561B: cal local patch some euhedral, local epi veins<10mm and alt<3cm along fracture = cataclasite?, slicken&step on coating(cal, chl)
15	fr	A, ±F	c	no	no	340	60		2	<0.5	?	?	?	no	0					
16	fr	A	c	?	?	120	90		2	?	?	?	?	no	5	w	plane, int. No. 19	weak crush at int. No. 14		
17	fr	A	c	?	?	10	55		2	?	?	?	?	no	0					
18	fr	A	c	?	?	20	45		2	?	?	?	?	no	10	w	fracture end			
19	fr	A	c	?	?	20	55		2	?	?	?	?	no	10	w	plane, int. No. 16			
20	fr	A	c	?	?	20	35		2	?	?	?	?	trace red	40	w	plane	end at stepped part of No. 14		
21	fr	A	c	?	?	50	85		2	?	p/s	chl?	?	no	70	w	plane, int. No. 23, 25			
22	fr	A	c	no	no	95	50		1	?	p/s	chl	100	no	100	w	plane			
23	FT	A, F	c	no	±cat<3, ±g<0.1	110	87	112	13	d	7	1-2	p-u/s	±epi <0.5- chl <1, cal <2, ±py, ±clay<1,	100	wk-mod red<5	100	w	plane	at 1553B: discontinuous/branched, epi-cataclasite?, two generations of cal, thick grey layer (healed gouge?) and white patch.
24	FT	A	c	no	±cat?<3, ±c<30	294	88		4	?	p/s	±epi?	?	±epi	80	±d	plane	// epi filled fracture or cataclasite? at 1555B roof. local crush zone between No. 25.		
25	FT?	A	c	no	±c<30	120	90		3	?	s-u/s	?	?	?	85	f	plane near int. No.21			
26	fr	A	c	?	?	8	65		4	?	u/s	±cal?	?	no	30	w	plane, int. No. 24, 25	curved fracture		

Appendix 3

Detailed Mapping - Site 1

No.	type	host	relation	ductile def.	fault rock (cm)	strike (deg)	dip	lineation	length (m)	aperture (mm)	roughness	coating / filling (mm)	f/c%	alteration (cm)	wet%	disch. type	discharge description	remarks
27	fr	A	c	?	?	123	78		3	?	p/s	chl?	?	no	50	w	plane	curved fracture
28	fr	A	c	no	no	48	85		3	?	p/p	chl	100?	no	70	±d	int. No. 27, plane	
29	FT?	A	c	?	?	322	80		4	?	p/s	cal?	?	?	100	d	plane	sinistral displacement?(1-2cm) of int. fracture, branched end
30	fr	A, F	f	?	?	332	75		2	?	?	?	?	?	40	±d	plane	following FGG vein
31	fr	A	c	?	?	350	38		4	?	p/s	chl?	?	no?	50	±d	plane	
32	fr	A	c	no	no	315	70		4	?	p/s	chl	100?	red 2	0			
33	fr	A	c	?	?	147	90		2	?	?	?	?	?	100	±d	plane	Fe, Mn precipitation in crush zone
34	fr	A	c	?	?	143	75		2	?	?	?	?	?	100	d	plane, fractured matrix	crush or excavation damage zone boundary
35	fr	A	c	?	?	137	80		2	?	?	?	?	?	100	d	plane, fractured matrix	near blast hole, crush or excavation damage zone boundary
36	fr	A	c	?	?	260	20		2	?	p/s	chl?	?	?	60	±d	fracture int., plane	shallow dipping fracture
37	fr	A	c	?	?	333	75		1	?	p/p	cal?	100	?	100	d	plane	splay of No. 14?
38	fr	A	f	no	no	162	65		2	?	s/s	chl	100?	no	100	w	plane	following margin of FGG vein(5cm)
39	fr	A, ±F	c	?	?	5	55		6	?	p/s	chl?	?	no	5	w	int. No. 40	
40	FT	A	c	no	±cat <3, ±c-b<30, ±g<0.1	113	84		9	1-2	p-u/st-s-p	chl <0.5, ±cal <2, ±clay<1	90	mod red 5-50 irregular	98	d	plane, crush zone	1566A: epi-cat? <3cm in rock 5cm away from sub-fault.
41	fr	A	c	?	no	126	74		3	?	?	?	?	?	60	d	fracture int., plane	
42	FT?	A	c	?	c-b 10-30	133	90		2	?	?	?	?	?	100	±d	plane, crush zone	in crush zone
43	fr	A, ±F	c	?	?	15	70		5	?	?	?	?	?	30	w	int. No. 42(c.z.), ±plane	
44	fr	A	c	?	?	15	65		1	?	?	?	?	?	100	w	plane, crush zone	Fe, Mn precipitation
45	fr	A	c	?	?	15	65		2	?	?	?	?	?	70	±d	plane	Fe, Mn precipitation
46	FT?	A	c	?	c-b<30	150	70		1	?	?	?	?	?	100	±d	plane, crush zone	Fe, Mn precipitation
47	fr	A	c	?	?	155	45		2	?	p/s	chl?	?	no	0			
48	fr	A, ±F	c	?	?	12	70		5	?	?	chl?	?	no?	50	d	plane	
49	fr	A	f, c	?	?	146	85		3	?	?	?	?	?	0			partly follow FGG vein
50	FT	A, ±F, ±m	c	no	±c-b<40, ±g	110	86		12	0.5-2	p-u/s-r	±epi<0.5, chl <0.5, cal <2, ±clay<0.5	90	±wk red?	90	d	plane	minor dextral displacement(<1cm?) of FGG vein at 1565B roof, cal local patch/layer
51	fr	A	c	?	?	156	83		4	?	p/s	chl?	?	red? 1	40	±d	plane	basically dry?
52	fr	A, ±F	c	no	no	290	75		3	?	p/s	chl, ±cal?	100	no	70	w	plane, int. No. 65	
53	fr	A	c	?	?	140	65		3	?	p/s	chl?	100?	?	95	d	plane	
54	fr	A	c	?	?	144	60		2	?	?	?	?	?	100	d	plane	Fe, Mn precipitation
55	fr	A	c	?	?	120	80		1	?	?	?	?	no	100	w	plane	

Appendix 3

Detailed Mapping - Site 1

No.	type	host	relation	ductile def.	fault rock (cm)	strike (deg)	dip	lineation	length (m)	aperture (mm)	roughness	coating / filling (mm)	f/c%	alteration (cm)	wet%	disch. type	discharge description	remarks
56	fr	A	c	?	?	122	90		2	?	p/s	chl?	?	no	0			
57	fr	A	c	?	?	295	85		1	?	p/s	chl?	?	no	10	w	near int. No. 58	
58	fr	A	c	?	?	340	75		2	?	?	?	?	no?	90	±d	plane	curved, dust/Mn precipitation
59	sp?	A	c	no	no	304	88		3	1	p-u/s	chl <0.5, cal <1	100	no	10	w	plane	cal patch
60	sp?	A	c	no	no	324	72		4	1	u/s	chl <0.5, ±cal <1	100	no	60	w	plane	cal local patch
61	fr	A	c	?	?	20	80		3	?	?	?	?	?	0			
62	fr	A	c	?	?	10	70		3	?	?	?	?	no	0			
63	fr	A	c	?	?	10	55		6	?	p/s	chl?	100?	no	0			
64	fr	A	c	?	?	138	90		2	?	?	?	?	?	50	±d	plane	
65	fr	A	c	?	?	280	5		4	?	p/s	±chl	70?	red?	100	±d	plane	
66	fr	A, ±F	c	?	?	290	15		6	?	p/s	±chl	20?	red	15	±d	plane	
67	fr	A	c	no	no	5	70		3	<0.5	p/s	chl	80?	no	30	w	plane, int. No. 66	
68	fr	A	c	no	no	5	60		6	<1	p/s	chl <0.5, ±cal <1	100	no	50	±d	plane, fracture int.	cal local patch
69	sp?	A	c	?	?	35	80		3	?	?	?	?	no	100	±d	plane	
70	sp?	A	c	?	?	30	80		2	?	?	?	?	?	100	±d	plane, int. No. 50	
71	fr	A	c	?	?	20	60		1	?	p/s	chl?	100	red + white at dry part	70	w	plane	
72	fr	A	c	?	?	312	80		2	?	p/s	chl?	?	?	40	d	plane	
73	fr	A	c	no	no	42	75		3	?	?	?	?	?	60	±d	plane, int. No. 50	
74	fr	A	c	no	no	20	70		6	<0.5	p/s	cal	50	no	10	w	plane, int. No. 50	
75	fr	A	c	no	no	5	65		5	<0.5	p/s	chl, cal	?	no	30	w	plane	
76	fr	A	c	?	?	24	83		6	?	p/s	chl?	?	no	60	±d	plane	fracture/breccia near int. No. 50
77	FT?	A	c	no	?	285	88		72	0.5-2	p-u/s	chl <1, ±cal <2	100?	no	90	d	plane	c-step of fault?, die out at B stronger A-side, cal local patch
78	FT?	A	c	?	?	105	85		2	?	?	?	?	?	15	d	plane	
79	FT?	A	c	no	?	104	73		4	<2	u-p/s	chl <1, cal <2	100	no	40	d	plane	die out on roof stronger A

Appendix 3

Detailed Mapping - Site 2

No.	type	host	relation	ductile def.	fault rock (cm)	strike (deg)	dip	lineation	length (m)	aperture (mm)	roughness	coating / filling (mm)	f/c%	alteration (cm)	wet%	disch. type	discharge description	remarks
1	FT	A	c	no	c-b<40, ±cat<3, g<0.2	142	87		9	0.5-3	p/s	epi<0.5, chl<1, cal<3, clay<2, ±grout<1	100	red <10, ±wk epi 50 in matrix	97	f	plane, crush zone, int. fracture, int. minor branch	roof, 2151B and 2159A total
2	sp?	A	c	no	no	55	70		1	?	p/s	chl	100?	no	20	w	plane	
3	sp?	A	c	no	no	60	75		2	?	p/s	chl	100	no	100	±d	plane	splay of No. 11
4	sp?	A	c	no	no	65	70		1	?	p/s	grout?	100?	?	100	w	plane, int. No. 11	
5	sp?	A	c	?	?	62	70		1	?	?	?	?	no?	0			
6	fr	A	c	?	?	110	85		3	?	p/s	chl, cal or grout<0.5	100	red 2	100	w	plane	
7	fr	A	f?	?	?	250	50		3	?	p/s	chl?	100?	no	20	w	plane, int. minor fractures	follow early foliation?
8	fr	A	c	?	?	144	83		3	?	p/s	±cal?	?	?	95	±d	plane	
9	fr	A	c	?	?	10	80		3	?	p/s	chl, ±cal	100	red 1-2	40	w	plane	cal: small patch
10	fr	A	c	?	?	51	88		2	?	p/s	±chl, ±cal	70?	no	0			cal: small patch
11	fr	A	c	no	no	128	85		5	?	p/s	±chl?, ±grout	20?	?	85	±d	plane, int. splays	
12	fr	A	c	?	?	122	70		2	?	?	?	?	?	50	±d	plane	
13	FT	A	c	no	±c<5	320	60		4	?	p/s	chl	100	red 2?	40	±d	plane	
14	FT?	A	c	no	no	318	48		3	?	u/s	chl	100	?	75	±d	plane	
15	fr	A	c	?	?	132	80		2	?	?	?	?	?	10	w	plane	
16	fr	A	c	?	?	133	75		3	?	p/s	chl?	?	?	100	±d	plane	
17	FT	A	c	?	±c<5	321	85		3	?	p/s	±chl?, ±grout	80?	±red <5	80	d	plane, crush zone	
18	FT	A	c	no	±c<10	142	88		7	0.5	p/s	chl?	100	red 20?	100	d	plane, int. No. 21	strong precipitation
19	FT	A, fg	c	?	±c-b<15	143	70		4	?	p/s	chl	100?	red 1-2?	100	d	d: crushed end in fg, w: plane	
20	FT	A, fg	c	no	±c<50	110	55		5	<0.5	p/s	chl<0.5	100?	red at cz	65	d	d: crush zone, w: plane	
21	FT	A	c	?	±c<15	50	80		3	?	p/p	chl	100	red at cz	80	±d	crush zone, plane	anti-clockwise step?
22	FT	A	c	?	c<5	36	65		3	?	u/s	chl	100	red 5	100	w	plane	
23	FT	A	c	?	c<20	252	80		2	?	s-p/s	chl?	?	red 20	100	w	plane	
24	fr	A	c	?	?	3	70		2	?	p/s	±grout	?	?	95	w	plane	
25	fr	A	c	?	?	60	70		2	?	p/s	chl	100	?	100	w	plane, int. other fractures	
26	FT	A	c	?	±c<5	130	85		2	?	p/s	chl?	100?	red 2	100	±d	plane, int. No. 28, 29	branching
27	fr	A	c	?	?	120	80		2	?	p/s	chl	100?	?	100	±d	plane, int. No. 28, 29	
28	fr	A	c	no	no	23	78		2	<1	p/s-r	chl<0.5, ±cal<1	100	no	100	±d	plane	
29	fr	A	c	?	?	40	90		1	?	?	?	?	?	100	±d	plane	
30	fr	fg	f	?	?	260	85		2	?	u/s	chl?	?	?	30	w	plane	
31	fr	fg, A	f	no	no	95	80		5	?	p-u/s	±chl?	?	?	100	d	plane	

Appendix 3

Detailed Mapping - Site 2

No.	type	host	relation	ductile def.	fault rock (cm)	strike (deg)	dip	lineation			length (m)	aperture (mm)	roughness	coating / filling (mm)	f/c%	alteration (cm)	wet%	disch. type	discharge description	remarks
32	fr	fg	f	?	?	83	70				3	?	p/s	chl	100	?	3	±d	plane	
33	FT	fg	c	?	c<30	240	80				3	?	?	chl?	?	?	100	±d	plane, fine fractures in crush zone	not well observed due to strong precipitation(Fe, Mn)
34	FT	fg, F	f	?	c-b<20	255	75				2	?	p-u/p-s	chl	100?	red?	0			
35	fr	A	c	?	?	90	70				2	?	p/s	±cal?	?	?	0			
36	fr	A	c	?	?	85	65				2	?	?	?	?	?	60	w	plane	
37	fr	A	c	?	?	12	60				2	?	p/s-r	±chl?	100	no	30	w	plane	
38	fr	A, ±F	c	no	no	160	75				4	<0.5	p/s	±chl	70?	red 1	50	w	plane	
39	FT	A, ±F	c	no	±cat<1	148	75				7	<2	p/s	epi<1, chl<1, ±cal?	100	red 2	40	±d	plane	2161R: sinistral displacement 20cm of F vein. 2164A: sinistral 15cm /normal 40cm displacement of pegmatite vein(5cm). 2165A: epi-cataclasite, fsp<5mm.
40	FT	A, ±F	c	no	cat 1-2, c-b<40, g<0.2	139	83	319	15	?	16	0.5-2	p-u/s	±epi<2, chl<0.5, ±cal<1, clay<2, -grout<0.5	100	wk red <10, clay or epi (white-green) <40	97	f	plane(at stepped part 2166.5A)	2161B-niche roof: dextral displacement 50cm of foliated granite(1-1.5m width, 85E/90, variation coarse to fine, composition S to F). dextral displacement 40cm of pagmatite vein(1cm). niche 2156B-B: extensive epi-cataclasite or vein 1-2cm. 2167A: epi-cataclasite, cal trace patch.
41	fr	A	c	?	?	133	80				1	?	p/s	±chl	?	red? 1?	50	w	plane	
42	FT?	A, F	c	?	±c<20	128	85				4	?	?	?	?	?	95	±d	plane, int. No. 36, 47, 48	
43	sp?	A	c	?	?	147	90				2	?	?	?	?	?	25	w	plane	
44	sp?	A	c	?	?	153	83				1	?	p/s	chl?	?	?	100	w	plane	
45	sp?	A	c	?	?	103	70				2	?	?	?	?	?	100	w	plane	
46	FT?	A, ±F	±f	?	?	315	80				1	?	p/s-p	chl?	100?	red 5?	70	w	plane	
47	fr	A, F	c	?	?	242	35				3	?	p/s-r	±chl?	?	?	5	w	plane, int. No. 39	shallow dipping
48	fr	A, F	c	?	?	230	20				2	?	p/s-r	±chl?	100?	?	5	w	int. No. 43	shallow dipping
49	fr	A	c	?	?	335	60				5	?	p/s	epi?	100?	?	10	w	plane?	
50	FT?	A, ±F	c	no	no	322	65				2	?	p/s	chl<0.5	100	no	100	w	plane	little displacement of F vein
51	fr	A	c	no	no	6	70				3	<0.5	p/s	chl<0.5	80	?	20	w	plane, int. fractures	
52	FT	A, ±F	c	no	±c<20	314	89	314	22.5	d?	11	1-2	p/p	epi<0.5, ±qtz?<2, chl<0.5, ±cal<2	100	no	50	d	plane	2168A: slicken on coating, dextral? step, epi-qtz vein 1-2mm. 2166.5R: dextral displacement c.a. 15cm of F vein(30cm).

Appendix 3

Detailed Mapping - Site 2

No.	type	host	relation	ductile def.	fault rock (cm)	strike (deg)	dip	lineation			length (m)	aperture (mm)	roughness	coating / filling (mm)	f/c%	alteration (cm)	wet%	disch. type	discharge description	remarks
53	sp?	A	c	?	?	260	80				1	?	?	?	no	100	w	plane		
54	sp?	A	c	?	?	65	75				2	?	p/s	chl?	no	15	±d	plane, int. crush zone		
55	FT?	A	c	?	?	345	80				4	<1	p/p	chl<1, -cal?	100	red?	3	w	plane	merge to No. 52
56	FT	A	c	no	no	63	45	250	10	?	6	1-2	u/s	chl<0.5, ±cal<2	100	red 2	0		slicken on coating, cal local patch	
57	FT	A, ±F	c	no	±c<5	318	89				7	<1	p/s	chl<0.5, -cal<1	100?	no	0		2167R: dextral displacement 10cm of F vein(30cm). end at both sides. cal trace patch.	
58	FT	A, ±F	c	no	±c-b<50	74	73				6	<1	p-u/s-r	chl<0.5, -cal<1	100	±red<1	50	w	plane	
59	fr	A	c	no	no	148	83				2	<0.5	p/s	chl<0.5, ±cal?	100	no	100	w	plane	
60	FT	A	c	no	no	143	85				6	<1?	p/p	chl<1	100	no	70	d	int. No. 31, plane	dextral 15cm displacement of pegmatite vein(1cm) and No. 61
61	fr	A	c	no	±cat?<1	340	50				6	<1	p/s-r	epi<10, ±qtz or fluo<2, ±chl?<0.5	100	red 8	7	w	plane(int. No. 63)	epi-cataclasite?: epi fine network to thick vein, grain size reduction not obvious.
62	sp?	A	c	no	no	50	85				1	?	p/p-s	chl	100	no	20	w	plane near int. No. 40	
63	sp?	A	c	no	no	40	85				1	?	p/s	chl	100	no	20	w	plane near int. No. 40	
64	FT	A	c	no	no	317	80				5	?	p/s	chl	100?	no	85	w	plane	dextral displacement 10cm of two pegmatite veins(1cm).
65	FT	A	c	no	no	326	80				1	?	p/s	chl?	?	no	40	w	plane	dextral displacement 4cm of pegmatite vein(1cm).
66	fr	A	c	no	no	140	80				2	?	p/s	chl?	?	no	15	w	plane	no displacement of vein
67	fr	A	c	no	no	335	80				2	?	?	?	no	0				no displacement of vein
68	fr	A	c	no	no	132	80				2	?	?	?	no	0				
69	sp?	A	c	no	no	317	55				2	0.5	p/s	no	0	no	100	w	plane	
70	fr	A	c	no	no	240	40				2	<0.5	p/s	chl<0.5, cal<0.5	100	wk red <1	30	w	plane	

Appendix 3

Detailed Mapping - Site 3

No.	type	host	relation	ductile def.	fault rock (cm)	strike (deg)	dip	lineation	length (m)	aperture (mm)	roughness	coating / filling (mm)	f/c%	alteration (cm)	wet%	disch. type	discharge description	remarks
1	FT	A	c	m 5-10, w<50	b-c<50	295	87		12	<8	u/s-p	epi<0.5, chl<1, cal<1, grout<8	100	red+epi<15	100	d	plane (not obvious)	not well observed due to reprecipitated grout. obvious mylonite foliation. dextral displacement 3m of F dike (3-5cm). red: extensive, epi: irregular/local.
2	sp?	A	c	no	no	140	30		1	<0.5	p/s	chl<0.5, ±epi<0.5, grout(Ca)<1	100	local epi	100	w	plane?	grout(Ca): grout and reprecipitated calcic material
3	sp?	A	c	no	no	260	75		2	0.5	p-u/s	chl<0.5, grout(Ca)<1	100	no?	100	w	plane?	
4	sp?	A	c	no	no	143	75		1	<0.5	p-u/s	chl<0.5, grout(Ca)<0.5	100	no	100?	w	plane?	
5	sp?	A	c	no	no	138	35		1	<0.5	p/s	chl<0.5, ±cal?<0.5, - grout(Ca)<1	100	no	100?	w	plane?	grout near No. 1
6	fr	A	c	no	no	165	10		2	0.5	p/s-r	no		no	0			
7	fr	A	c	no	no	292	35		3	0.5-1	p/s	epi<0.5, chl<0.5, cal<0.5, - qtz<0.5	100	no	0			
8	fr	A	c	no	no	195	15		4	<0.5	p/s-r	±chl	20?	red 5	0			
9	fr	A	c	no	no	55	35		3	<0.5	p/s	chl<0.5, cal<0.5	100	local red	0			
10	sp?	A	c	?	?	320	85		2	?	p/s	chl, ±grout	100	no	0			
11	fr	F/A	f	no	no	198	80		3	<0.5	p/s	chl, ±grout(Ca)	90	no	0			boundary of F vein.
12	fr	A	c	?	?	213	85		2	?	p/s	chl?, ±grout(Ca)	?	no	60	w	plane	
13	fr	A	c	?	?	70	65		1	?	p/r-s	chl?, ±grout(Ca)	70	wk red?	50	w	plane	
14	fr	A	c	?	?	120	90		1	?	?	?	?	?	100	w	plane	
15	fr	A	c	?	?	193	35		1	?	p/s	chl, Fe-Ox	100	red 1?	0			
16	fr	A	c	?	?	75	60		5	?	p/s	chl, ±grout(Ca)	100	wk red 5?	40	w	plane	
17	fr	A	c	?	?	70	55		3	?	p/s	chl, ±grout(Ca)	80?	wk red 3	30	w	plane	
18	FT?	A	c	no	no	299	83		4	0.5?	p/s	chl, ±grout(Ca)	?	no?	70	d	d: fracture end, w: plane	
19	fr	A	c	no	no	325	80		4	<0.5	p/s	chl<0.5, ±cal?<0.5	100	wk red? 10	60	±d	plane	
20	fr	A	c	no	no	256	26		5	0.5-1?	p/s	chl<0.5, ±cal?, grout(Ca)<0.5	100	red 3	70	±d	plane	gently dipping
21	fr	A	c	?	?	50	75		1	?	p/s	grout(Ca)	100	?	0			
22	fr	A	c	?	?	5	80		1	?	p/s	grout(Ca)	100	?	0			
23	FT?	A	c	?	?	114	80		2	?	p/s	chl?, ±grout(Ca)	100?	?	50	±d	plane	a part of master fault
24	fr	A	c	no	±c<10	40	80		1	<0.5	p/s	chl?<0.5	100?	no	50	d	plane	

Appendix 3

Detailed Mapping - Site 3

No.	type	host	relation	ductile def.	fault rock (cm)	strike (deg)	dip	lineation	length (m)	aperture (mm)	roughness	coating / filling (mm)	f/c%	alteration (cm)	wet%	disch. type	discharge description	remarks
25	FT	A	c	m<3	b 2-3, c<20, ±cat<4, g<0.2	326	78		4	0.5-1	p-u/s	chl<0.5, epi<0.5, ±cal<1, clay<2, ±grout(Ca)<0.5	100?	mod red 5	100	f	plane	branch of No. 1. local epi-mylo 3cm. gouge: clay, chl, fragments
26	FT	A	c	no	±c	315	86		4	0.5-2	p/s	chl<0.5, grout<2	100	no?	50	d	near int. NO. 41	branch of No. 1. mostly grouted (visible layer). dextral displacement 15cm of F vein (1-2cm).
27	FT	A	c	m<5	±cat<3, g<0.2	129	87	300 20 ?	4	0.5-2	p-u/s	±qtz+fluo<1, ±qtz+epi 1-2, chl<0.5, cal<1, clay<2	100	red?, (str Fe precip)	100	f	plane	merge to mylonite of No. 1. epi-mylo 5cm, consistent. gouge: clay, chl, ±fragments. dextral displacement 1m of F vein (1-2cm).
28	FT?	A	c	no	no	140	80		1	<0.5	p/s-r	±chl<0.5	80	red?	100	±d	plane	alteration not certain due to intersection with coated subhorizontal plane of No. 47.
29	fr	A	c	no	no	48	80		2	0.5	p-u/s	chl<0.5	100	?	100	w	plane	
30	FT?	A	c	no	no	306	85		2	<1	p/s	chl<0.5, cal<1	100	red? 3	100	d	plane	Cal: film - patch
31	fr	A	c	no	no	110	90		1	<0.5	p/s	chl<0.5	100	?	100	±d	plane	
32	FT?	A	c	no	no	290	85		2	<0.5	p/s	chl<0.5?	100	mod red 2	100	d	plane	merge to No. 36.
33	fr	A	c	no	no	307	80		1	<0.5	p/s	?	?	no	100	±d	plane	
34	FT?	A	c	no	no	300	80		1	<0.5	p/s	?	?	?	100	d	plane	merge to No. 36.
35	fr	A	c	no	no	334	78		2	?	p-u/s	chl?	?	no	70	w	plane	
36	FT	A, ±F	c	?	±c<10	121	84		11	?	p/s	chl, ±cal?, grout(Ca)	?	no	20	d	plane, int. No. 32	mostly grouted. dextral displacement 50cm of F dike (10cm).
37	fr	A	c	?	?	15	45		5	?	p/s	chl, ±grout(Ca)	100	mod red 20	20	w	plane, int. No. 17	
38	fr	A	c	?	?	235	70		1	?	p/s	chl?, grout(Ca)	?	?	15	±d	plane	
39	fr	A	c	?	?	52	90		2	?	p/s	chl	100	wk red 5?	0			
40	fr	A	c	?	?	328	85		2	?	p/s	chl?	?	?	5	w	plane	
41	FT?	A	c	no	no	309	88		1	0.5-1	p/s	chl<0.5, cal<1	100	no	100	d	plane	reactivating epi vein.
42	fr	A	c	no	no	141	90		1	0.5	p/s	chl<0.5, ±cal?<0.5	100?	wk red 2	70	d	plane	
43	FT	A	c	no	no	336	80		1	0.5-1	p/s	epi<0.5, chl<0.5, ±cal<1, clay<1	100	red?±epi?	70	w	plane	right-side up displacement 1cm at open crack.
44	fr	G	c	no	no	126	85		1	<0.5	p/s	no		no	100	f	plane	// minor fractures in G.
45	fr	A	c	no	no	134	85		2	<0.5	p-u/s	no		no	100	?		

Appendix 3

Detailed Mapping - Site 3

No.	type	host	relation	ductile def.	fault rock (cm)	strike (deg)	dip	lineation	length (m)	aperture (mm)	roughness	coating / filling (mm)	f/c%	alteration (cm)	wet%	disch. type	discharge description	remarks
46	FT	G	c	w?<2	b<10, c<30, ±g<0.1	133	83		2	0.5-1	u/s	epi<0.5, chl<0.5, ±cal<1, -qtz5-20, ±clay<1	100	epi 2-12	100	w	plane	right-side down shear lense, sheared qtz vein - block/lense 2cm thick. wk mylo? (foliation?) or epi±qtz vein/breccia 2cm.
47	fr	A	c	no	no	345	15		5	0.5	p/s-st	chl<0.5	100	mod red 5	?			possibly conductive open subhorizontal fracture.
48	fr	A	c	no	no	265	5		3	<0.5	p/s	?	?	no?	0?			
49	FT	A	c	no	±c-b<10	8	10		5	1-2	p/s	epi<1, qtz<1	100	mod red 5-entire	0?			dextral displacement 7cm of peg vein (1cm)
50	fr	A	c	no	no	85	20		1	<0.5	p/s	±chl	10?	no?	0?			
51	fr	A, G	c	no	no	200	25		1	<0.5	p/s	no?	?	no?	0?	f	int. No. 44	strong flow spots at int. of minor fractures.
52	fr	A, G	c	no	no	108	10		2	<0.5	p/r-s	chl<0.5, ±cal<0.5	100	wk red 10-entire	0?			// horizontal fractures
53	fr	A	c	no	no	125	10		2	<0.5	p/s-r	chl<0.5	100	wk red 1?	0			
54	fr	G, ±A	c	no	no	120	20		1	?	p/s	±chl?, ±epi?	?	epi entire	0?			
55	fr	G	c	no	no	105	25		1	<0.5	p/s	±chl<0.5	20?	epi?	?			
56	sp?	G	c	no	no	110	60		1	<0.5	p-u/s	chl?	?	?	?			
57	sp?	G	c	no	no	112	35		1	<0.5	p/s	chl, ±epi?	100?	?	?			

Appendix 3

Detailed Mapping - Site 1 sidewall

No.	type	fault rock (cm)	strike (deg)	dip	lineation	length (m)	aperture (mm)	roughness	coating / filling (mm)	f/c%	alteration (cm)	remarks		
8	fr	no	210	65			5	1-2	p/s	chl 1-2, cal 0.2	100?	no	reactivated vein boundary	
14	FT	±c<10, g<0.1	332	73	340	10	s	5	0.5-2	p-u/s	chl <1, ±epi<0.5, ±cal patch<2, grey clay<1	100	mod red<3	1545A-1. Slicken by chl stretch, cal growth in groove.
14	FT	±cat<3, ±c<10, g<0.2	335	83	330	10	s	4	0.5-2	u/s-p	±epi <1, chl <0.5, cal <2, clay<2	100	local epi?	1561B-1. cal local patch some euhedral, local epi veins<10mm and alt<3cm along fracture = cataclasite?, slicken&step on coating(cal, chl)
23	FT	g<0.1	99	78	105	15	d?	4	1	u/s	chl<0.5, ±epi?<0.5, grey±white cal<2, ±py, clay<1	100	±mod red<5	1553B-2: two generations of cal, thick grey layer (healed gouge?) and white patch.
23	FT	cat<3, ±g?	300	83	118	10	d	4	2	p-u/s	epi<0.5 - chl<1, grey cal<1, white cal<1	100	±wk red<2?	1553B-3, no gouge?
23	fr	no	107	78				2	<0.5	p/s-r	±cal patch, ±py	40	±red	1553B-4, irregular and extensive red alteration.
40	FT	±cat <3, ±c<5, ±g<0.1	108	87	102	5	d?	4	1-2	u/st-s	chl <0.5, ±cal <2, ±clay<1	90	mod red 5-50 irregular	1566A-1 total: epi-cat? <3cm in rock 5cm away from sub-fault.
50	FT	±c-b<40, ±g	110	86				12	0.5-2	p-u/s-r	±epi<0.5, chl <0.5, cal <2, ±clay<0.5	90	±wk red?	minor dextral displacement(<1cm?) of FGG vein at 1565B roof, cal local patch/layer
65	fr	?	280	5				4	?	p/s	±chl	70?	red?	
66	fr	?	290	15				6	?	p/s	±chl	20?	red	
68	fr	no	5	60				6	<1	p/s	chl <0.5, ±cal <1	100	no	cal local patch
77	FT?	no	285	88				12	0.5-2	p-u/s	chl <1, ±cal <2	100?	no	c-step of master faults, die out at B stronger A-side, cal local patch
79	FT?	no	104	73				4	<2	u-p/s	chl <1, cal <2	100	no	die out on roof stronger A
1545A-3	FT	no	340	73	152	10	?	4	<2	p-u/s	chl<0.5, epi<0.5, ±cal<2, ±py	100	±wk red<3	F=pegmatite, trace striation.
1545A-4	fr	no	40	75				2	<0.5	p-s/s	no	0	no	
1545A-5	fr	no	28	60				2	<0.5	p/s	±cal<0.5	?	no	
1545A-6	FT	±c, ±g	344	68	170	3	s?	4	0.5	p-s/s	chl<0.5, ±epi<0.5, cal<0.5	100	mod red<2	trace striation on chl and cal.
1561B-2	fr	no	330	55				2	0.5	p/s	chl<0.5	100	?	
1566A-5	fr	no	195	13				3	<0.5	p/s	no	0	wk red<1	
1566A-6	fr	no	168	10				3	<0.5	p-u/s	chl<0.5	90?	trace red?<1	
1566A-7	fr	no	335	15				2	<0.5	p/s	±chl?<0.5, ±epi<1, ±cal<0.5	90?	±wk red<2	epidote fracture
1566A-8	sp?	no	165	15				1	<0.5	p/s	±chl<0.5, ±epi<0.5, ±cal<0.5	100	±wk red<1	// minor fractures
1573A-3	FT	±g	208	88				4	<0.5	p/s-r	±chl?<0.5, ±cal<0.5	?	?	
1573A-5	fr	no	357	60				6	<0.5	p/s	±cal?	?	red<1	
1573A-6	fr	no	232	25				3	<0.5	p/s	chl<0.5, -cal<0.5	90	no	


Appendix 3

Detailed Mapping - Site 2 sidewall

No.	type	fault rock (cm)	strike (deg)	dip	lineation			length (m)	aperture (mm)	roughness	coating / filling (mm)	f/c%	alteration (cm)	remarks
1	FT	c-b<40, ±cat<3, g<0.2	142	87				9	0.5-3	p/s	epi<0.5, chl<1, cal<3, clay<2, ±grout<1	97	red <10, ±wk epi 50 in matrix	roof, 2151B and 2159A total
20	FT	±c<50	110	55				5	<0.5	p/s	chl<0.5	100?	red at cz	
39	FT	±cat<1	148	75				7	<2	p/s	epi<1, chl<1, ±cal?	100	red 2	2161R: sinistral displacement 20cm of F vein. 2164A: sinistral 15cm /normal 40cm displacement of pegmatite vein(5cm). 2165A: epi-cataclasite, fsp<5mm.
40	FT	cat 1-2, c-b<40, g<0.2	139	83	319	15	?	16	0.5-2	p-u/s	±epi<2, chl<0.5, ±cal<1, clay<2, -grout<0.5	100	wk red <10, clay or epi (white-green) <40	2161B-niche: dextral displacement 50cm of foliated granite(1-1.5m width, 85E/90, variation coarse to fine, composition S to F). 2167A: epi-cataclasite, cal trace patch. niche 2156B-roof: dextral displacement 40cm of pagmatite vein(1cm). niche 2156B-B: ext
52	FT	±c<20	314	89	314	22,5	d?	11	1-2	p/p	epi<0.5, ±qtz?<2, chl<0.5, ±cal<2	100	no	2168A: slicken on coating, dextral? step, epi-qtz vein 1-2mm. 2166.5R: dextral displacement c.a.15cm of F vein(30cm).
56	FT	no	63	45	250	10	?	6	1-2	u/s	chl<0.5, ±cal<2	100	red 2	slicken on coating, cal local patch
57	FT	±c<5	318	89				7	<1	p/s	chl<0.5, -cal<1	100?	no	2167R: dextral displacement 10cm of F vein(30cm). end at both sides. cal trace patch.
58	FT	±c-b<50	74	73				6	<1	p-u/s-r	chl<0.5, -cal<1	100	±red<1	
59	fr	no	148	83				2	<0.5	p/s	chl<0.5, ±cal?	100	no	
69	sp?	no	317	55				2	0.5	p/s	no	100	no	
70	fr	no	240	40				2	<0.5	p/s	chl<0.5, cal<0.5	100	wk red <1	

Appendix 3

Detailed Mapping - Site 3 sidewall

No.	type	mylonite int.	fault rock (cm)	strike (deg)	dip	lineation	length (m)	aperture (mm)	roughness	coating / filling (mm)	f/c%	alteration (cm)	remarks
1	FT	m 5-10, w<50	b-c<50	295	81		12	<8	u/s-p	epi<0.5, chl<1, cal<1, grout<8	100	red+epi<15	not well observed due to reprecipitated grout. obvious mylonite foliation. dextral displacement 3m of F vein (3-5cm). red: extensive, epi: irregular/local.
2	sp?	no	no	140	30		1	<0.5	p/s	chl<0.5, ±epi<0.5, grout(Ca)<1	100	local epi	grout(Ca): grout and reprecipitated calcic material
3	sp?	no	no	260	75		2	0,5	p-u/s	chl<0.5, grout(Ca)<1	100	no?	
4	sp?	no	no	143	75		1	<0.5	p-u/s	chl<0.5, grout(Ca)<0.5	100	no	
5	sp?	no	no	138	35		1	<0.5	p/s	chl<0.5, ±cal?<0.5, -grout(Ca)<1	100	no	grout near No. 1
6	fr	no	no	165	10		2	0,5	p/s-r	no		no	
7	fr	no	no	292	35		3	0.5-1	p/s	epi<0.5, chl<0.5, cal<0.5, -qtz<0.5	100	no	
8	fr	no	no	195	15		4	<0.5	p/s-r	±chl	20?	red 5	
9	fr	no	no	55	35		3	<0.5	p/s	chl<0.5, cal<0.5	100	local red	
25	FT	m<1	b 2-3, c<20, ±cat<4, g<0.2	326	78		4	0.5-1	p-u/s	chl<0.5, epi<0.5, ±cal<1, clay<2, ±grout(Ca)<0.5	100?	mod red 5	branch of No. 1. local epi-myo 3cm. gouge: clay, chl, fragments
27	FT	m<5	±cat<3, g<0.2	129	87	300 20 ?	4	0.5-2	p-u/s	±qtz+fluo<1, ±qtz+epi 1-2, chl<0.5, cal<1, clay<2	100	red?, (str Fe precip)	merge to mylonite of No. 1. epi-myo 5cm, consistent. gouge: clay, chl, ±fragments
30	FT?	no	no	306	85		2	<1	p/s	chl<0.5, cal<1	100	red? 3	Cal: film - patch
31	fr	no	no	110	90		1	<0.5	p/s	chl<0.5	100	?	
41	FT?	no	no	309	88		1	0.5-1	p/s	chl<0.5, cal<1	100	no	reactivating epi vein.
42	fr	no	no	141	90		1	0,5	p/s	chl<0.5, ±cal?<0.5	100?	wk red 2	
43	FT	no	no	336	80		1	0.5-1	p/s	epi<0.5, chl<0.5, ±cal<1, clay<1	100	red?±epi?	right-side up displacement 1cm at open crack. 
44	fr	no	no	126	85		1	<0.5	p/s	no		no	// minor fractures in G.
45	fr	no	no	134	85		2	<0.5	p-u/s	no		no	
46	FT	w?<2	b<10, c<30, ±g<0.1	133	83		2	0.5-1	u/s	epi<0.5, chl<0.5, ±cal<1, -qtz5-20, ±clay<1	100	epi 2-12	right-side down shear lense, sheared qtz vein - block/lense 2cm thick. wk mylo? (foliation?) or epi±qtz vein/breccia 2cm.
47	fr	no	no	345	15		5	0,5	p/s-st	chl<0.5	100	mod red 5	possibly conductive open subhorizontal fracture.
49	FT	no	±c-b<10	8	10		5	1-2	p/s	epi<1, qtz<1	100	mod red 5-entire	dextral displacement 7cm of peg vein (1cm)
50	fr	no	no	85	20		1	<0.5	p/s	±chl	10?	no?	
52	fr	no	no	108	10		2	<0.5	p/r-s	chl<0.5, ±cal<0.5	100	wk red 10-entire	// horizontal fractures
53	fr	no	no	125	10		2	<0.5	p/s-r	chl<0.5	100	wk red 1?	
55	fr	no	no	105	25		1	<0.5	p/s	±chl<0.5	20?	epi?	
57	sp?	no	no	112	35		1	<0.5	p/s	chl, ±epi?	100?	?	

Appendix 4

Report of the XRD measurement

Enheten för berggrundsgéologi

Handläggare, direkttelefon/Our reference, telephone

Sven Snäll, tel. 018-179319

Terralogica AB

Att. Eva-Lena Tullberg

Box 4140

443 14 GRÅBO

XRD-analyser av prover med beteckningar 1553B, 1561B, 1575A, 2151B, 2156B och 2198A.

Fraktionering

Proverna fraktionerades i destillerat vatten genom omröring sedimentation och avsugning av lermaterialet i två kornstorleksfraktioner, i en fraktion $<2 \mu\text{m}$ och en $>2 \mu\text{m}$ med följande resultat:

Prov	$<2 \mu\text{m}$ (vikt-%)	$>2 \mu\text{m}$ (vikt-%)
1553B	27	73
1561B	30	70
1575A	13	87
2151B	38	62
2156B	50	50
2198A	35	65

XRD-analyser

Prov 1553B

Fraktion $<2 \mu\text{m}$

XRD-analyserna av lerfraktionen (orienterade prover) gav de diagram som visas i Bilaga 1. Det svarta diagrammet är upptaget på naturligt material som dispergerats i natriumhexametafosfat och det röda är upptaget på etylenglykolmättat material.

Analyserna visar att materialet består av klorit och ett svällande blandskikt-mineral som tolkas som corrensit (se Jasmund & Lagaly, 1993, kopia av sid. 59 bifogas, Bilaga 1). Kloriten har sin högsta topp vid 7 Å (002-toppen). Kloritens 14 Å-topp (001-toppen) är normalt lägre än 7 Å-toppen men i detta prov är den

ter0108

ss 2001-08-14

Organisationsnr. 202100-2528

Huvudkontor / Head Office:

Box 670
SE 751 28 Uppsala, Sweden
Besök - Visit: Villavägen 18 Uppsala
Tel: 018 17 90 00 - 46 18 17 90 00
Fax: 018 17 92 10 - 46 18 17 92 10
E-mail: sgu@sgu.se

Filial / Regional Office:

Geovetarcentrum
Guldhedsgatan 5A
SE 413 20 Göteborg, Sweden
Tel: 031-708 26 50 - 46 31 708 26 50
Fax: 031-708 26 75 - 46 31 708 26 75
E-mail: gb@sgu.se

Filial / Regional Office:

Kiliansgatan 10
SE 223 50 Lund, Sweden
Tel: 046-31 17 70 - 46 46 31 17 70
Fax: 046 31 17 99 - 46 46 31 17 99
E-mail: lund@sgu.se

Filial / Regional Office:

Skolgatan 4
SE 930 70 Malmö, Sweden
Tel: 0953 346 00 - 46 953 346 00
Fax: 0953 216 86 - 46 953 216 86
E-mail: mala@sgu.se

Filial / Regional Office:

Box 16247
SE 103 24 Stockholm, Sweden
Besök - Visit: Drottninggatan 33
Tel: 08 54 52 15 00 - 46 8 54 52 15 00
Fax: 08 24 68 14 - 46 8 24 68 14
E-mail: stockholm@sgu.se

högre. Detta betyder att provet innehåller en betydande mängd av blandskiktmineralet.

Fraktion >2 µm

Det grövre materialet består enligt XRD-analysen (analys av malda, packade prover) av klorit, järnrik glimmer (alt. järnrik illit), kvarts, plagioklas, flusspat, kalcit och ev. något rutil (se Bilaga 2).

Prov 1561B

Fraktion <2 µm

XRD-analyserna av lerfraktionen (orienterade prover) gav de diagram som visas i Bilaga 3. Det svarta diagrammet är upptaget på naturligt material som dispergerats i natriumhexametfosfat och det röda är upptaget på etylenglykolmättat material.

Lermaterialet i detta prov består också av klorit och det svällande blandskiktmineralet, tolkat som corrensit. I detta provmaterial är klorithalten högre än i prov 1553B och halten av blandskiktmineral lägre. Blandskiktmineralet är inte heller lika välkristalliserat (diffusare toppar) som i prov 1553B.

Fraktion >2 µm

Det grövre materialet består enligt XRD-analysen av klorit, dåligt kristalliserad illit), kvarts, plagioklas, kalcit och möjligen dolomit. Toppen vid $d=2.9018$ har tolkats som dolomit (se Bilaga 4) men en del av toppen kan också härröra från epidot. Epidoten har även en relativt stark topp vid 5.0 Å vilken finns med i diagrammet (nämligen i samma läge som för illitens 002-topp).

Prov 1575A

Fraktion <2 µm

XRD-analyserna av lerfraktionen (orienterade prover) gav de diagram som visas i Bilaga 5. Det svarta diagrammet är upptaget på naturligt material som dispergerats i natriumhexametfosfat och det röda är upptaget på etylenglykolmättat material.

Lermaterialet i detta prov består till övervägande del av det svällande blandskiktmineralet, tolkat som corrensit. Något klorit ingår också samt kalcit

och flusspat. Utbildningen av blandskiktmineralet är dock något olika i proverna. I detta prov är topparna i intervallet 29-32 Å dåligt utvecklade.

Fraktion >2 µm

Det grövre materialet består enligt XRD-analysen av blandskiktmineralet (tolkat som corrensit), något klorit, illit (järnrik) samt kvarts plagioklas, kalcit, flusspat och ev. också något rutil (se Bilaga 6).

Prov 2151B

Fraktion <2 µm

XRD-analyserna av lerfraktionen (orienterade prover) gav de diagram som visas i Bilaga 7. Det svarta diagrammet är upptaget på naturligt material som dispergerats i natriumhexametfosfat och det röda är upptaget på etylenglykolmättat material.

Lermaterialet i detta prov består också av klorit och det svällande blandskiktmineralet, tolkat som corrensit. Halten av det svällande blandskiktmineralet är dock jämförelsevis låg i detta prov. Det finns också kalcit i lermaterialet och kvarts i mycket liten mängd.

Fraktion >2 µm

Det grövre materialet består enligt XRD-analysen av klorit, kvarts, plagioklas, kalcit (hög halt), flusspat och möjligen också något rutil (toppen vid $d=3.240$), se Bilaga 8).

Prov 2156B

Fraktion <2 µm

XRD-analyserna av lerfraktionen (orienterade prover) gav de diagram som visas i Bilaga 9. Det svarta diagrammet är upptaget på naturligt material som dispergerats i natriumhexametfosfat och det röda är upptaget på etylenglykolmättat material.

Det svällande blandskiktmineralet, tolkat som corrensit, dominerar i lerfraktionen av detta prov. Klorit ingår också som enskilt mineral (se 7.2 Å toppen i det EG-mättade materialet).

Fraktion >2 µm

Det grövre materialet består enligt XRD-analysen av det blandskiktmineralet, tolkat som corrensit (hög halt), klorit, kvarts, flusspat, plagioklas, kalcit, sannolikt också dolomit och möjligen också något rutil (toppen vid $d=3.224$, se Bilaga 10).

Prov 2198A

Fraktion <2 µm

XRD-analyserna av lerfraktionen (orienterade prover) gav de diagram som visas i Bilaga 11. Det svarta diagrammet är upptaget på naturligt material som dispergerats i natriumhexametafosfat och det röda är upptaget på etylenglykolmättat material.

Lermaterialet i detta prov domineras av klorit. En mindre mängd av det svällande blandskiktmineralet, tolkat som corrensit, ingår också.

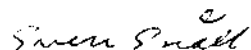
Fraktion >2 µm

Det grövre materialet består enligt XRD-analysen av klorit, kvarts, plagioklas, kalcit (hög halt), flusspat, epidot (topp vid $d=5.027$ och topp vid $d=2.8995$ som sammanfaller med dolomitens högsta topp), ev. dolomit och möjligen också något rutil (toppen vid $d=3.228$), se Bilaga 12).

Litteratur:

Jasmund K. Och Lagaly G., 1993: Tonminerale und Tone. – Steinkopff Verlag Darmstadt.

Med vänlig hälsning



Sven Snäll

2.3.1 Minerale mit regelmäßiger ABAB-Wechselagerung

Die Minerale mit regelmäßiger Wechselagerung geben ein Röntgendiagramm mit einer rationalen Serie von Basisreflexen, wobei sich der d -Wert des ersten Basisreflexes aus der Summierung der Basisabstände beider Schichttypen ergibt. Den Mineralen mit regelmäßiger Wechselagerung dürfen eigene Mineralnamen gegeben werden. Bisher sind in der Literatur folgende Tonminerale dieser Art beschrieben worden:

Rectorit:	Muskovit/Montmorillonit
Rectorit:	Paragonit/Montmorillonit
Tosudit:	dioktaedrischer Chlorit/Smectit
Corrensit:	Chlorit/Vermiculit
Corrensit:	Chlorit/trioktaedrischer Smectit
Aliettit:	Talk/Saponit
Hydrobiotit:	Biotit/Vermiculit

Weitere Minerale mit regelmäßiger oder fast regelmäßiger AB-Wechselagerung, die keine eigenen Namen erhalten haben, sind beschrieben z. B. als: Illit/Smectit, Glaukonit/Smectit, Kaolinit/Smectit, Kaolinit/Chlorit, Serpentin/Chlorit.

Zusammenstellungen der regelmäßigen AB-Wechselagerungsminerale mit einschlägigen Literaturangaben finden sich bei Reynolds (218, 219).

In den Sedimentgesteinen kommen die Wechselagerungsminerale gemeinsam mit anderen Tonmineralen vor, meistens mit Chloriten und Illiten. Sie sind fast immer aus einer ihrer Komponenten durch Verwitterung oder unter Bedingungen der Diagenese bzw. leichten Metamorphose oder durch hydrothermale Vorgänge entstanden. Die Teilchengrößen liegen wie bei anderen Tonmineralen vorwiegend unter $2\ \mu\text{m}$ \varnothing . Die regelmäßige Wechselagerung und die Art der wechselagernden Komponenten läßt sich am besten unter dem hochauflösenden Durchstrahlelektronenmikroskop erkennen, und zwar an Ultramikrotomschnitten senkrecht zur Basis, wenn die quellbaren Komponenten mit n -Alkylammoniumionen aufgeweitet werden (256). Einen Schnitt durch Corrensit zeigt die Abbildung 2.15.

Minerale mit regelmäßiger AB-Wechselagerung lassen sich in Tonproben anhand ihres ersten Basisreflexes im $24 - 30\ \text{\AA}$ -Bereich erkennen. Bei streng regelmäßiger Wechselagerung tritt eine rationale Serie von Basisreflexen auf (Tabelle 2.40). Als Beweis für eine rationale Abfolge der Basisreflexe darf hierbei nach einem Vorschlag des AIPEA-Nomenklaturkomitees die relative Standardabweichung (bezogen auf: $1 \cdot d_{(001)}$) nicht größer als 0,75 % sein (5). Vorausgesetzt wird dabei, daß mindestens 10 Basisreflexe gemessen werden.

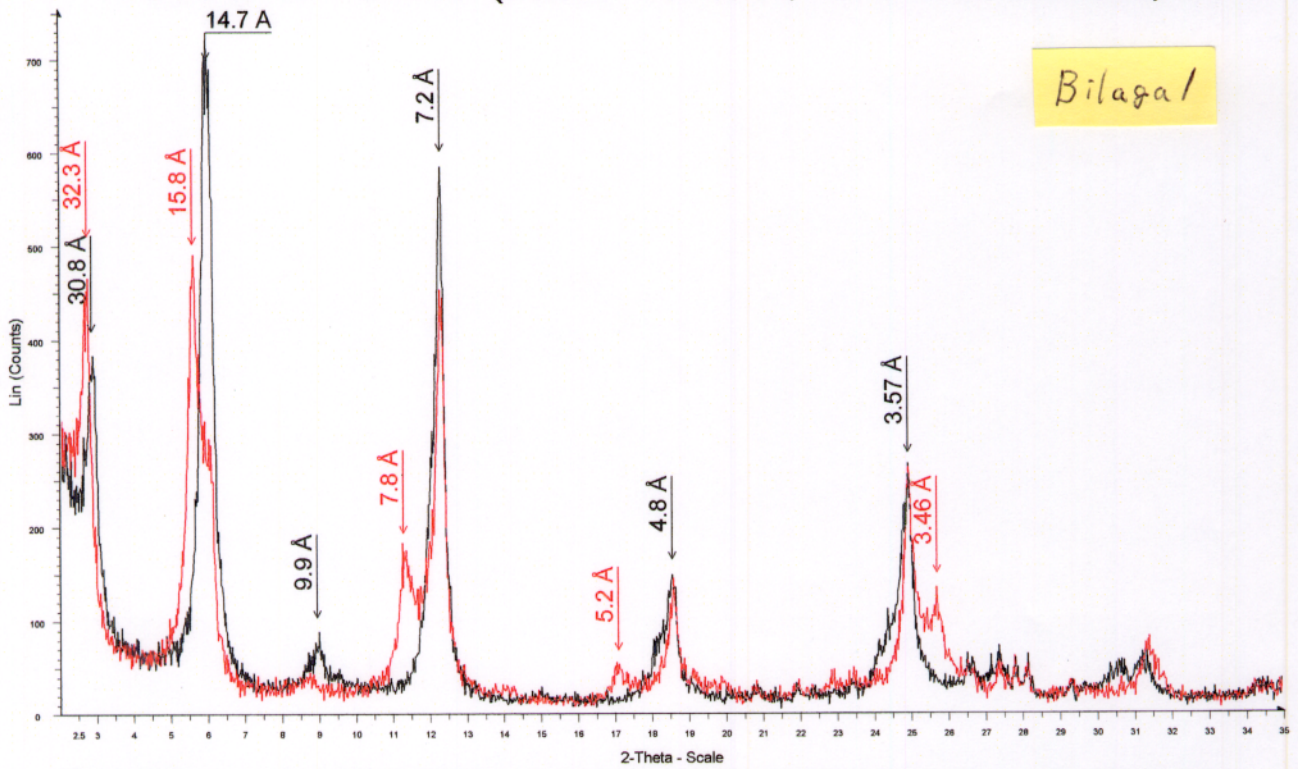
Zur röntgenographischen Identifizierung der Minerale mit regelmäßiger Wechselagerung werden zweckmäßig Texturpräparate verwendet (Kap. 1.5.3) und in die quellbaren Schichten Glycerin oder Ethylenglycol eingelagert. Neben dem Quellverhalten ist die Schrumpfung der Minerale bei kurzzeitigem Erhitzen von lufttrockenen Texturpräparaten auf $550\ ^\circ\text{C}$ für die röntgenographische Erkennung der wechselagernden Schichttypen wichtig.

Die Verfahrensweise ist bei Moore und Reynolds (183), die theoretischen Grundlagen sind bei Reynolds (218, 219) eingehend beschrieben.

Rectorit (Allevardit) ist ein dioktaedrisches Wechselagerungsmineral von Glimmer- und Smectitschichten (25, 53). In Frankreich wurde das Mineral zuerst als Alle-

1553B <2 micron (black=natural, red=EG saturated)

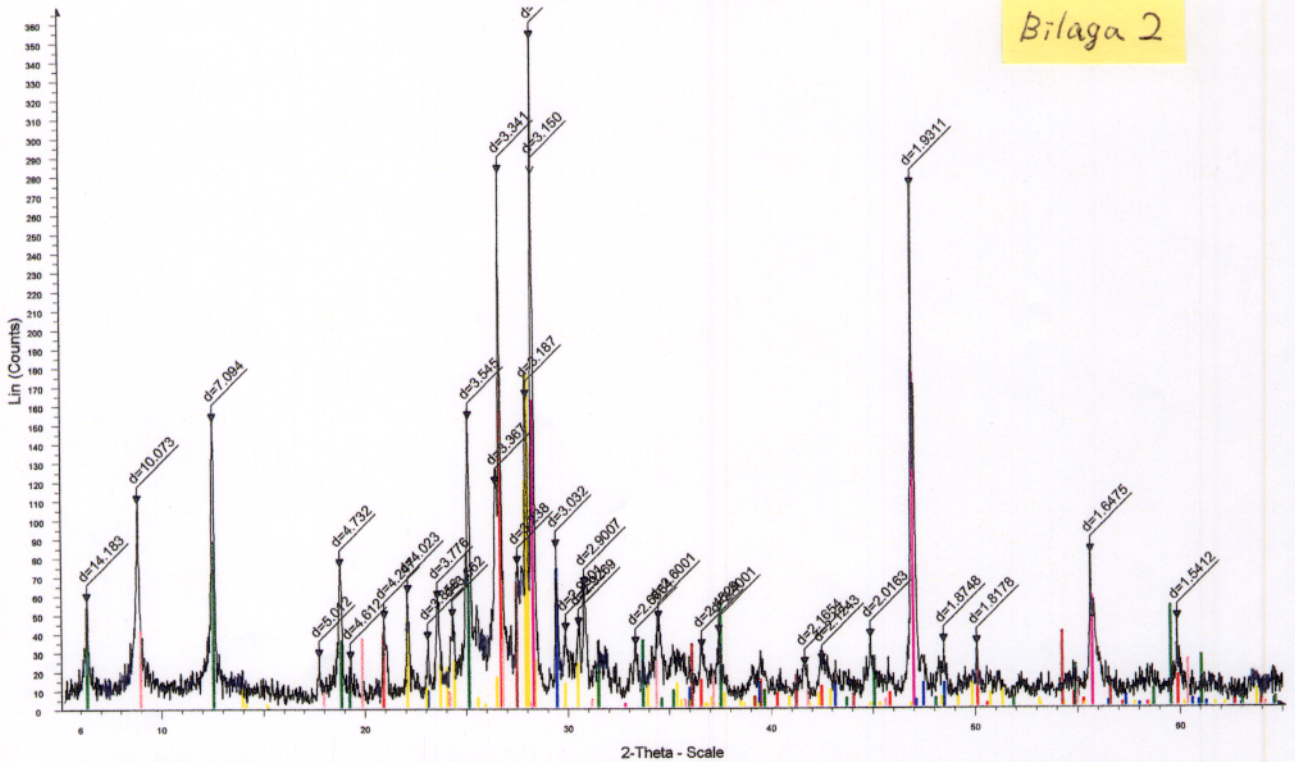
Bilaga 1



C:\Sven\Uppdrag\Terralogica\1553B-2mc.RAW - File: 1553B-2mc.RAW - Type: 2Th/Th locked - Start: 2.000 ° - End: 35.000 ° - Step: 0.020 ° - Step time: 1.0 s - Temp.: 27.0 °C - Time Starter: Operations: Import
 C:\Sven\Uppdrag\Terralogica\1553B-2mc+EG.RAW - File: 1553B-2mc+EG.RAW - Type: 2Th/Th locked - Start: 2.000 ° - End: 35.000 ° - Step: 0.020 ° - Step time: 1.0 s - Temp.: 27.0 °C - Tin Operations: Import

1553B >2 micron

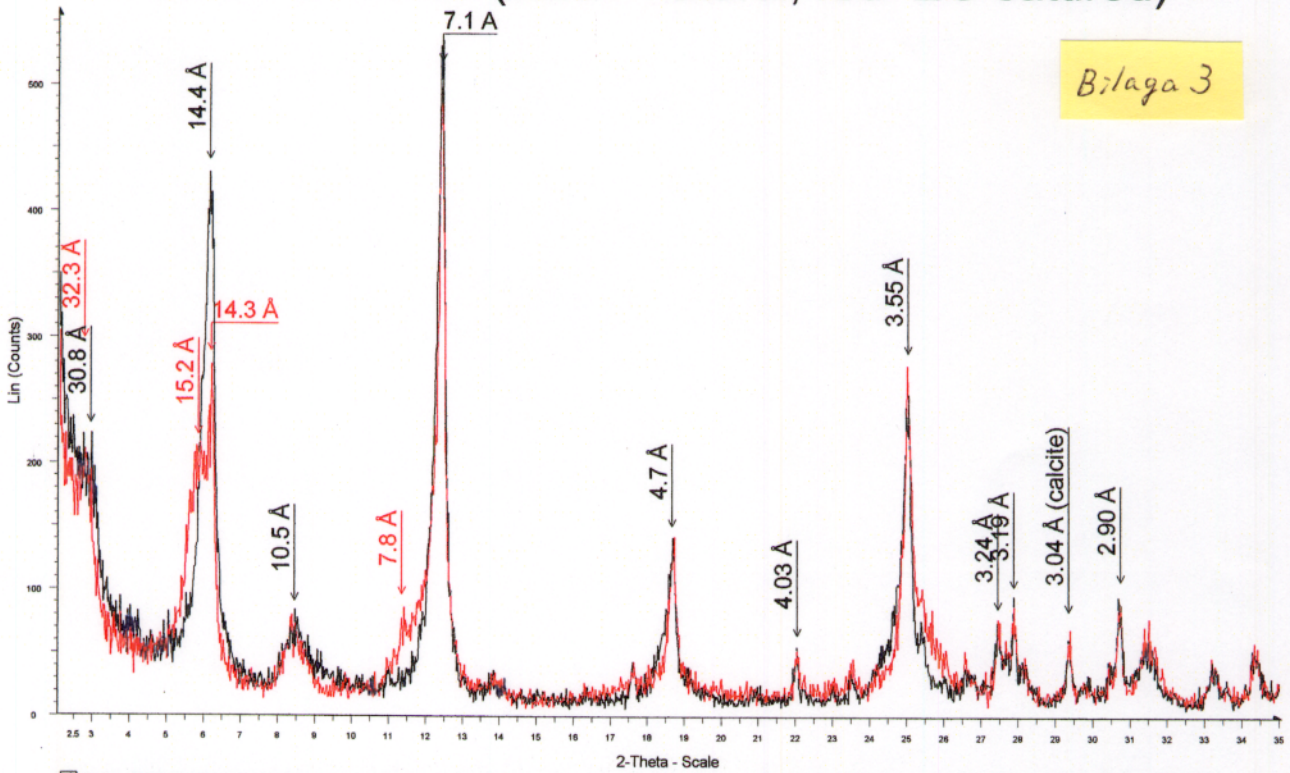
Bilaga 2



C:\Sven\Uppdrag\Terralogica\1553B+2mc.RAW - File: 1553B+2mc.RAW - Type: 2Th/Th locked - Start: 2.000 ° - End: 35.000 ° - Step: 0.020 ° - Step time: 1.0 s - Temp.: 27.0 °C - Time Starter: Operations: Displacement -0.417 | Import
 33-1161 (*) - Quartz, syn - SiO2 - Y: 50.00 % - d x by: 1.000 - WL: 1.54056
 05-0586 (*) - Calcite, syn - CaCO3 - Y: 20.83 % - d x by: 1.000 - WL: 1.54056
 41-1480 (I) - Albite, calcian, ordered - (Na,Ca)Al(Si,Al)3O8 - Y: 50.00 % - d x by: 1.000 - WL:
 35-0816 (*) - Fluorite, syn - CaF2 - Y: 50.00 % - d x by: 1.000 - WL: 1.54056
 09-0343 (D) - Illite, trioctahedral - K0.5(Al,Fe,Mg)3(Si,Al)4O10(OH)2 - Y: 11.46 % - d x by: 1.
 16-0362 (N) - Clinocllore-1Mla, ferroan - (Mg,Fe,Al)6(Si,Al)4O10(OH)8 - Y: 25.00 % - d x by

1561B <2 micron (black=natural, red=EG saturated)

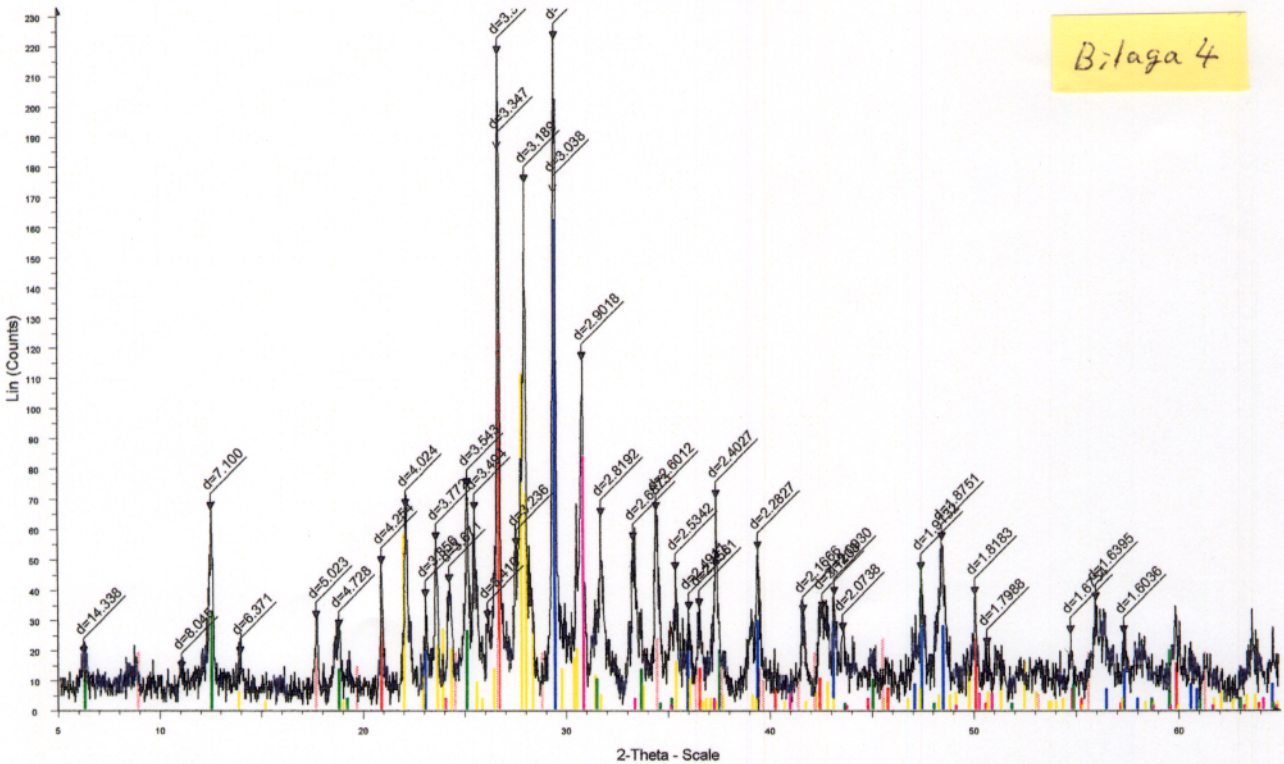
Bilag 3



C:\Sven\Uppdrag\Terralogica\1561B-2mc.RAW - File: 1561B-2mc.RAW - Type: 2Th/Th locked - Start: 2.071 ° - End: 35.068 ° - Step: 0.020 ° - Step time: 1.0 s - Temp.: 27.0 °C - Time Start
 Operations: Displacement -0.250 | Import
 C:\Sven\Uppdrag\Terralogica\1561B-2mc+EG.RAW - File: 1561B-2mc+EG.RAW - Type: 2Th/Th locked - Start: 2.071 ° - End: 35.068 ° - Step: 0.020 ° - Step time: 1.0 s - Temp.: 27.0 °C - Tin
 Operations: Displacement -0.250 | Import

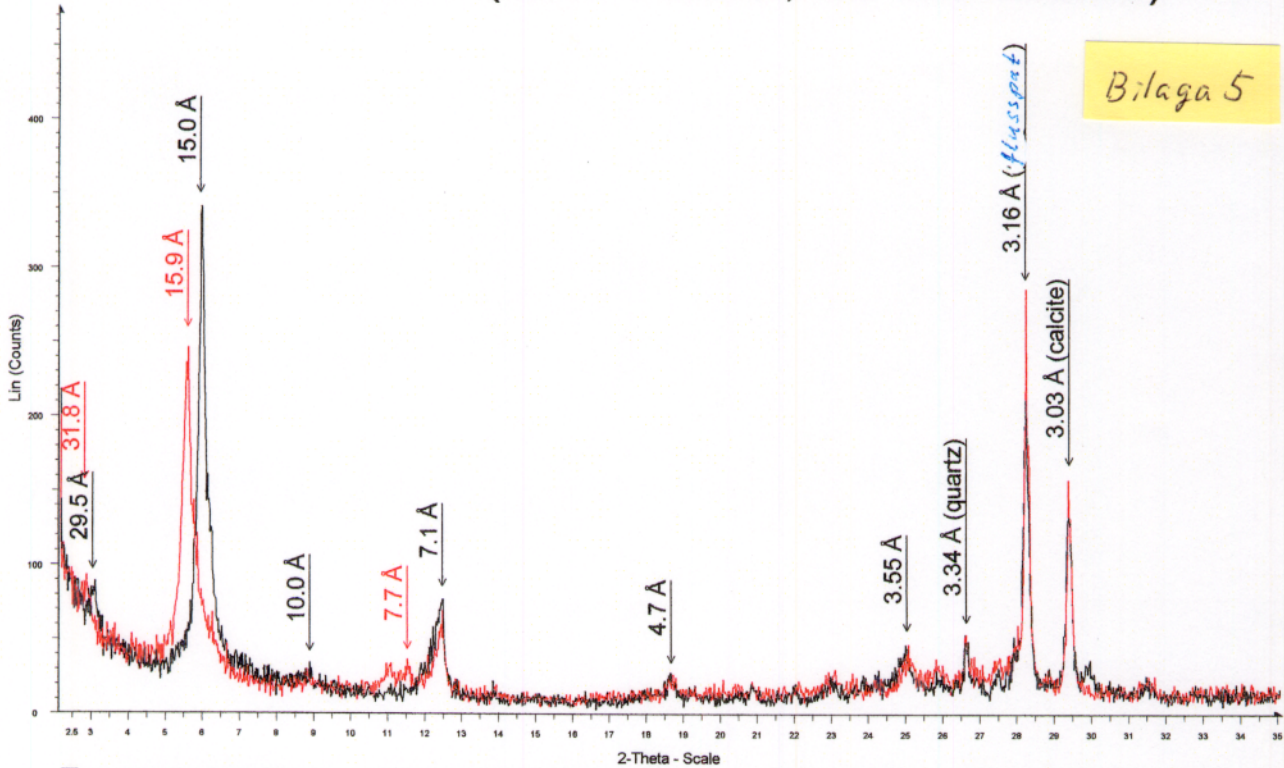
1561B >2 micron

Bilag 4



C:\Sven\Uppdrag\Terralogica\1561B+2mc.RAW - File: 1561B+2mc.RAW - Type: 2Th/Th locked - Start: 5.000 ° - End: 65.000 ° - Step: 0.020 ° - Step time: 1.0 s - Temp.: 27.0 °C - Time Start
 Operations: Import
 33-1161 (*) - Quartz, syn - SiO₂ - Y: 75.00 % - d x by: 1.000 - WL: 1.54056
 05-0586 (*) - Calcite, syn - CaCO₃ - Y: 72.92 % - d x by: 1.000 - WL: 1.54056
 20-0548 (D) - Albite, calcian, ordered - (Na,Ca)(Si,Al)4O₈ - Y: 50.00 % - d x by: 1.000 - WL: 1.54056
 16-0362 (N) - Clinocllore-1Mia, ferroan - (Mg,Fe,Al)8(Si,Al)4O₁₀(OH)8 - Y: 14.58 % - d x by: 1.000 - WL: 1.54056
 02-0462 (D) - Illite, 1M - KAl₂(Si₃AlO₁₀)(OH)₂ - Y: 10.42 % - d x by: 1.000 - WL: 1.54056
 34-0517 (D) - Dolomite, ferroan - Ca(Mg,Fe)(CO₃)₂ - Y: 37.50 % - d x by: 1.000 - WL: 1.54056

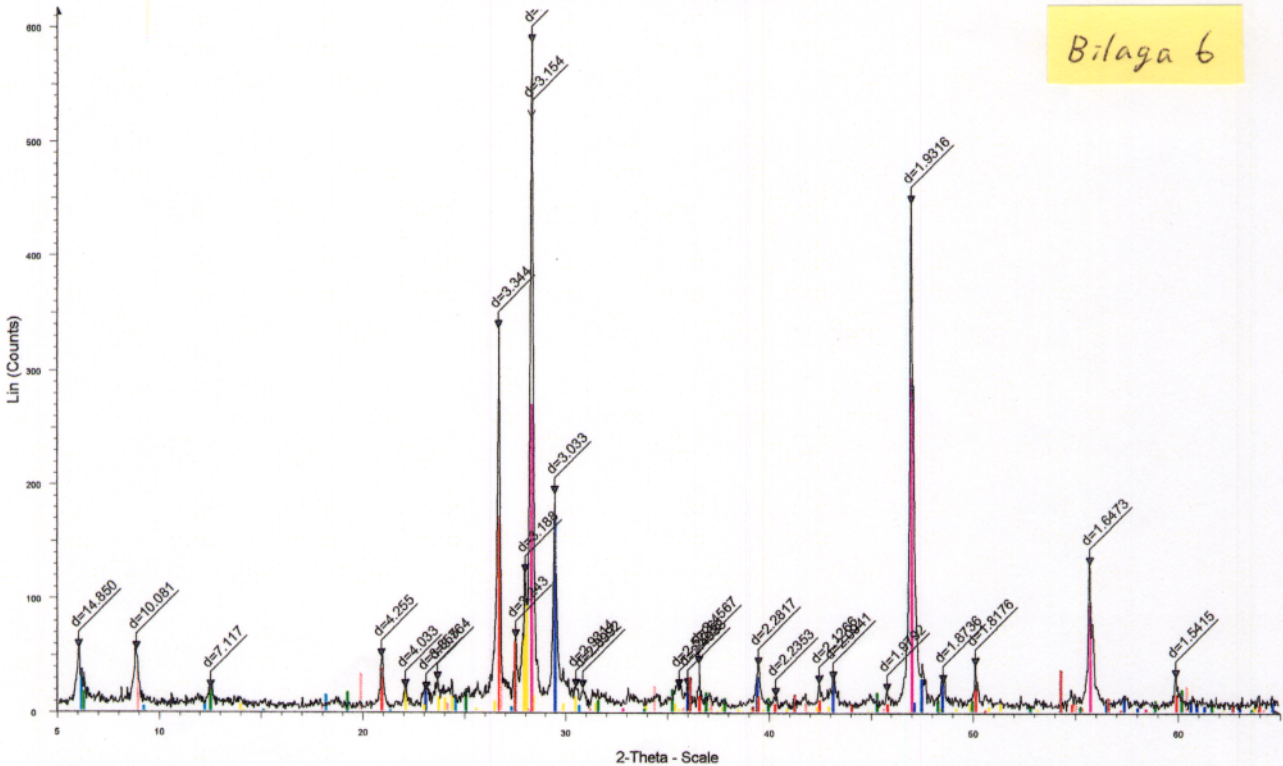
1575A <2 micron (black=natural, red=EG saturated)



Bilaga 5

A: C:\Sven\Uppdrag\Terralogica\1575A-2mc.RAW - File: 1575A-2mc.RAW - Type: 2Th/Th locked - Start: 2.119 ° - End: 35.114 ° - Step: 0.020 ° - Step time: 1.0 s - Temp.: 27.0 °C - Time Starter
 Operations: Y Scale 0.750 | Displacement -0.417 | Import
 A: C:\Sven\Uppdrag\Terralogica\1575A-2mc+EG.RAW - File: 1575A-2mc+EG.RAW - Type: 2Th/Th locked - Start: 2.119 ° - End: 35.114 ° - Step: 0.020 ° - Step time: 1.0 s - Temp.: 27.0 °C - Tin
 Operations: Y Scale 0.750 | Displacement -0.417 | Import

1575A >2 micron

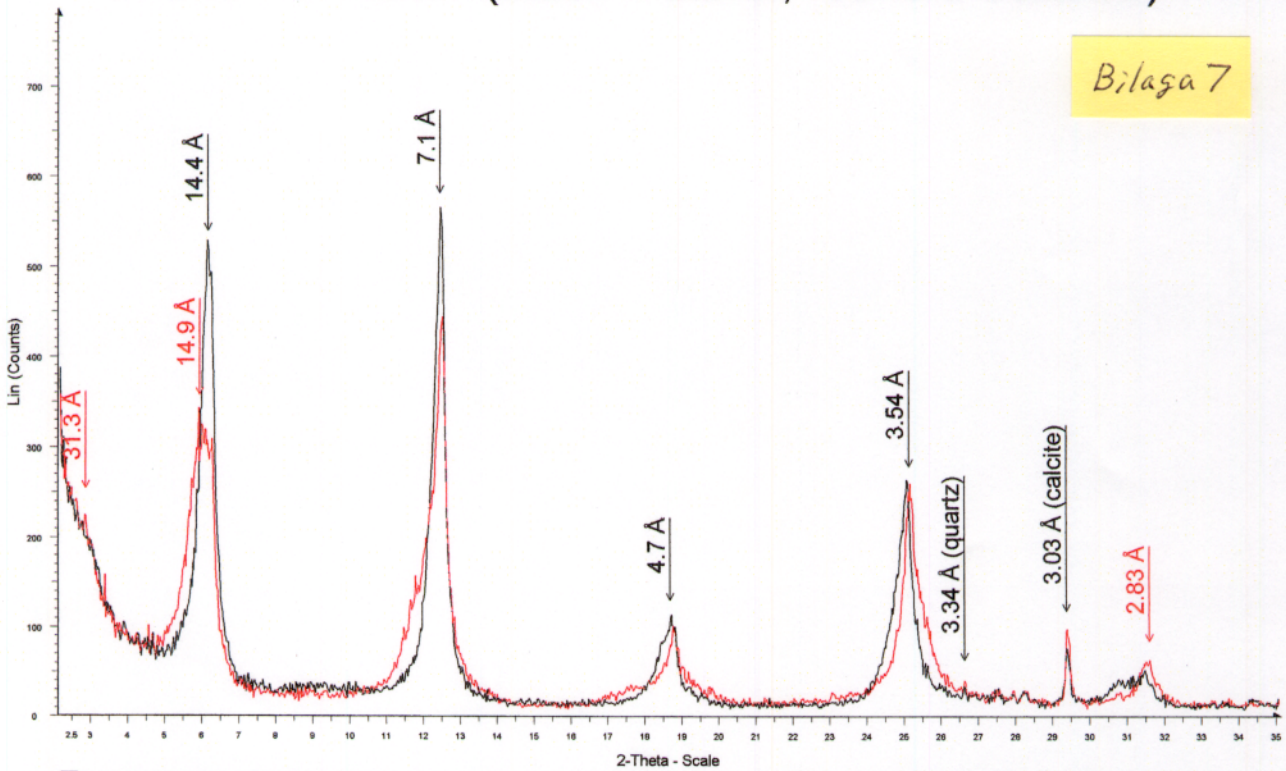


Bilaga 6

A: C:\Sven\Uppdrag\Terralogica\1575A+2mc.RAW - File: 1575A+2mc.RAW - Type: 2Th/Th locked - Start: 2.119 ° - End: 35.114 ° - Step: 0.020 ° - Step time: 1.0 s - Temp.: 27.0 °C - Time Starter
 Operations: Displacement 0.083 | Displacement 0.167 | Import
 05-0586 (*) - Calcite, syn - CaCO₃ - Y: 29.17 % - d x by: 1.000 - WL: 1.54056
 33-1161 (*) - Quartz, syn - SiO₂ - Y: 29.17 % - d x by: 1.000 - WL: 1.54056
 41-1480 (l) - Albite, calcian, ordered - (Na,Ca)Al(Si,Al)₃O₈ - Y: 16.67 % - d x by: 1.000 - WL:
 35-0816 (*) - Fluorite, syn - CaF₂ - Y: 50.00 % - d x by: 1.000 - WL: 1.54056
 13-0190 (D) - Corrensite - Mg₈Al₃(Si₆O₂₀(OH)10.4H₂O - Y: 6.25 % - d x by: 1.000 - WL: 1.5
 19-0749 (D) - Clinocllore-2Mlib - Mg₅Al(Si₃Al)O₁₀(OH)₈ - Y: 4.17 % - d x by: 1.000 - WL: 1
 09-0343 (D) - Illite, trioctahedral - K_{0.5}(Al,Fe,Mg)₃(Si,Al)₄O₁₀(OH)₂ - Y: 6.25 % - d x by: 1.0
 21-1276 (*) - Rutile, syn - TiO₂ - Y: 10.42 % - d x by: 1.000 - WL: 1.54056

2151B <2 micron (black=natural, red=EG saturated)

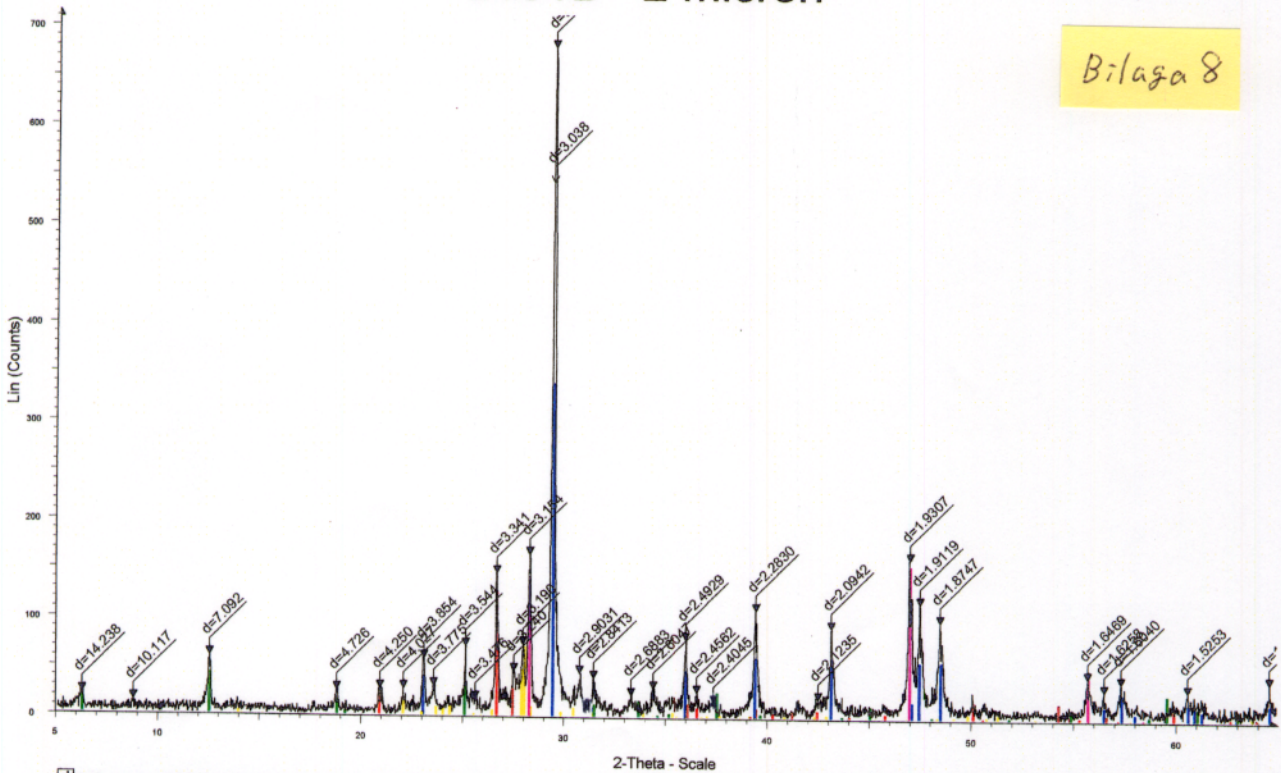
Bilaga 7



C:\Sven\Uppdrag\Terralogica\2151B-2mc.RAW - File: 2151B-2mc.RAW - Type: 2Th/Th locked - Start: 2.119 ° - End: 35.114 ° - Step: 0.020 ° - Step time: 1.0 s - Temp.: 27.0 °C - Time Start:
 Operations: Y Scale 0.750 | Displacement -0.417 | Import
 C:\Sven\Uppdrag\Terralogica\2151B-2mc+EG.RAW - File: 2151B-2mc+EG.RAW - Type: 2Th/Th locked - Start: 2.143 ° - End: 35.136 ° - Step: 0.020 ° - Step time: 1.0 s - Temp.: 27.0 °C - Tin
 Operations: Y Scale 0.750 | Displacement -0.500 | Import

2151B >2 micron

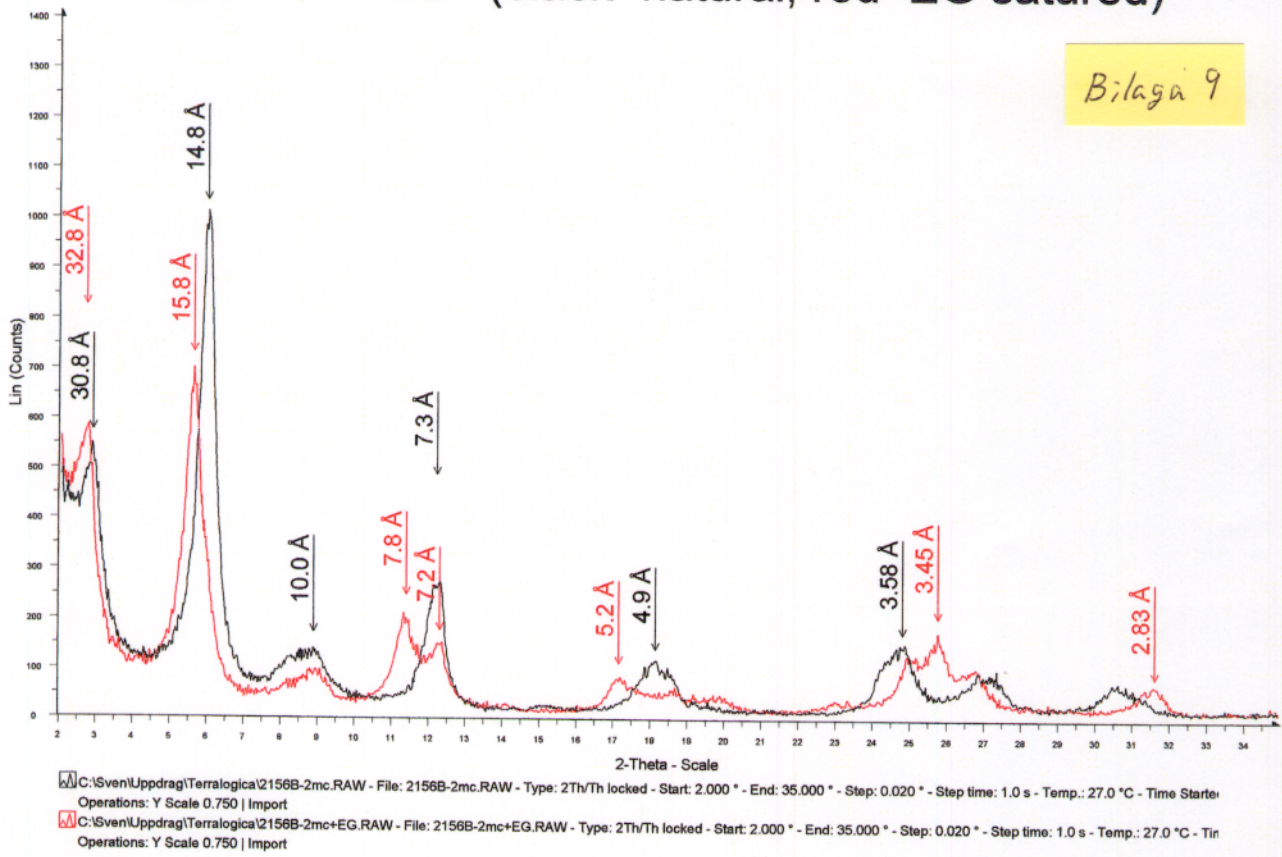
Bilaga 8



C:\Sven\Uppdrag\Terralogica\2151B+2mc.RAW - File: 2151B+2mc.RAW - Type: 2Th/Th locked - Start: 5.000 ° - End: 65.000 ° - Step: 0.020 ° - Step time: 1.0 s - Temp.: 27.0 °C - Time Start:
 Operations: Import
 33-1161 (*) - Quartz, syn - SiO₂ - Y: 18.75 % - d x by: 1.000 - WL: 1.54056
 05-0586 (*) - Calcite, syn - CaCO₃ - Y: 50.00 % - d x by: 1.000 - WL: 1.54056
 41-1480 (I) - Albite, calcian, ordered - (Na,Ca)Al(Si,Al)₃O₈ - Y: 10.42 % - d x by: 1.000 - WL: 1.54056
 35-0816 (*) - Fluorite, syn - CaF₂ - Y: 22.92 % - d x by: 1.000 - WL: 1.54056
 16-0362 (N) - Clinochlore-1Mla, ferroan - (Mg,Fe,Al)₆(Si,Al)₄O₁₀(OH)₈ - Y: 6.25 % - d x by: 1.000 - WL: 1.54056
 21-1276 (*) - Rutile, syn - TiO₂ - Y: 4.17 % - d x by: 1.000 - WL: 1.54056

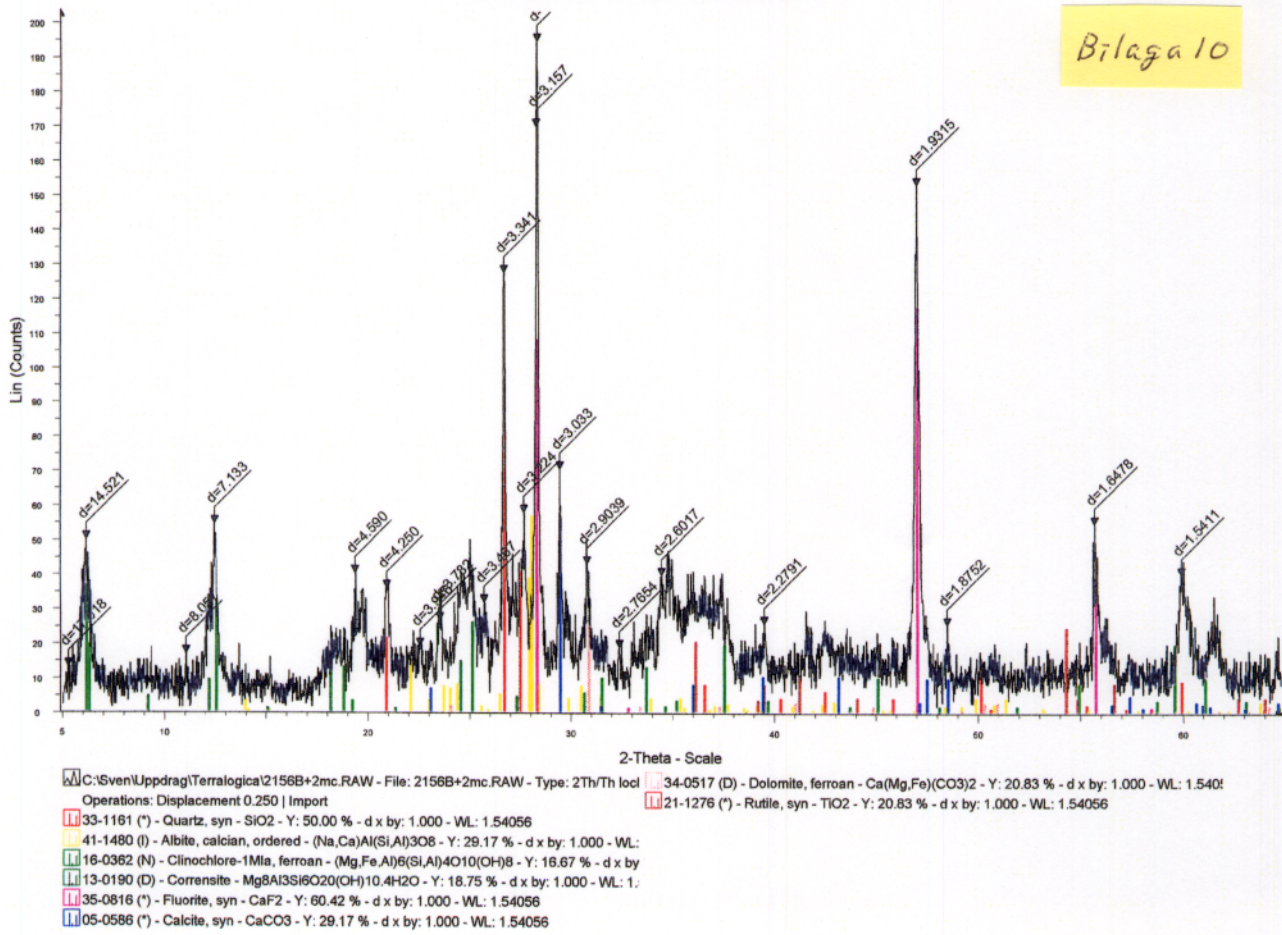
2156B <2 micron (black=natural, red=EG saturated)

Bilaga 9



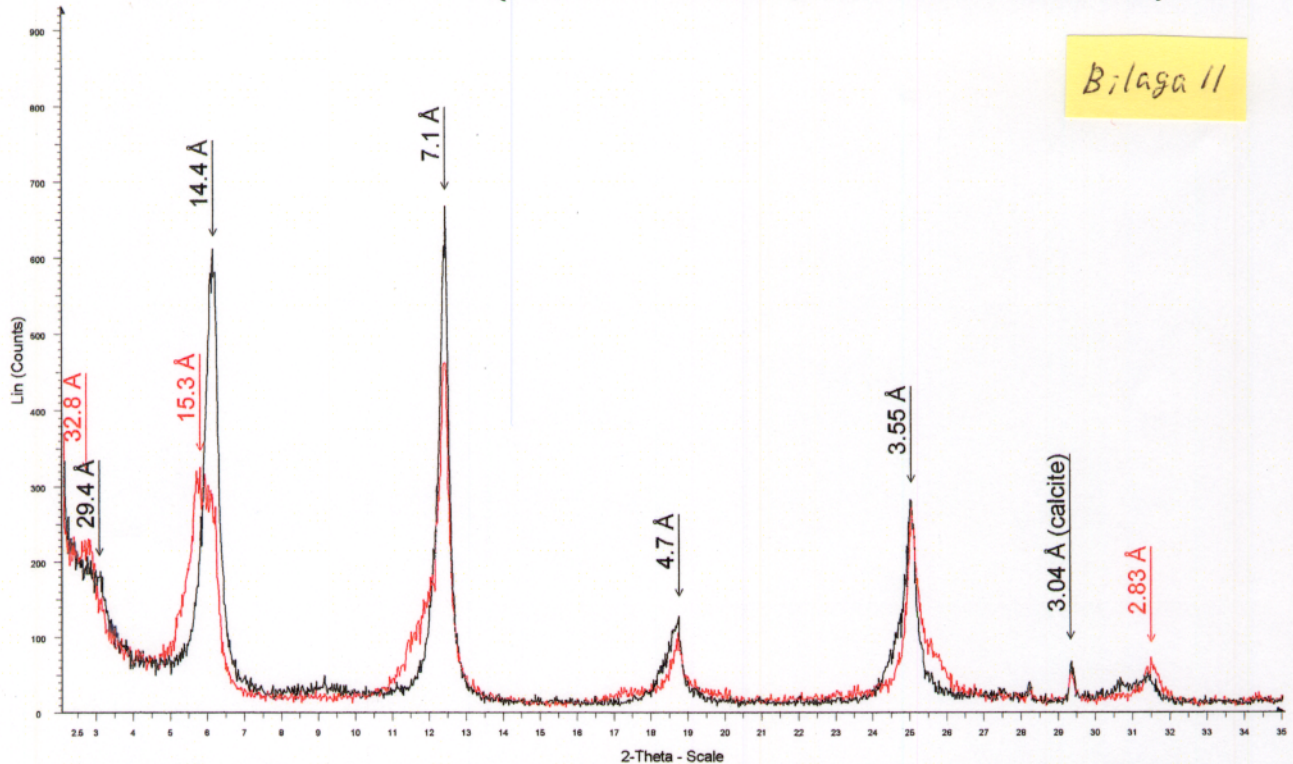
2156B >2 micron

Bilaga 10



2198A <2 micron (black=natural, red=EG saturated)

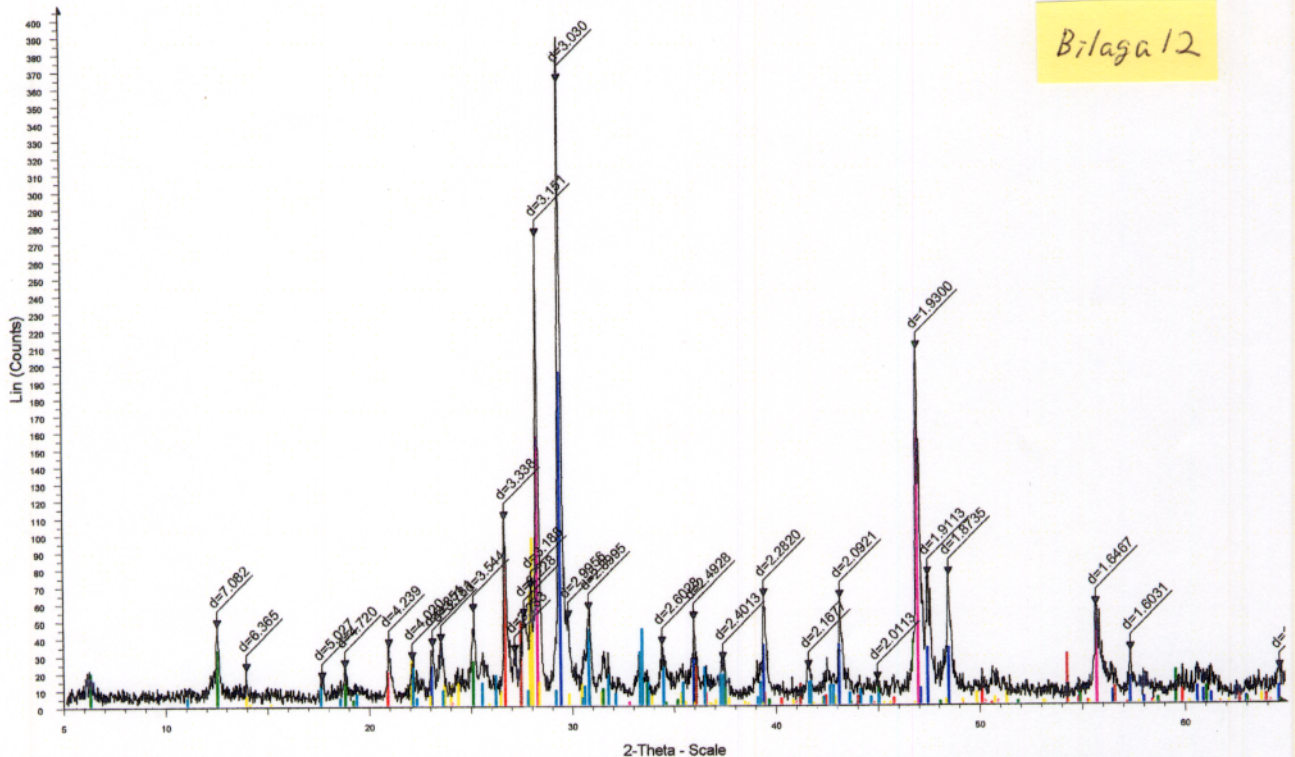
Bilaga 11



[A] C:\Sven\Uppdrag\Terralogica\2198A-2mc.RAW - File: 2198A-2mc.RAW - Type: 2Th/Th locked - Start: 2.095 ° - End: 35.091 ° - Step: 0.020 ° - Step time: 1.0 s - Temp.: 27.0 °C - Time Start: 0.000 s - Operations: Y Scale 0.750 | Displacement -0.333 | Import
 [C] C:\Sven\Uppdrag\Terralogica\2198A-2mc+EG.RAW - File: 2198A-2mc+EG.RAW - Type: 2Th/Th locked - Start: 2.071 ° - End: 35.066 ° - Step: 0.020 ° - Step time: 1.0 s - Temp.: 27.0 °C - Time Start: 0.000 s - Operations: Y Scale 0.750 | Displacement -0.250 | Import

2198A >2 micron

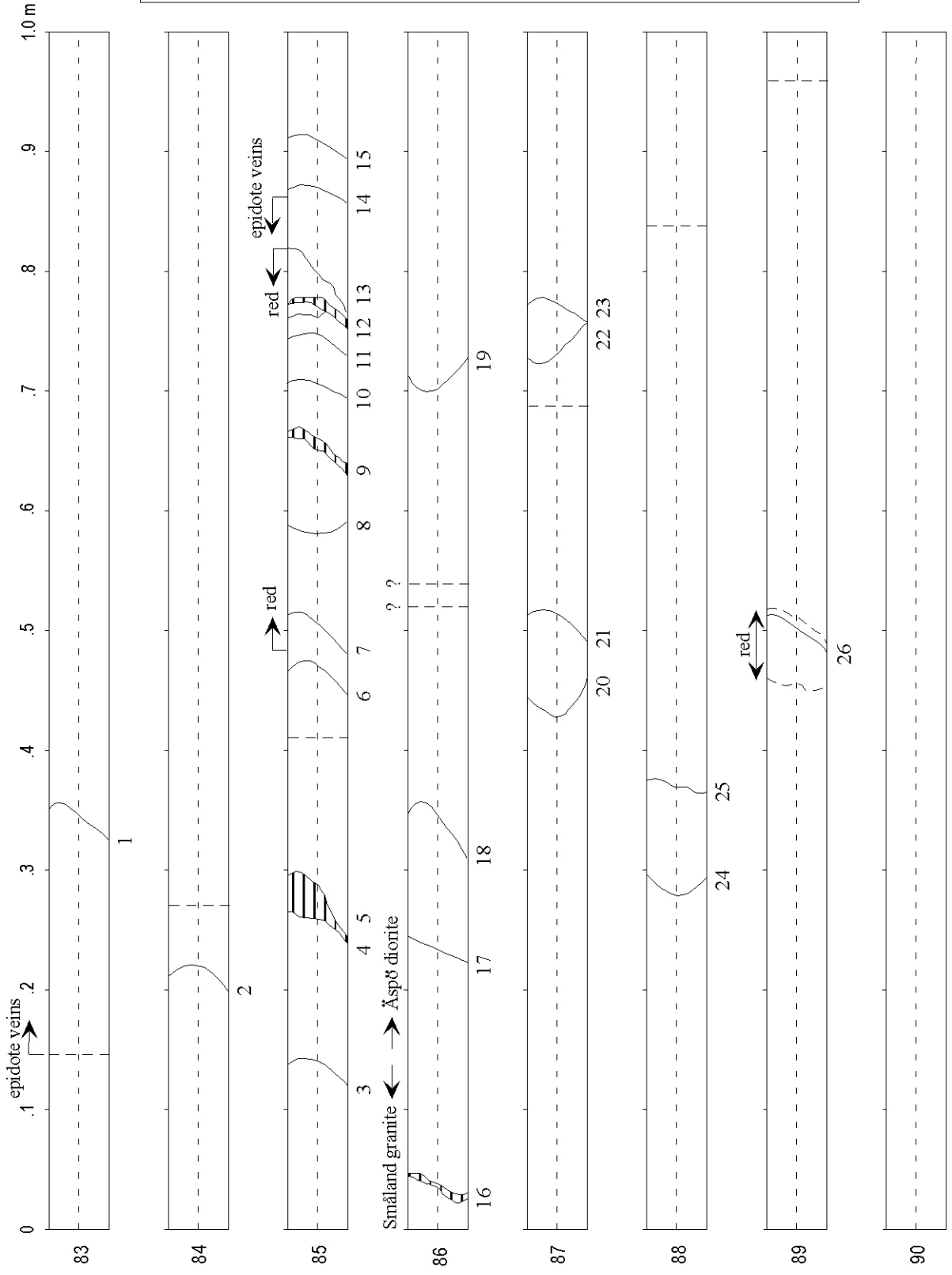
Bilaga 12



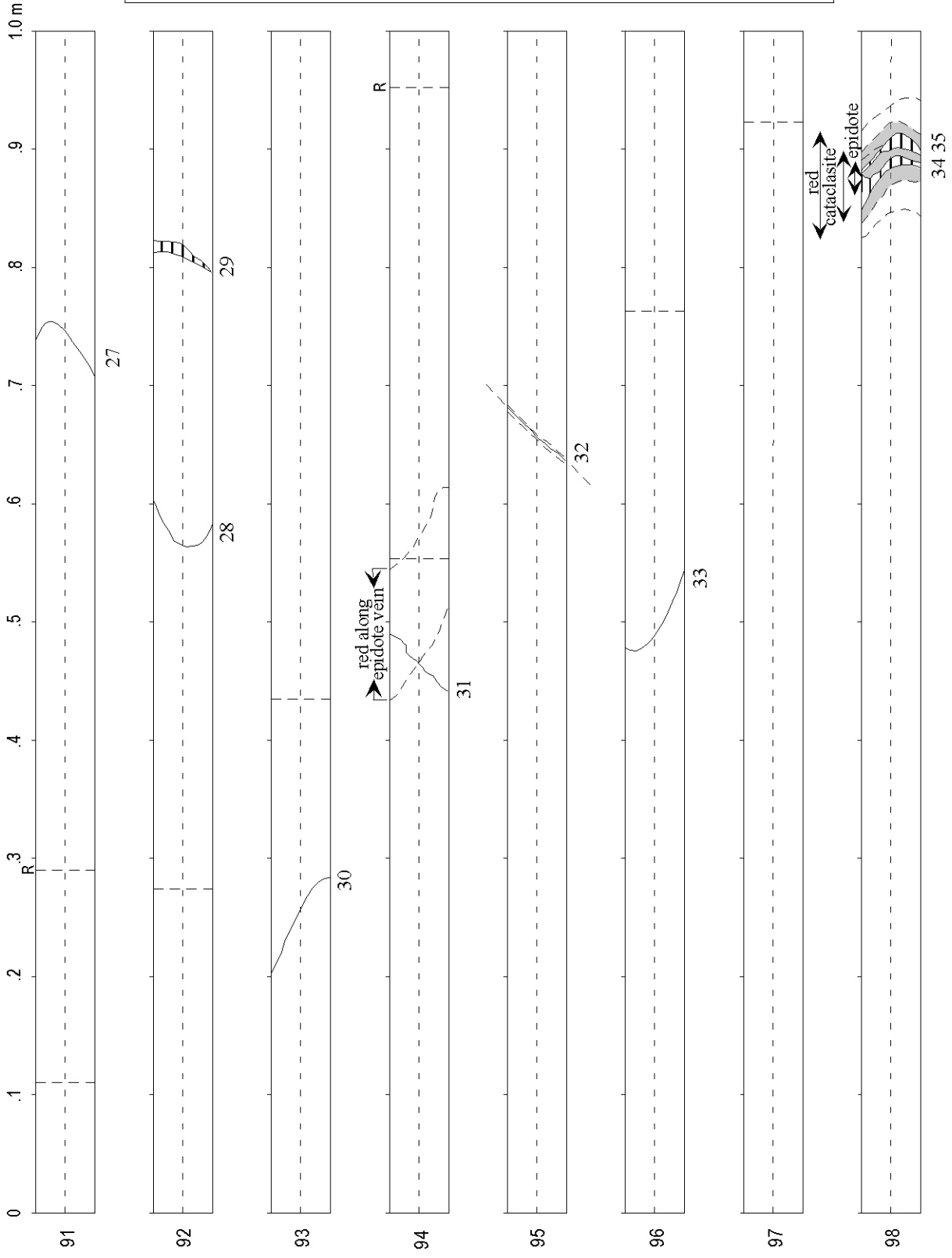
[A] C:\Sven\Uppdrag\Terralogica\2198A+2mc.RAW - File: 2198A+2mc.RAW - Type: 2Th/Th locked - Start: 2.095 ° - End: 35.091 ° - Step: 0.020 ° - Step time: 1.0 s - Temp.: 27.0 °C - Time Start: 0.000 s - Operations: Displacement 0.000 | Displacement 0.250 | Displacement 0.000 | Import
 [L] 16-0362 (N) - Clinocllore-1M1a, ferroan - (Mg,Fe,Al)6(Si,Al)4O10(OH)8 - Y: 8.33 % - d x by: 1.000 - WL: 1.54056
 [I] 17-0514 (I) - Epidote - Ca2Al2Fe(SiO4)(Si2O7)(O,OH)2 - Y: 11.46 % - d x by: 1.000 - WL: 1.54056
 [T] 33-1161 (*) - Quartz, syn - SiO2 - Y: 22.92 % - d x by: 1.000 - WL: 1.54056
 [L] 05-0586 (*) - Calcite, syn - CaCO3 - Y: 50.00 % - d x by: 1.000 - WL: 1.54056
 [I] 35-0816 (*) - Fluorite, syn - CaF2 - Y: 43.75 % - d x by: 1.000 - WL: 1.54056
 [L] 41-1480 (I) - Albite, calcian, ordered - (Na,Ca)Al(Si,Al)3O8 - Y: 25.00 % - d x by: 1.000 - WL: 1.54056
 [L] 21-1276 (*) - Rutile, syn - TiO2 - Y: 12.50 % - d x by: 1.000 - WL: 1.54056
 [L] 34-0517 (D) - Dolomite, ferroan - Ca(Mg,Fe)(CO3)2 - Y: 10.42 % - d x by: 1.000 - WL: 1.54056

Appendix 5

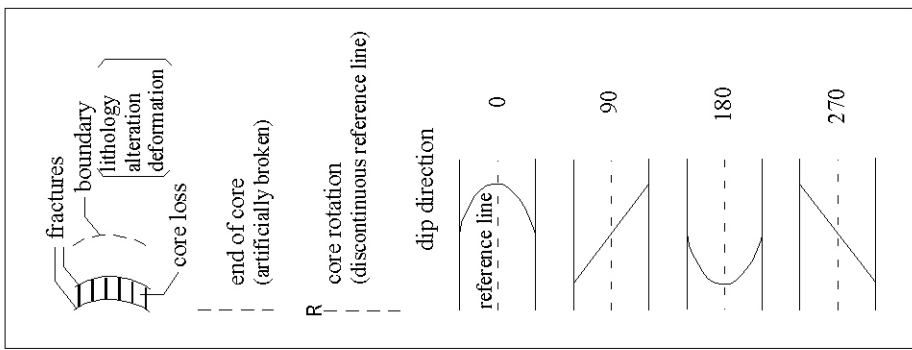
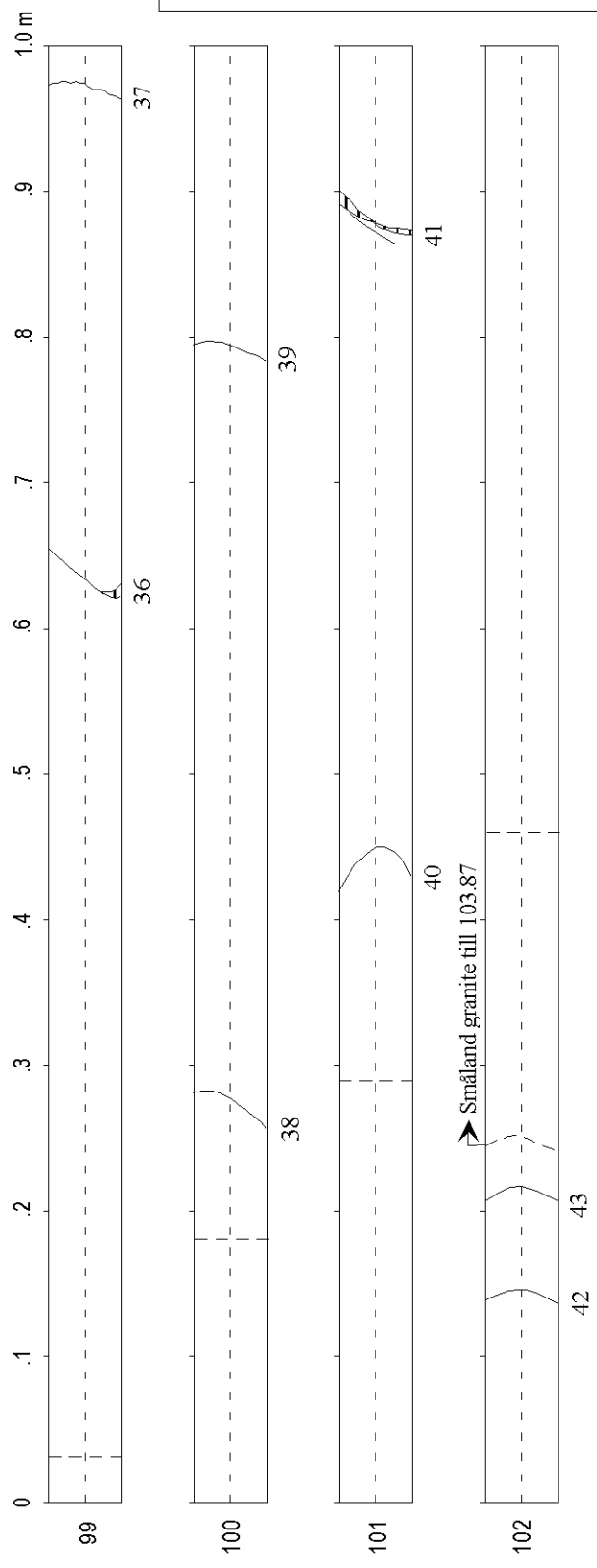
Maps of the core mapping

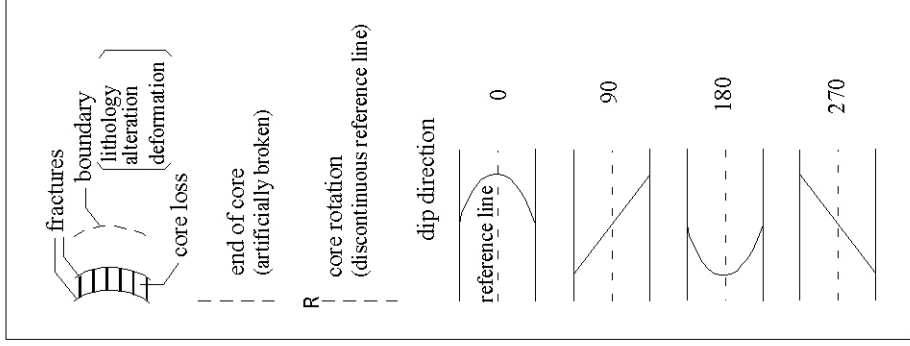
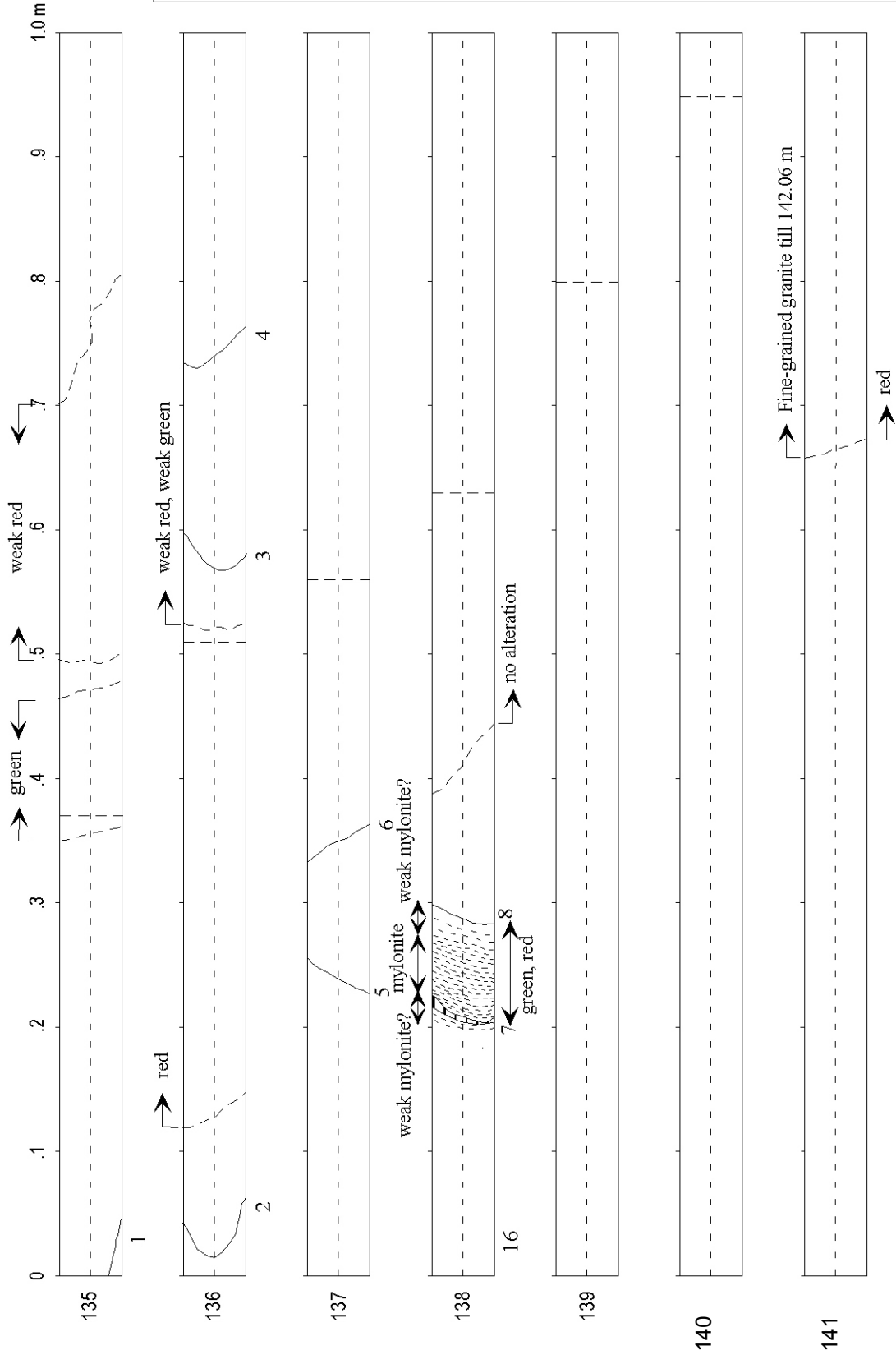


Core Mapping - Section 1 (1/3)
Appendix 5



Core Mapping - Section 1 (2/3)





Appendix 6

Tables of descriptions for the core mapping

Appendix 6: Core mapping description

LEGEND

No.	reference number in the map
type	type of the feature
	fr fracture displacement/slip along fracture is not obvious
	ft fault displacement/slip along fracture is observed or positively assumed
host	host rock
	A Äspö diorite
	S Småland granite
	F Fine-grained granite (including dikes/veins of leuco-granite and pegmatite)
	G green stone (±: subordinate)
relation	relationship to the host rock
	c cutting
	f following
ductile def.	intensity of ductile deformation (mylonitization) along the feature, and width in cm.
	w weak
	m moderate
	s strong
fault rock	type cohesive and incohesive fault rock, intensity as above and width in cm.
	cat cataclasite lithified fault breccia
	c fault crush fragments>90% matrix <10%
	b fault breccia fragments 90-30% matrix <10%
	g fault gouge fragments<10% matrix <10% (±: subordinate)
dip dir.	angle from reference line to dip direction (0 to 360 deg. In clockwise)
dip CA	dip angle from core axis.
linea. dir.	angle from reference line to plunge direction of lineation (0 to 360 deg. In clockwise)
linea. CA	plunge angle from core axis.
slip	d dextral
	s sinistral
aperture	visual estimation in cm.
	0,1 no visible aperture, tight fracture with good fitting of planes
	0,2 not obvious aperture, a little loose fracture but good fitting of planes.
	? not available due to bad fitting of planes.
fitness	f good fitting of fracture planes (±f: partly open).
	o open fracture, poor fitting of fracture planes (±o: partly fit).
plane	shape of fracture plane
	s stepped
	u undulating
	p planar
rough	plane surface condition
	r rough
	s smooth
	p polished
filling/coating	nature and thickness (mm) of fracture filling/coating materials, ordered from outer to inner
	cal calcite
	chl chlorite
	clay clay minerals
	epi epidote
	py pyrite
	grout grout cement (±: subordinate)
f/c%	approximate area filled/coated in a feature
alteration	nature and width (cm) of alteration halo perpendicular to fracture

Appendix 6

Core Mapping - Section 1

No.	type	host	relation	ductile def. (cm)	fault rock (cm)	dip dir.	dip CA	linea. dir.	linea. CA	slip	aperture (mm)	fitness	plane	rough	filling/coating (mm)	f/c (%)	alteration (cm)	remarks
1	fr	S-A	c	no	no	330	50				0,2	f	u	s	cal<0.2	100	no	many epi veins till No. 14.
2	fr	S-A	c	no	no	340	40				0,1	f	p	s	cal<0.1, ±py(p)	100	no	
3	fr	S-A	c	no	no	330	45				0,1	f	p	s	cal<0.1	100	no	
4	fr	S-A	c	no	no	315	45				?	o	p-u	s-r	±cal<0.1	50	no	lost broken pieces between No.4 and 5.
5	fr	S-A	c	no	no	300	30				?	o	p-u	s-r	±cal<0.1	30	no	
6	fr	S-A	c	no	no	330	45				0,1	f	p	s	cal<0.1	100	no	
7	fr	S	c	no	no	310	45				0,2	f	p	s-st	cal=<0.1	100	entire red	// cal filled fractures nearby.
8	fr	S	c	no	no	160	75				0,1	f	p	s	cal<0.2	100	entire red	*{many // minor open/closed fractures nearby. many random fine network of epi veins. entire reddening of fsp. silicified?}
9	fr	S	c	no	no	295	45				>0.2	o	p	s-st	cal<0.2, -epi	80	entire red	*
10	fr	S	c	no	no	310	60				0,2	f	p	s	cal<0.2	100	entire red	*
11	fr	S	c	no	no	315	60				0,1	f	p	s	cal=<0.1, py?<0.1	100	entire red	*, grey obscure py?
12	fr	S	c	no	no	320	60				?	o	p	r	chl<0.2, cal<0.2, -py(p)	70	entire red	*
13	fr	S	c	no	no	290	40				0,1	f	p	r	chl<0.1, ±cal<0.1	100	entire red	*
14	fr	S	c	no	no	325	65				0,1	f	p	s	cal<0.2, ±py?	100	no	grey obscure py?
15	fr	S	c	no	no	325	60				0,1	f	p	s	cal<0.2	100	no	
16	fr	S	c	no	no	250	65				>0.2	±f	u-s	s-r	cal<0.2, -clay?	90	no	light grey clay?, fracture partly fit
17	fr	A	c	no	no	270	70				0,1	f	u	s	±chl<0.1, ±cal<0.1, -py(e)	90	no	euhedral py dissemination with grey clay.
18	fr	A	c	no	no	300	40				0,2	±f	p	r	cal=<1	100	no	
19	fr	A	c	no	no	220	40				0,2	f	p	r	epi?<0.1, cal<0.1	100	no	epi or clay?
20	fr	A	c	no	no	150	45				0,1	f	p	r	±cal<0.1	70	no	
21	fr	A	c	no	no	320	45				0,1	f	p	r	±cal<0.1	50	no	
22	fr	A	c	no	no	100	55				0,1	f	p-u	r	cal<0.1, -py(p)	100	no	
23	fr	A	c	no	no	325	50				0,1	f	p	r	cal<0.1	70	no	
24	fr	A	c	no	no	170	65				0,1	f	u	r	chl?<0.1, cal<0.2	100	no	grey chl?
25	fr	A	c	no	no	285	75				0,1	f	u	r	chl<0.2	100	no	
26	fr	A	c	no	no	295	60				0,2	f	p	s-r	±epi<0.1, cal=<0.1, ±clay<0.3	100	epi<0.5, red<1	grey clay.
27	fr	A	c	no	no	325	35				0,1	f	p	r	±cal<0.1	30	no	
28	fr	A	c	no	no	195	35				0,1	f	p	r-s	cal<0.1	100	no	
29	fr	A	c	no	no	305	45				>0.2	±0	p	r	±cal<0.1	10	no	broken, only a portion fits.
30	fr	A	c	no	no	280	25				0,1	f	u	r	chl<0.1	100	no	spherulitic chl?
31	fr	A	c	no	no	280	40				0,1	f	u	r	chl<0.1, ±cal<0.1	100	entire red	red alteration along fine epi veins.
32	fr	A	c	no	no	250	35				0,2	f	p	s	epi<3, cal<0.5, -py(e)	100	no	
33	fr	A	c	no	no	105	25				0,1	f	p	s-r	chl=<1, ±py(p)	100	no	

Appendix 6

Core Mapping - Section 1

No.	type	host	relation	ductile def. (cm)	fault rock (cm)	dip dir.	dip CA	linea. dir.	linea. CA	slip	aperture (mm)	fitness	plane	rough	filling/coating (mm)	f/c (%)	alteration (cm)	remarks
34	ft	A	c	no	cat; mod<2, wk<5	20	35					o	p	s	epi<0.3, chl<0.2, \pm cal<0.2	100	red<10	re-activated cataclasite; epi veins 3-5mm with fragments, weak grain size reduction, chl in matrix, filling/breccia is lost and fitting is bad.
35	ft	A	c	no	same as above	25	40				0,2	\pm f	p-u	s	chl<0.2, \pm cal<0.1, -clay	100	red<10	same as above.
36	ft	A	c	no	no	265	55	240	45	?	0,1	f	p	s	\pm chl<0.1, cal<0.1, -py(p)	100	no	weak lineation (groove/striation).
37	fr	A	c	no	no	305	70				0,1	f	p-u	r	chl<0.1, \pm cal?<0.1	100	no	grey cal?
38	fr	A	c	no	no	300	55				0,1	f	p-u	s-r	chl<0.1, \pm cal<0.1	100	no	
39	fr	A	c	no	no	305	60				0,1	f	u	s-r	chl<0.1, \pm cal?	100	no	
40	fr	A	c	no	no	10	40				0,2	f	p	s	clay<0.2	80	no	olive green clay?
41	fr	A	c	no	no	230	55				<0.3	\pm o	p-u	s	epi?<0.1, cal<0.3	100	no	
42	fr	A	c	no	no	15	65				0,1	f	p	s	\pm ?	?	no	weakly altered surface.
43	fr	A	c	no	no	345	55				0,1	f	p-s	s	\pm ?	?	no	weakly altered surface.

Appendix 6

Core Mapping - Section 2

No.	type	host	relation	ductile def. (cm)	fault rock (cm)	dip dir.	dip CA	linea. dir.	linea. CA	slip	aperture (mm)	fitness	plane	rough	filling/coating (mm)	f/c (%)	alteration (cm)	remarks
1	fr	A	c	no	no	145	20				0,1	f	u	r	chl<0.1, cal<0.2, -clay?, -py(e)	100	wk red<3, ±green	brown clay or mud?
2	fr	A	c	no	no	170	30				0,1	f	u	r	chl<0.1, cal<0.1, -clay?	100	entire wk green, ±red	brown clay or mud?
3	fr	A	c	no	no	190	30				0,1	f	p-s	r-s	±cal<0.1	10	entire wk red, green	many irregular high angle chl filled fractures with red alteration.
4	fr	A	c	no	no	120	55				0,1	f	p	r	chl<0.1, clay<0.1	100	entire wk red, green	grey clay.
5	fr	A	c	no	no	285	55				0,1	f	p	r-s	cal=<0.3	80	entire wk red, ±green	
6	fr	A	c	no	no	95	55	75	52		0,2	f	p	s	chl<0.2, clay<0.1	100	wk red<5, ±green	grey clay.
7	ft	A	c	s<6, w?<2	±b?	230	65				<5?	o	p-u	r-s	epi(vein)=<10, ±cal<0.2, -clay?, -py(e)	100	mod red<20, mod green<7?	following edge of mylonite with foliation defined by very fine epi veins. grains not visible due to mylonitization. fracture not fit, probably apperture<5mm. ±b?; minor epidotized ragments. clay/gouge washed out?
8	fr	A	c	no	no	250	65	265	63		0,2	f	p-u	s-st	chl<0.2, cal=<1.0, ±py(p,e)	100	mod red<20, mod green<8?	following edge of trace mylonite?